SSSU 55
ISSN 0140 3818

UNIVERSITY OF SOUTHAMPTON

DEPARTMENT OF SHIP SCIENCE

FACULTY OF ENGINEERING AND APPLIED SCIENCE

WIND TUNNEL TESTS ON A 1/16TH-SCALE LASER MODEL

by

Dr. R.G.J. Flay
Visiting Senior Lecturer

Ship Science Report No. 55

June 1992

WIND TUNNEL TESTS ON A 1/6th-SCALE LASER MODEL

By Dr. R.G.J. Flay
Visiting Senior Lecturer*

Ship Science Report No. 55

* On Sabbatical leave at Department of Ship Science from The University of Auckland, New Zealand, January - June 1992.

SUMMARY

An analysis of full-scale wind structure relevant to sailing yachts is carried out in order to develop a target model for wind-tunnel simulations. Unavoidable differences between real onset yacht flows and idealised wind-tunnel simulations are pointed out. Detailed measurements of the actual wind-tunnel flows developed for the present tests are discussed in depth, and are compared to idealised cases, concluding that although the simulations are not as good as physically possible, they are perfectly adequate for the present test programme.

Measurements of the forces and moments acting on a 1/6th scale model of a Laser yacht for apparent wind directions of 30 and 60 degrees, for heel angles of 0, 10, 20, and 30 degrees, and for smooth and turbulent sheared flow are presented. The results are discussed in terms of sail aerodynamics, and a transformation procedure is developed which leads to an excellent collapse of the measured results on the basis of calculated sail lift and drag coefficients.

ACKNOWLEDGEMENTS

I should like to thank Professor W.G. Price, Head of the Department of Ship Science for his support and encouragement, and for making the facilities of the Department available to me during my January to June 1992 Sabbatical Leave in the Department of Ship Science.

At the inception stage of the test programme reported herein, the help of Dr. A.F. Molland was invaluable in sorting out various pieces of hardware, especially a suitable balance (dynamometer). Mr. S.R. Turnock contributed significantly by writing a data acquisition program to drive the balance voltmeter, and then by actually running the program during the testing phase. Thanks also to Mr. G. Baldwin for operating the wind-tunnel throughout the tests and for making the many adjustments to the model setup.

The discussions with Dr. J.F. Wellicome and Mr. I.M.C. Campbell concerning model yacht-sail wind-tunnel testing procedures, and sail aerodynamics were of much interest, and very helpful. The data analysis could not have advanced without the help of Mr. P.A. Wilson in sorting out my various problems in learning to operate the Departmental computers.

I should like to thank Mrs. Sue Garside for typing this report, and for carrying out the necessary tasks for its completion after the end of my Sabbatical Leave in the Department.

Finally, I should like to thank my wife Linda for taking on the lion's share of looking after our young family away from home during my Sabbatical Leave.

CONTENTS

1. INTRODUCTION

The wind tunnel is a very useful tool for carrying out tests on yacht models to enable predictions of full-scale performance to be made. However, aerodynamically yachts are very complicated devices and there is not necessarily a one to one correspondence between wind tunnel performance measures and real performance of the full-scale prototype. This arises through a variety of reasons, but is mainly due to the difficulty of adequately simulating the full-scale onset flow to the yacht in the wind tunnel where the model is stationary. Other difficulties arise such as getting adequate sail shapes when the models are too small.

A practical difficulty when undertaking wind tunnel tests is deciding on appropriate sail configurations to test. A sail requires a minimum of say 10 variables to specify its shape, and to cover various ranges of heel angle and apparent wind angle, as well as wind speed requires an inordinate number of individual tests unless simplifications are made.

One outcome of the Conference on The Science of Sail Design at the University of Western Ontario, in June 1982 (Ref. 1) was that it was agreed that a "standard" sail should be selected and tested to enable comparisons to be made among the results from different facilities. This is done in calibrating Aeronautical wind-tunnels (standard AGARD models) and Wind Engineering wind-tunnels (CAARC model). The laser yacht (Fig. 1) was selected as the standard because it simply has a single mainsail, and it is a very common design worldwide.

Following on from some earlier wind-tunnel investigations where America's Cup designs had been tested by the Mechanical Engineering Department at the University of Auckland, (12 metre and K class designs), it was decided that a detailed study of various shapes of mainsails flying on a Laser model would be carried out. This study was carried out as a Master of Engineering research project (Ref. 2), and involved the systematic testing of a large number of different sails in different configurations on a 6th scale model Laser yacht, with a stiff cantilevered mast (Fig. 2). It was felt that it would be useful to continue the tests on this model, concentrating in particular on the effects of heel. Thus the present studies of the effects of heel, and also the effects of testing in smooth and a turbulent shear flow, were carried out at the University of Southampton in the 7'x5' wind-tunnel while the author was there during part of his Sabbatical leave, January - June 1992.

The test programme on which this report was based was carried out during the 7th, 8th and 9th of April, and although it would have been desirable to have had a longer test period, this was not possible due to the pressure of wind-tunnel bookings for commercial testing.

The report describes the apparent wind structure of the onset flow in full scale and points out the simplifications which have to be made in practical wind-tunnel tests. It then presents the actual wind-tunnel flow, and discusses how this differs from the flow which was ideally desired. The results are then presented and analysed and compared to relevant results in the literature. The effectiveness of the method used to non-dimensionalise and collapse the results is discussed.

2. APPARENT WIND STRUCTURE

2.1 Velocity Profile

The apparent wind structure seen by the sailing laser depends on the true wind speed, and the direction the yacht is heading. This study will be confined to the upwind sailing case, and it will be assumed that the true wind speed, V_S = 5 m/s = 9.7 knots, a fairly pleasant wind speed for sailing. Furthermore, it will be assumed that this speed

applies at a reference height of 40% of the mast height of 6m, or 2.4m, as it has been found previously that the centre of pressure of sails is around this height. Assuming that the true wind angle β_T is 45° and the boat to true wind speed ratio,

$$\frac{V_S}{V_T} = 0.5 \tag{1}$$

gives the velocity triangle shown.

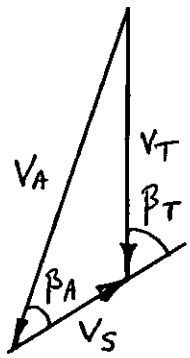

$$V_A = (V_S^2 + V_T^2 + 2V_S V_T \cos\beta_T)^{1/2} \tag{2}$$

$$\beta_A = \sin^{-1}\left(\frac{V_T}{V_A}\sin\beta_T\right) \tag{3}$$

Thus the apparent wind speed is

$$V_A = (5^2 (0.5^2 + 1) + 2 \times 0.5 \times 5^2 \cos 45)^{1/2}$$

$$V_A = 6.995 \text{ m/s}$$

and

$$\beta_A = \sin^{-1}\left(\frac{5}{6.995}\sin 45\right)$$

$$\beta_A = 30.4°$$

The drag coefficient of the water surface, and consequently the roughness length, Z_o, depends on the mean wind speed, as increased wind speed (and fetch) increases the height of the waves, and consequently the surface roughness. However, aerodynamically waves turn out to be very smooth, probably because they are rounded, and in general are translating in the mean wind direction. One correlation for roughness length as a function of the mean wind speed at a height of 10m, V_{10} is available in Cook (Ref. 3) and is

$$Z_o = 5\text{x}10^{-5} V_{10}^2/g \tag{4}$$

At elevations below about 50-100m, in the absence of thermal effects, the true wind velocity profile is described by the simple log-law

$$\bar{V} = \frac{U^*}{0.4} \ln \frac{Z}{Z_o} \tag{5}$$

Guessing that Z_o = 0.2mm allows the speed at 10m height to be estimated

$$\frac{\bar{V}_{10}}{5} = \frac{\ln \frac{10}{0.0002}}{\ln \frac{2.4}{0.0002}}$$

giving $\bar{V}_{10} = 5.76$ m/s

and hence $Z_o = 5\text{x}10^{-5} (5.76)^2/9.81$

$= 0.17$mm

which is close enough, so we shall assume $Z_o = 0.2$mm for subsequent calculations.

The motion of the yacht affects the "apparent" roughness length Z_A, as the sails are of course sensitive only to the apparent wind formed by the vector sum of the boat speed and true wind speed. Sailing upwind tends to flatten the velocity profile as far as the yacht is concerned, whereas sailing downwind tends to make it more non-uniform. For the rather contrived cases of sailing directly upwind or downwind ($\beta_T = 0$ and 180° respectively) the effect of hull motion on the incident wind is simply to modify the actual roughness length Z_o to an apparent roughness:

$$\frac{Z_A}{Z_o} = \frac{1}{f} \text{ (upwind)} \quad ; \quad = f \text{ (downwind), where } f = (\frac{h}{Z_o}) \frac{Vs}{V_T} \qquad (6)$$

where h is the reference height, in this case 2.4m.

For the present case, if β_T were 0°, the apparent roughness length would be

$$Z_A = 0.2/(\frac{2.4}{0.0002})^{0.5}$$

$$= 0.002\text{mm}$$

or reduced by a factor of about 100. If β_T were 180°, Z_A would be increased to about 20mm.

For the real upwind case the situation is more complicated, and the apparent wind varies in speed and direction with height so that the velocity profile appears twisted. The variation of apparent wind speed with height is given by

$$V_A(Z) = (V_s^2 + V_T(Z)^2 + 2V_s\, V_T(Z) \cos\beta_T)^{1/2} \qquad (7)$$

where from (5)

$$V_T(Z) = \frac{0.213}{0.4} \ln \frac{Z}{0.0002} \qquad (8)$$

and

$$\beta_A(Z) = \sin^{-1} (\frac{V_T(Z)}{V_A} \sin \beta_T) \qquad (9)$$

Apparent speed profiles for various values of β_T, and $V_S/V_T = 0.5$ are given in

Fig. 3, in conjunction with the true wind velocity variation with height. When extrapolated to zero speed, it is clear how the apparent roughness length is diminished for upwind cases, and increased for downwind cases. When the speed profiles are normalised by the speed at a height of 10m, the differences are more apparent (Fig. 4). The real upwind case where β_T = 45° has quite a similar velocity profile to the contrived case where β_T = 0. The biggest changes occur for downwind cases, and this can be seen more clearly in Fig. 5 where the height axis is linear, and the speed is dimensionless.

The variation of apparent wind direction (ideally) is shown in Fig. 6. For upwind cases the variation in direction is small, but it increases as β_T increases. The difference in wind direction with height (i.e. twist) with respect to the wind direction at 0.5m height (near boom) is shown in Fig. 7. Here, the angle scale has amplified the change in direction compared to the previous figure, and whereas for β_T = 30° the change in direction over the sail is only a few degrees (2), when β_T is 150° it is increased to almost 13° twist. In practice, wind twist may be less than indicated here for the upwind case and more for the downwind case, due to the flow tending to accelerate at low levels as it rises to pass over the hull. In so doing, the velocity component perpendicular to the hull centreline is increased which causes this effect. (Ref. 4).

The preceding comments illustrate that there is some legitimacy in conducting wind tunnel tests of yachts sailing upwind as far as the velocity profile is concerned, but that for the downwind case, the compromises required will be more severe.

For the present example where it is desired to simulate the flow for a yacht sailing upwind with (say) β_T = 45°, the speed profile should be based on a log-law distribution, with Z_0 around 0.002mm in full-scale. Since the test model is one-sixth of full-scale, this means that Z_0 in the wind-tunnel should be 0.002/6 $\simeq$ 0.0003mm, a very small value. The wind speed variation over the height of the sail is thus relatively small, but is nonetheless still significant.

2.2 Turbulence Intensity

The wind engineering community accepts (Ref. 5) that it is essential to model the spectrum of turbulence (Ref. 6) accurately in building aerodynamic studies in order for the model flow field to truly represent full-scale. This is because turbulence in flow has two aerodynamic effects. It promotes early transition of laminar boundary-layers (Ref. 7), and it must therefore be modelled correctly to reproduce boundary layer behaviour in attached flow, and the associated pressure distributions and occurrence of separation. Turbulence also increases the rate of entertainment in shed shear layers in separated flows, thus reducing their radius of curvature (Ref. 8). In turn this affects the pressure in the wake, or base pressure, which can increase or decrease depending on the afterbody shape and can even change the direction of lift on certain bluff bodies by promoting reattachment and thus altering the direction of the wake. In wind tunnel studies of buildings, the state of the boundary layers on the model is not usually significant in determining the loads, except in certain cases where the shapes are very rounded, and the main function of turbulence modelling in the wind tunnel flow is to reproduce wakes and separation bubbles which mimic full-scale behaviour.

Surprisingly, most vehicle aerodynamic studies have been done in relatively low turbulence wind tunnels (Ref. 9), when one would expect from wind engineering studies that the turbulence generally present in flows onset to vehicles (except for the case of no traffic and no wind) would affect the aerodynamic behaviour. Recently some analysis of the turbulence relevant to vehicles has been carried out (Ref. 10), and it is likely that this point will receive more attention in the future with the drive towards cars with good handling and low drag in the normal situation of turbulent onset flow.

Yachts can only sail when it is windy, and since they operate at the bottom of the earth's boundary layer, they always operate in a turbulent shear flow. As shown in the

previous section, the sea is aerodynamically quite smooth, and this means that over the range of typical mast heights, the turbulence intensity will be of the order of 10%, much less the 15-40% typical for buildings.

The effect of atmospheric turbulence on full-scale sails is not known with certainty, and indications in the literature are confusing. For example, in Ref. 11 it was found that the critical Reynolds number for the drag of a sphere was not affected by atmospheric turbulence whereas in wind tunnels it was found that a small amount of fine scale turbulence had a major effect on the resulting coefficients. Since it is not known what effect it really has on yacht sails, it is difficult to say whether it is important to model it accurately in wind tunnel simulations.

In the author's work, a pragmatic approach has been taken where it has been attempted to model as well as possible the approach turbulence as seen by the moving yacht in full-scale. Since to the author's knowledge there are no published data of turbulence measured by a sensor attached to a sailing yacht, it is useful to try to deduce what the appropriate turbulence level is to give guidance on what it should be in the wind tunnel. The following analysis for the Laser yacht under consideration follows the method developed in Ref. 12.

The turbulence has to be considered with respect to a moving reference frame attached to the yacht. This is similar to the approach taken in Ref. 13 concerning turbulence with respect to moving ground vehicles. The yacht motion, however, can be considered as consisting of two parts, a mean part, plus a dynamic part. The dynamic part occurs because the yacht *reacts* to turbulence, particularly large low frequency gusts, and thus it performs a filtering function.

Rectilinear translation of a vessel through the boundary layer does not alter variance of the turbulence, provided that the relative velocity of the vessel to the wind is not less than one third of the mean wind speed. This assumption is therefore valid for a vessel speed of half the mean wind speed, except at very low heights when sailing downwind where the relative wind speed becomes very small (Ref. 14). It does change the apparent frequency of the turbulence however. Using the analysis of Ref. 13, it can be seen in Fig. 8 that for sailing upwind ($\beta_T = 0°$) the apparent frequency is increased and vice versa for downwind ($\beta_T = 180°$) compared with the stationary yacht case.

These atmospheric wind spectra illustrate that most of the turbulence is at relatively low frequencies, in the region of 0.01 Hz or 1 cycle in about 2 minutes. For a Laser yacht, which reacts quickly to "gusts" this is a very low frequency. The helmsman continually alters the orientation of the Laser to generally keep the heel angle roughly constant, and he would see a gust at this low frequency as simply a variation in the mean wind speed. A cut-off frequency between high frequency turbulence likely to be important in sail aerodynamics, and low frequency turbulence can be deduced if, for example, it is assumed that gusts with wavelengths greater than say 10 boat lengths are simply changes in the same wind speed. For a yacht length of say 4m, this is $\lambda = 40$m, and for an apparent wind speed of say 5m/s, a gust of this wavelength would take 8 seconds to pass the boat. Changes in the boat's heading will filter out changes in wind direction, whereas low frequency changes in speed are not really filtered out, just assumed to manifest themselves as changes in mean wind speed. Furthermore, rather surprisingly, it was found in Ref. 8 that the wake behaviour behind bluff models in turbulent flows could be reproduced by introducing a wire upstream of the model on the stagnation streamline. From this it would also appear that fine-scale turbulence is also the key in controlling wake behaviour.

Based on the aforementioned arguments, we shall then deduce the relevant part of the turbulence spectrum as far as the yacht is concerned, on the premise that the high frequency part is the most important. If we suppose that the yacht acts like a first-order high-pass filter, with a half-power point at n_c, then the effect on the wind spectrum is as

illustrated for the stationary yacht case in Fig. 9. Here it has been assumed that $n_c = 1/8 = 0.125$ Hz, but this was a somewhat arbitrary selection.

This means that much of the turbulence in the normal atmospheric wind spectrum can be omitted, as frequencies less than about 0.03 Hz are not that important, leaving only the high frequency part. This is an enormous help, because it is the large low frequency eddies which are most difficult to generate in wind tunnel simulations, usually requiring rather lengthy test sections. We need only generate some suitable fine scale turbulence, and this can be done using bars and grids in a relatively short test section.

It can be shown by integration of the filtered spectrum in Fig. 9 that the contribution to the turbulence variance is reduced to about

$$\sigma_{uf}^2 = 0.16\,\sigma_u^2, \tag{10a}$$

so,

$$\sigma_{uf} = 0.4\,\sigma_u \tag{10b}$$

It turns out that the turbulence variance is not affected by apparent wind direction (unless the relative wind speed becomes too small, as mentioned earlier), but the apparent turbulence intensity $T_{uf} = \sigma_{uf}/V_A$ *is* affected by translation of the yacht because this changes the apparent wind speed in the denominator.

If it is assumed that the apparent velocity profile can be described by a log-law with suitable choice of apparent roughness length, i.e.

$$\frac{V_A}{u_*} = \frac{1}{k} \ln \frac{Z}{Z_A}, \tag{11}$$

(where k is von Karman's constant = 0.4).

and further, if it is assumed that

$$\sigma_u = 2.5\,u_* \tag{12}$$

as observed by measurement (Ref. 15), then the apparent turbulence intensity for a yacht, as a function of height, is given by

$$Tu_{Z,\,A} = \frac{0.4}{\ln \frac{Z}{Z_A}} \tag{13}$$

Turbulence intensity profiles for upwind, downwind and yacht stationary conditions are plotted in Fig. 10. For the upwind case, it can be seen that the idealised turbulence intensity should be about 3%.

3. TURBULENCE GRID DESIGN

The normal procedure at the University of Auckland for creating a sheared, turbulent onset flow for yacht studies is to generate it with a grid of appropriately spaced circular bars spanning the test section upstream of the model. A computer program from Ref. 16 using methods based on theories by Cowdrey, and Owen and Zienkiewicz was used for this purpose. A listing is given in Appendix 1, along with input and output from the present run.

The program requires the user to input a power index n to describe the velocity profile shape, i.e.

$$\frac{u}{u_{ref}} = \left(\frac{Z}{Z_{ref}}\right)^{1/n} \tag{14}$$

the test section height in inches, h, a value for the pressure drop coefficient k0, the bar diameter in inches, and an error tolerance.

In the present design 5/8" diameter aluminium alloy tubes were used as they were readily available. By curve fitting a power-law profile to the ideal log-law profile in the sail region (Fig. 11) a value n=12 was selected. For the 7'x5' test section, h=60, and by trial and error it was found that k0=0.25 and tol=0.002 gave 16 bars which appeared to offer reasonable blockage. A schematic drawing of the grid is shown in Fig. 12.

It needs to be noted at this point that the grid design method does not consider turbulence, and the selection of the pressure drop coefficient, and tube diameter has to be done on the basis of experience in order to attempt to get the correct turbulence levels.

4. THE FLOW SIMULATION

4.1 Data Acquisition and Analysis

The flow simulation was measured by attaching a hot-wire and pitot-static probe to a traversing rig borrowed from Wolfson MTIA as shown in Fig. 13. The pitot-static probe was connected to a Betz manometer and pressures recorded manually, whereas the hot-wire output was connected to an analogue to digital input channel on a CED 1401, an Intelligent Interface, manufactured by Cambridge Electronic Design Ltd., Science Park, Milton Road, Cambridge CB4 4FE. The voltage output from a potentiometer on the traverse, attached to the screw thread, and giving a signal proportional to height above the floor was also connected to a CED A/D analogue input channel. The CED was driven by a program called TURBOAD written by Wolfson MTIA staff.

After appropriate calibration, text-files of heights and corresponding means and standard deviations of the hot-wire voltages were created. Each data point corresponded to measurements at 100 Hz for 20 seconds. This process allowed velocity and turbulence intensity profiles for the smooth flow (grid out) and turbulent flow (grid in) cases to be obtained at the model test position near the downstream end of the test section (see Fig. 13). The manually tabulated pitot-static probe readings confirmed the accuracy of the hot-wire for the mean velocity measurements.

In addition, at heights above the floor of 200, 400 and 800mm, 16384 samples were saved in separate files to enable the power spectral densities to be evaluated. These data were obtained at a sampling frequency of 2000 Hz with a low pass filter setting of 1000 Hz

4.2 Velocity and Turbulence Profiles

In Section 2.1, it was argued that Z_A for the upwind sailing case should be about $2x10^{-6}$m. At 1/6th-scale in the wind tunnel, this gives

$$Z_{Am} \simeq 3x10^{-7}m.$$

The vertical profile measurements were taken when the reference pitot-static probe (mounted upstream of the turbulence grid about 200mm from the wall, 1m above the floor, on the left hand side looking upstream) measured a pressure difference of 3mm of water. At the test position reference height of 40% of mast height, taken as 400mm above the floor, this gave a velocity of about 7m/s. This can be seen in Fig. 15 which shows the 2 sets of smooth flow results, and one set of turbulent flow measurements. A curve corresponding to the ideal case is also shown (Z_{Am} = $3x10^{-7}$m) which has been matched to the measured turbulent profile at 400mm height. The agreement is good for the height range 200 - 900mm, but is poor at lower heights. The same results are shown in Fig. 16 with power-law axes, and in Fig. 17 with log-law axes.

Since they both have log height axes, Figs. 16 and 17 expand the graphs at lower heights, exaggerating the differences between ideal and measured. Clearly the measured profiles are not as good as they might be, although in Fig. 17, extrapolating the velocity profile curve downwards from readings about Z = 200mm would give an estimate for Z_{Am} close to that actually desired.

It is clear that the velocity profiles are all too low at low levels. There is even quite a boundary layer for the smooth flow case as well. The reason for the discrepancy in the turbulent flow case probably lies partly with the grid design program which assumes uniform onset flow to the grid. The distance from the grid to model was 3.5m, which also gives the boundary layer plenty of fetch to thicken. A step in the floor height of around 100mm at the front of the moving belt ground plane could have also produced a separation bubble, thus thickening the boundary layer as well. The suction system to bleed off this boundary layer was not used in the present tests.

The measured turbulence intensity profiles are compared with the ideal upwind profile in Fig. 18. This figure shows the good flow quality of the test section in the smooth flow case away from the floor, where the turbulence intensity is typically about 0.2%. As for the velocity profile, the idealised and measured turbulent profiles agree quite well at heights above about 200mm, but at lower heights the actual flow is far too turbulent. This applies to the grid out results too, for heights below about 100mm.

These results indicate that the grid tube density was too high near the ground, and that the model was placed too far downstream in the test-section. Unfortunately, it was not possible within the test programme to right these two problems. There was no time available to re-test with a different turbulence grid, and the model had to be located at the downstream end of the test section because the moving belt ground plane was installed in the test section floor and was not able to be removed for these two tests. Thus measurements of forces and moments on the Laser model were taken with the onset flow as it is shown here.

4.3 Wind Spectra

The turbulence grid design method does not consider turbulence at all, just the velocity profiles. Spectra at heights of 200, 400 and 800mm above the floor were therefore measured at the model test location to see if they had any resemblance at all to the desired shapes developed in Section 2.2.

16384 samples were obtained at 2000 Hz at each height, and these were then analysed as 8 blocks of 2048 samples. A fast Fourier transform was run on each of the 8

blocks. The 8 spectral estimates at each frequency were then averaged to reduce the standard error. In addition, the samples were averaged over frequency as well, over 13 equal log-frequency bands, to finally give 13 spectral estimates. Since there are more samples in each band at higher frequencies, the statistical reliability of the estimates improves as frequency increases. These spectra had a bandwidth from f_1 = 2000/2048 = 0.977 Hz to f_2 = 2000/2 = 1000 Hz.

In order to improve the statistical reliability of the results at frequencies around 1 Hz, it was decided to digitally filter the raw samples by simply adding each eight consecutive samples up to obtain new samples approximately equivalent to sampling at 1000/8 - 125 Hz, resulting in one block of 2048 samples for each height. Spectral estimates were therefore also obtained for these lower frequency samples over the bandwidth f_3 = 125/2048 = 0.06104 Hz to f_4 = 125/2 = 62.5 Hz. Block averaging obviously could not be carried out, but frequency averaging over 13 equally spaced log-frequency bands was carried out as before.

The resulting smoothed spectra can be seen in Fig. 19. Pairs of full and dotted lines correspond to the measured spectra. There is reasonable agreement where each set overlaps, which confirms that the averaging process used to obtain the larger bandwidth overlapped spectra behaved properly. Spectra at 800mm height were very similar to the 400mm curves, so are not shown to improve readability. It can be seen that the peak of the 200mm height spectrum is at around 6 Hz, and the peak of the 400mm spectrum is at around 20 Hz, some 3 times higher. However, the idealised spectrum has a peak at around 1-3 Hz which is much lower. This curve is the same one as the dotted curve in Fig. 9 except that it has been normalised so that the area under it is unity, and it has been shifted on the frequency axis to preserve the correct reduced frequency, i.e.

$$\left(\frac{nL}{V}\right)_{model} = \left(\frac{nL}{V}\right)_{full\text{-}scale}$$

$$n_m = n_{fs}\left(\frac{V_m}{V_{fs}}\right)\left(\frac{L_{fs}}{L_m}\right)$$

Thus, $n_m \simeq n_{fs}\,(1)\,(6)$

$$n_m \simeq 6n_{fs}$$

It is clear that the bar grid generates turbulence at too high a frequency by a factor of about 8. The vortex shedding frequency of the bar can be found from the Strouhal number, giving

$$n_s = 0.2\,\frac{V}{D}$$

For V = 7m/s and D = 5/8" = 15.87mm

$$n_s = 0.2 \times 7/0.016$$

$$= 88 \text{ Hz.}$$

It is interesting, and perhaps rather surprising that there is no evidence of the bar

vortex shedding frequency in the spectra. This is probably because the measurements were taken some 220 bar diameters downstream of the turbulence grid.

To summarise, it can be seen that the turbulence simulation is not particularly good as far as its spectral content is concerned, and that larger bars, or possibly some other method is required to generate turbulence spectra which resemble the desired shapes more exactly. However, the variance of the turbulence is only slightly less than that desired ideally.

5. MODEL AND SAIL DETAILS

The model used in this, and the earlier study (Ref. 2) at the University of Auckland was a simplified 1/6th scale model of a Laser sailing dinghy. A rigid mast made of a uniform 11mm OD steel tube was used rather than a scaled down version of the flexible prototype. The mainsail was attached with a bolt-rope to a thin slot cut in the mast. It was cantilevered in two deep-groove roller bearings located inside the hull, and was thus able to rotate freely. The model mast height was 1m (measured from heel axis near the hull bottom to the top of the tested sail).

Sail trim was adjusted using electric winches located inside the hull which controlled mainsheet and boom vang tension. During testing it was found that the boom vang winch was not powerful enough, and it was difficult at times to get enough leach tension. The mainsheet winch worked well. The mainsail foot was attached to the boom by an outhaul at the clew only. No gap between the sail and boom resulted from this means of attachment.

The test rig was attached to the balance as shown in Fig. 20 by an arrangement which allowed vertical height adjustment, and rotation about the heel axis fitting near the bottom of the hull. The hull could be separated to give access to the winches and heeling mechanism. During testing the model was located in a circular cutout in the test section floor. A cardboard surround was taped over most of this, leaving a vertical gap of less than 5mm between the hull and surround. When the hull was heeled to 20 and 30°, it was raised on the 4 threaded studs as required so that there was no contact between it and the test-section floor. This vertical height shift was measured so that the actual distance between the balance horizontal axis and the reference axis (taken as the heel axis near the hull bottom) could be used in subsequent moment calculations.

The mainsail was constructed from the lightest grade of Mylar sail cloth obtainable at the time. Initially the Sailmaker (TM) sail mould development program was set up to plot the required panels on sail cloth, however, as the seam shape was so small, the plotted panels were not of sufficient accuracy. Thus based on the advice of a local NZ sailmaker, a more old fashioned method was adopted, as described below.

The approximate outline of the complete mainsail was marked out on a single sheet of sailcloth. Using cross-cut panels, the seam shape (curve) and taper were marked out at various luff heights. Seam shape was drawn using a flexible metal strip that formed the required curve across the chord. Keeping the curvature of the strip constant, the same form of seam curve could be drawn at various luff heights. By increasing the curvature, the camber (draught) could be increased, and by moving the location fore and aft, its chord-wise location could be shifted.

Individual panels were cut and joined. The curved panel edge was placed onto the straight panel edge of the adjacent panel which had double-sided tape attached. After the panels were joined, the correct luff curve for the mast was drawn on the developed mainsail. Finally, the leech curve was drawn to form the final planform of the mainsail.

The sail used in the present tests had a 913mm luff, a 360mm foot, a luff/foot ratio of 2.5 and a maximum camber of about 13% at 50% of the chord at a height of

about 33% up the luff. A reference area of 0.1642 m^2 was used for the tests. For moment coefficients a reference length of 1m was used, the distance between the heel axis fitting and the sail head.

6. BALANCE DETAILS

There was some difficulty in obtaining a suitable balance for the sail tests at the University of Southampton, as the low test speed required of around 7 m/s meant that the loads were much smaller than normally obtained in common wind tunnel tests there. Dynamometers used for keel tank tests were available, but could measure lift and drag only, whereas it was desired to measure heeling moment as well. In the end a compromise solution was reached whereby a 5-component (vertical force not measured) dynamometer developed especially for wind tunnel tests of rudders (Ref. 17) was used. It is a very strong and stiff dynamometer (hereafter referred to as balance), and is capable of measuring loads of about 100lbs. The rudder and skeg can be mounted and rotated independently on it. The overall balance can be seen in Fig. 21, and a cross-section showing the roll centres in Fig. 22.

The model yacht was mounted where the rudder is shown in Fig. 22, and the lower handwheel was used to alter the direction of the model (to obtain the desired test apparent wind angles) so that the yacht and balance axes were always parallel. In other words body, not wind axes were used. The top handwheel was used once only to centre the top balance plate for the tests.

The balance was extensively calibrated around 1977, and has not been recalibrated since. A check calibration was carried out to verify the repeatability and linearity of the balance for the rather small anticipated loads, and this was found to be good for lift, drag, and heeling moment, but the pitching moment output was clearly erroneous. This didn't matter, as measurements of pitching moment were regarded as of secondary importance.

The balance was repeatable to about $\pm 0.3\mu V$, and signals during testing of about $20\mu V$ were expected, giving an accuracy of about $\pm 2\%$.

7. DATA PROCESSING

7.1 Data Acquisition

The balance strain gauges were connected directly to a strain gauge amplifier and power supply (Manufactured by Fylde) by purpose built cables and plugs. This was connected to a very accurate Schlumberger voltmeter (Model No. 7061) which used a special patented averaging method to give average voltages from each channel to $0.1\mu V$. This unit was controlled from software written by Stephen Turnock, a Research Fellow in the Department of Ship Science. This software scanned through each of the 5 data channels or the supply voltage channels the number of times specified (usually 10) and recorded the resulting voltages, averaged over the (say) 10 consecutive scans to 7 decimal places in an ASCII text file. In addition, information concerning the test was added as needed, such as heel angle, wind on or off, turbulence grid in or out etc.

A separate file was obtained for each test, (eg for a particular apparent wind angle), where each file simply contained the unprocessed voltages and experiment information as described above. This hard copy allowed "by hand" verification to be made of the software used to analyse the test data files.

7.2 Preliminary Data Reduction

The data acquisition program had been adapted from a version used for rudder tests, and as such, it actually recorded some additional extranious information which was

not required in the present work. A program called EXTRACT was developed by the writer to extract only the pertinent mean results for the present tests, and the experiment information, and to write them to a file. The data were then scaled for variation in the supply voltages V_s, and zero offset voltages V_o in all channels, assuming a linear variation in these values with scan number between measurements of them. Thus the recorded bridge voltage V_T was scaled to give a voltage V proportional to the applied force at the original calibrated voltage V_c:

$$V = (V_T - V_o) \times V_c/V_s$$

The original calibration of the balance in Ref. 16 quantified the interaction between the five components of the balance. The matrix expression given below uses the interaction matrix and incorporates the calibration constants to give the sideforce, thrust, yaw, roll and pitch (F_1 through F_5 respectively) in N and Nm.

$$\begin{bmatrix} F_1 \\ F_2 \\ F_3 \\ F_4 \\ F_5 \end{bmatrix} = \begin{bmatrix} 0.338035 & -1.1881\times10^{-03} & -3.952\times10^{-04} & -1.4848\times10^{-03} & -3.2605\times10^{-03} \\ 2.12\times10^{-05} & 0.252512 & -6.659\times10^{-04} & 1.6823\times10^{-03} & -9.901\times10^{-04} \\ -1.82\times10^{-04} & 2.845\times10^{-04} & 3.9366\times10^{-02} & 1.344\times10^{-04} & 3.2\times10^{-04} \\ 7.002\times10^{-04} & -2.37\times10^{-05} & -3.4036\times10^{-03} & 6.34925\times10^{-02} & 2.049\times10^{-04} \\ -3.3\times10^{-06} & 6.333\times10^{-04} & 1.47\times10^{-05} & -3.008\times10^{-04} & 4.8468\times10^{-02} \end{bmatrix} \begin{bmatrix} V_1 \\ V_2 \\ V_3 \\ V_4 \\ V_5 \end{bmatrix}$$

where V_1 - V_5 are the corrected balance voltages in μV.

However, there was one "fiddle" done in the application of the interaction matrix. As noted previously, the pitching moment voltage V_5 was incorrect, and it was felt that this incorrect voltage would generate errors in the other channels through the interaction matrix. To eliminate the source of error, an estimate of what V_5 should have been was made, based on the thrust voltage V_2 by assuming that the pitching moment was due entirely to the thrust force acting at 40% of the mast height.

$$V_5 = 0.2525 \times V_2 \times h/4.84685 \times 10^{-2}$$

where h is the vertical height above the balance axis of a point 400mm along the mast. V_5 was estimated as shown before the balance matrix was applied to each set of corrected balance voltages.

The next manipulation to the data was to move the moment centre from the balance to the reference centre in the boat. This was defined to be the point corresponding to the intersection of the mast and the heel axis. This point was 0.085m in front of the vertical axis of the balance, and 0.122+h above the balance axis, where h is a variable distance which depended on heel, and was measured at each test. Moments based on the yacht reference centre were calculated as follows from the forces and moments (F_1 - F_5) resulting from application of the interaction matrix.

$$M_3 = F_3 + 0.085 \times F_1 \text{ (yaw)}$$
$$M_4 = F_4 - F_1 \times (0.122 + h) \text{ (roll)}$$
$$M_5 = F_5 - F_2 \times (0.122 + h) - F_6 \times 0.085 \text{ (pitch).}$$

F_6 is the estimated vertical force (positive downwards) assuming that the sideforce acts perpendicular to the mast, i.e.

$$F_6 = F_1 \times \tan \phi$$

where ϕ is heel angle.

M_3 and M_5 are of no real interest; indeed pitch was measured incorrectly, but

they were processed in any event for completeness.

The final part of the preliminary data reduction was to convert the measured forces and moments into coefficients. Since all tests were done with the wind tunnel pitot-static probe measuring 3mm of water, this was done with the following set of equations:

$$
\begin{aligned}
C_s &= F_1/3 \times 9.81 \times A \times r \\
C_t &= F_2/3 \times 9.81 \times A \times r \\
C_{ym} &= M_3/3 \times 9.81 \times A \times r \times L \\
C_{rm} &= M_4/3 \times 9.81 \times A \times r \times L \\
C_{pm} &= M_5/3 \times 9.81 \times A \times r \times L \\
C_v &= F_6/3 \times 9.81 \times A \times r
\end{aligned}
$$

where the reference area A = 0.1642 m^2 and the reference length for moments L = 1m. r is the ratio of the dynamic pressure at a point 400m along the mast from the heel axis to the dynamic pressure on the wind tunnel probe. For smooth flow r = 1.03. For turbulent flow r varies with height above the wind tunnel floor, h. Curve fitting the turbulent flow calibration velocity profile in the region h = 400mm gave the following empirical expression for r:

$$r = 0.76239 + 0.0005326 \times h$$

where h here is height above the floor in mm.

The preliminary data reduction process described above resulted in force and moment coefficients based on the boat moment reference centre, where all the force and moment coefficients are in horizontal and vertical directions. These basic coefficients are manipulated in the following sections in order to collapse the data in a meaningful way.

8. MEASURED DATA

The preliminary data reduction process described in the foregoing results in the following coefficients of particular interest = C_t (thrust) and C_s (sideforce) in the horizontal plane, and C_{mh} (heeling moment). These are plotted as a function of heel in Figs. 23, 24 and 25.

The thrust coefficient in Fig. 23 for an apparent wind angle of 30° shows almost no variation with the range of heel angles tested from 0 to 30°. The coefficients for both the smooth and turbulent flow case also for this apparent wind angle show amazingly good agreement, and in all cases are about 0.4, with a slight drop to 0.3 for ϕ = 30°. Clearly the use of the dynamic pressure at 40% mast height works well. For the β_A = 60° results (smooth flow only measured) the coefficients are higher (around 1.0) and show a more significant drop for ϕ = 20 and 30°, which is well fitted by a cosine heel squared function.

The sideforce coefficients results in Fig. 24 do not show such a perfect collapse of the smooth and turbulent results for β_A = 30° as for thrust, but nonetheless, it is still good. The reduction in C_s with heel is fitted well by a cosine heel function. The C_s results for β_A = 60° show no consistent variation with heel. Not surprisingly, because the sail has been let out further, C_s for β_A = 60° is much less (about 2/3) of the β_A = 30° values.

The rolling moment coefficient (or heel coefficient) is due to the sideforce acting part way up the mast (about 40%), and to the vertical force acting out at some distance horizontally from the heel axis. Because it arises mainly from the sideforce, it can be seen that the variation of C_{rm} with ϕ (Fig. 25) is somewhat similar to the variation of C_s with ϕ (Fig. 24) although smaller. Note that Deakin (18) found that C_{rm} reduced

with ϕ according to $\cos^{1.3}\phi$. If it is assumed that the side and vertical force components act in such a way that the net force is perpendicular to the mast, then the height of application of this force can be estimated.

Referring to Fig. 26 we have:

$$C_{rm}\, L = C_S d\cos\phi + C_V d\sin\phi$$

and by assuming that

$$\frac{C_V}{C_S} = \tan\phi$$

it follows that

$$\frac{d}{L} = \frac{C_{rm}}{C_S(\cos\phi + \frac{\sin^2\phi}{\cos\phi})} = \frac{C_{rm}\cos\phi}{C_S}$$

The result of this calculation is shown in Fig. 27 for all test cases. Heel angle clearly has little effect apart from increasing the scatter at 30° heel and, on average, the force acts about 37% of the way along the mast, close to the 40% reported by many workers.

A similar kind of analysis cannot be applied to the thrust results to get its height of application because the balance measurements of pitching moment were in error.

9. SAIL AERODYNAMICS

The foregoing section merely discussed the display of the measured data, the only assumption being in Fig. 26 where it was assumed that the side component of the sail force acted perpendicular to the mast. The results verified that the dynamic pressure at 40% mast height gives a good collapse of the coefficients, and indeed, the results verified that the sideforce does in fact act near that height. However, one would really like to be able to predict the various coefficients at various heel angles and so on, based on a knowledge of the sail aerodynamics. In other words, it would be very convenient to be able to predict the performance of the sail rig at various heel angles from the results of measurements at a single heel angle.

In this section we will suppose that a yacht sail of given shape produces an aerodynamic force which can be described by conventional lift and drag coefficients which are a function of the angle of attack between a reference chord line on the sail, and the component of the wind resolved in a plane which is horizontal in the fore and aft direction, and inclined at the heel angle ϕ in the beam direction. It can be loosely described as the plane of the deck. It is convenient to sub-divide this angle of attack into two further angles, the effective wind angle, β_E which is the angle between the wind component and the centreline of the yacht, and the sail sheeting angle, δ, the angle between the yacht centreline and a reference sail chord line which we will take as the boom direction, measured in the deck plane. These angles are shown in Fig. 28.

In this inclined plane, and for a particular sail shape, we have

$$C_L = C_L(\beta_E - \delta)$$
$$C_D = C_D(\beta_E - \delta)$$

and from Fig. 28 it can be seen that the thrust (horizontal), and sideforce (inclined at ϕ) coefficients are related to the sail coefficients by

$$C_{T\phi} = C_L \sin \beta_E - C_D \cos \beta_E$$
$$C_{s\phi} = C_L \cos \beta_E + C_D \sin \beta_E$$

Resolving these into the horizontal plane gives

$$C_T = C_{T\phi} \text{ is already horizontal)}$$

$$\text{so} \quad C_T = C_L (\beta_E - \delta) \sin \beta_E - C_D (\beta_E - \delta) \cos \beta_E \qquad (1)$$

and since $C_s = C_{s\phi} \cos\phi$, it follows that

$$C_s = [C_L \cos \beta_E + C_D \sin \beta_E] \cos\phi \qquad (2)$$

Equations (1) and (2) enable the sail lift and drag coefficients to be deduced from measurements of C_s and C_T in the horizontal plane by the balance.

$$C_T = C_L (\beta_E - \delta) \sin \beta_E - C_D (\beta_E - \delta) \cos \beta_E \qquad (1)$$

$$C_s/\cos\phi = C_L (\beta_E - \delta) \cos \beta_E + C_D (\beta_E - \delta) \sin \beta E \qquad (2)$$

Re-arranging leads to

$$C_L (\beta_E - \delta) = \frac{C_s}{\cos\phi} \cos \beta_E + C_T \sin \beta_E \qquad (3)$$

$$C_D (\beta_E - \delta) = \frac{C_s}{\cos\phi} \sin \beta_E - C_T \cos \beta_E \qquad (4)$$

Further, by assuming that the heeling moment arises wholly from the elevated action of the sideforce, we get

$$C_{rm} L = C_{s\phi} h = \frac{C_s}{\cos\phi} h$$

where L is the reference length, and h is the height of application of the sideforce. Hence,

$$C_{rm} = \frac{h}{L} \frac{C_s}{\cos\phi} = \frac{h}{L} \left[C_L (\beta_E - \delta) \cos \beta_E + C_D (\beta_E - \delta) \sin \beta_E \right]$$

Finally, if the lift and drag coefficients in the wind tunnel axes are required, the following pair of equations carry out the rotation necessary (see Fig. 29):

$$C_{LW} = C_s \cos \beta_A + C_T \cos \beta_A$$

$$C_{DW} = C_s \sin\beta_A - C_T \cos \beta_A$$

The Effective Wind Angle, β_E

This angle was introduced above. We now consider its geometrical interpretation. We take the case of a yacht at an apparent wind angle β_A, apparent wind speed V_A heeled at an angle ϕ (see Fig. 30). The apparent wind velocity component parallel to the yacht centreline is $V_A\cos\beta_A$, and the component perpendicular to the centreline, and in a plane inclined at the heel angle ϕ is $V_A\sin\beta_A\cos\phi$. These two components form a right-angled triangle in the deck plane, and the effective wind angle, β_E, is given by

$$\tan\beta_E = \frac{V_A \sin\beta_A \cos\phi}{V_A \cos\beta_A}$$

whence $\beta_E = \tan^{-1}(\tan\beta_A \cos\phi)$

For β_A and $\phi < \sim 30°$ this can be approximated to

$$\beta_E = \beta_A \cos\phi$$

When the boom is out to leeward from the yacht centreline an angle δ, then the sail angle of attack is

$$\beta_S = \beta_E - \delta = \tan^{-1}(\tan\beta_A \cos\phi) - \delta$$

We now have a set of equations which enable the sail coefficients to be obtained from the balance measurements and presented as functions of $\beta_S = \beta_E - \delta$. If for a given sail shape the sail coefficients can be described by $C_L(\beta_S)$ and $C_D(\beta_S)$, then universal curves corresponding to these functions should be able to be obtained from wind tunnel measurements at various values of β_A, ϕ and δ. If a good collapse can be obtained, then this means that such results can be used in a predictive manner.

10. RESULTS AND DISCUSSION

As mentioned previously, the sail test programme involved two apparent wind angles β_A = 30 and 60°, 4 heel angles - 0, 10, 20 and 30°, and tests in both smooth and sheared turbulent flow. For each test case corresponding to a particular flow type and apparent wind angle the sail was set by adjusting the mainsheet and boom vang to get maximum thrust at nominally zero heel. The sail controls were not altered as the heel was changed, and the luff and foot tensions were not altered at all t hroughout the test programme. It was also found that in all cases the boom vang tension needed to be as tight as possible - the winch was driven until it stalled. In the β_A = 30° tests the boom was pulled in over the deck and the vertical component of the sheet tension tended to keep the sail leech tighter than for the β_A = 60° test cases where it had less effect and the leech twisted away more noticeably.

The model design used a rotating straight mast cantilevered from within the hull which was perpendicular to the heel axes. This means that, in theory, for a constant boom vang tension, altering the sheet tension (changing δ) should not alter the sail shape significantly - it should simply rotate with the mast. This was not quite the case in the present test arrangement because of the reduction in the vertical component of the sheet tension as δ increased, but nonetheless, it was decided to compare the β_A = 30 and 60° results as if they resulted from the same sail shape.

The sail lift and drag coefficients were calculated for all test cases and are shown plotted in Fig. 31. When β_A = 30°, the angle δ from the centreline to the boom was 5°, and when β_A = 60° it increased to 35°. Thus it can be seen that all results lie in the

relatively small sail angle range 20 to 25°. The lift coefficient is about 1.5 and the drag coefficient about 0.5. The smooth and turbulent flow results are in relatively good agreement which is somewhat surprising given the substantial differences between the flows. The β_A = 60° results show lower lift and higher drag coefficients.

The comparison between the two apparent wind angle results is not entirely fair because of the increased sail twist at β_A = 60° noted already. Some allowance for this can be made by simply setting δ to some larger effective angle. The effect of setting δ = 40° is illustrated in Fig. 32. This figure shows C_L reducing in a somewhat linear fashion towards 0 as β_E-δ is decreased, and the trend of C_D is now to increase at the same time.

It is clear now that the tests have been completed that it would have been useful to have had data for a range of smaller values of β_E-δ as well. To discover whether there are universal functions $C_L(\beta_S)$ and $C_D(\beta_S)$ for a particular sail shape for various values of ϕ, β_A and δ requires that the sail shape be maintained in all cases. For a Laser with a cantilevered mast this should be able to be achieved by keeping the boom vang tension constant. However, although such tests are interesting aerodynamically they are not particularly relevant to sailing where the sails are always adjusted for a given apparent wind angle to maximise thrust, providing the heeling moment is not too large. In fact, one can argue that the sails should be adjusted to maximise the ratio thrust/sideforce, corresponding to the low windspeed sailing condition, and to maximise thrust for a given sideforce (or heeling moment) in the case of the high windspeed sailing condition.

Nonetheless, the present results have illustrated that for β_A = 30° the sail coefficients, as defined herein, are virtually identical for the smooth and turbulent cases, and the β_A = 60° results show lower lift and higher drag, as could be expected from the somewhat more twisted shape in this test case.

11. CONCLUSIONS

The ideas of wind engineering and mechanics can be used to develop models of onset flow to sailing yachts. Such models show that it is more legitimate to wind-tunnel test yachts sailing upwind than downwind because in the former case wind twist is smaller and the velocity profile is more uniform than in the latter case.

An analysis of wind turbulence has shown that only the high frequency end of the atmospheric wind spectrum is important as far as yacht sail aerodynamics is concerned, and thus only this part needs to be modelled in wind-tunnel simulations.

A grid of horizontal bars can be used to generate velocity and turbulence intensity profiles which simulate these parameters quite well, but the spectrum of turbulence generated this way shows that the turbulence length scale is really too low, and in the present case the turbulence spectrum was energetic at frequencies which were too high by a factor of about eight.

The simplified yacht model was adequate for the test programme apart from the boom vang winch which was under-powered so that it proved difficult to get sufficient leach tension. The high capacity, stiff dynamometer (balance) used in the tests had acceptable accuracy for thrust, sideforce, and heeling moment, but it would have been interesting to have had measurements of pitching moment and vertical force as well.

The 30 deg apparent results showed essentially constant thrust and effective-height-of-sideforce with change in heel angle, but the sideforce reduced according to cos(heel) and the associated rolling moment coefficient showed little change with heel. This was the same for both the turbulent and smooth results.

The 60 deg apparent results were somewhat different. The sideforce, and rolling moment coefficient were all essentially invariant with change in heel angle, but the

effective-height-of-sideforce showed a small reduction with heel and the thrust coefficient showed a reduction proportional to $\cos^2$ heel).

When the measured forces and moments were converted to lift and drag coefficients based on a wind axis system in a plane perpendicular to the mast, the collapse of the data was quite spectacular. The angle between the apparent wind direction and the boom was about 23 deg in all test cases, and gave a mean lift coefficient of about 1.5, and a mean drag coefficient of about 0.5. By making some allowance for sail twist, and increasing $\beta_E - \delta$ by 5 deg for the 60 deg apparent results, C_L showed a reduction as $\beta_E - \delta$ reduced. It was also clear that the 60 deg results had a higher drag coefficient than the 30 deg results, probably resulting from the more twisted sail shape in the former case. It would thus appear that this method of collapsing wind-tunnel data is a worthy candidate for further study.

12. REFERENCES

1. Jackson, P.S. The science of sail design. Proc. of a Conf. held at the Boundary Layer Wind Tunnel Laboratory, University of Western Ontario, London, Ontario, Canada, June 21-22 1982.

2. Shaw, D.A. Yacht mainsail aerodynamics. M.E. Thesis, Mechanical Engineering Dept, University of Auckland, Private Bag 92019, Auckland, New Zealand, 1991.

3. Cook, N.J. The designer's guide to wind loading of building structures. Part 1, Butterworths, 1985.

4. Wellicome, J.F. Private communication. Dept. of Ship Science, University of Southampton.

5. Aerodynamics Committee of the American Society of Civil Engineers, Manual of practice for wind-tunnel testing of buildings and structures. January 1986.

6. Engineering Sciences Data Unit, Characteristics of the atmospheric environment near the ground. Part 2, single point data for strong winds (neutral atmosphere), ESDU 85020, ESDU International plc, London, UK, 1985.

7. Mueller, T.J., Pohlen, L.J., Congigliano, P.E., Jansen, B.J. The influence of freestream disturbances on low Reynolds number airfoil experiments. Experiments in fluids, 1, 3-14, 1983.

8. Gartshore, I.S. The effects of freestream turbulence on the drag of rectangular two-dimensional prisms, University of Western Ontario, Canada, BLWT-4-73, 1973.

9. Waudly-Smith, P.M. and Rainbird, W.J. Some principles of automotive aerodynamic testing in wind tunnels with examples from slotted wall test section facilities, Paper 850284, SAE Intl. Congr. and Exp., Detroit, Michigan, USA, February-March 1985.

10. Cooper, K.R. The wind tunnel simulation of wind turbulence for surface vehicle testing. J.W.E. and IA, 38, 71-81, 1991.

11. Millikan, C.B., Klein, A.L. The effect of turbulence: an investigation of the maximum lift coefficient and turbulence in wind tunnels and in flight. Aircraft Engineering, August, pp169-174, August 1933.

12. Flay, R.G.J. and Jackson, P.S. Flow simulation for wind-tunnel studies of sail aerodynamics. Eighth International Conf. on Wind Engineering, London, Ontario,

Canada, July 1991.

13. Cooper, R.K. Atmospheric turbulence with respect to moving ground vehicles. Aerodynamics of Transportation - II. The winter annual meeting ASME, Boston, Mass., pp53-63, 13-18 November 1983.

14. Teunissen, H.W. Characteristics of the mean wind and turbulence in the planetary boundary layer, UTIAS Review 32, Institute for Aerospace Studies, University of Toronto, Toronto, Canada, 1970.

15. Flay, R.G.J. Structure of a rural atmospheric boundary layer near the ground. Mechanical Engineering Department, University of Canterbury, New Zealand, Ph.D. Thesis, 1978.

16. Raine, J.K. Modelling the natural wind: Wind protection by fences. Vol. II, Ph.D. Thesis, University of Canterbury, NZ, October 1974.

17. Molland, A.F. The design, construction and calibration of a five component strain gauge wind tunnel dynamometer. SSSU 1/77, ISSN 0140-3818.

18. Deakin, B. The development of stability standards for UK sailing vessels. RINA Meeting, 23rd April 1990, London

Fig. 1: Full-scale Laser yacht.

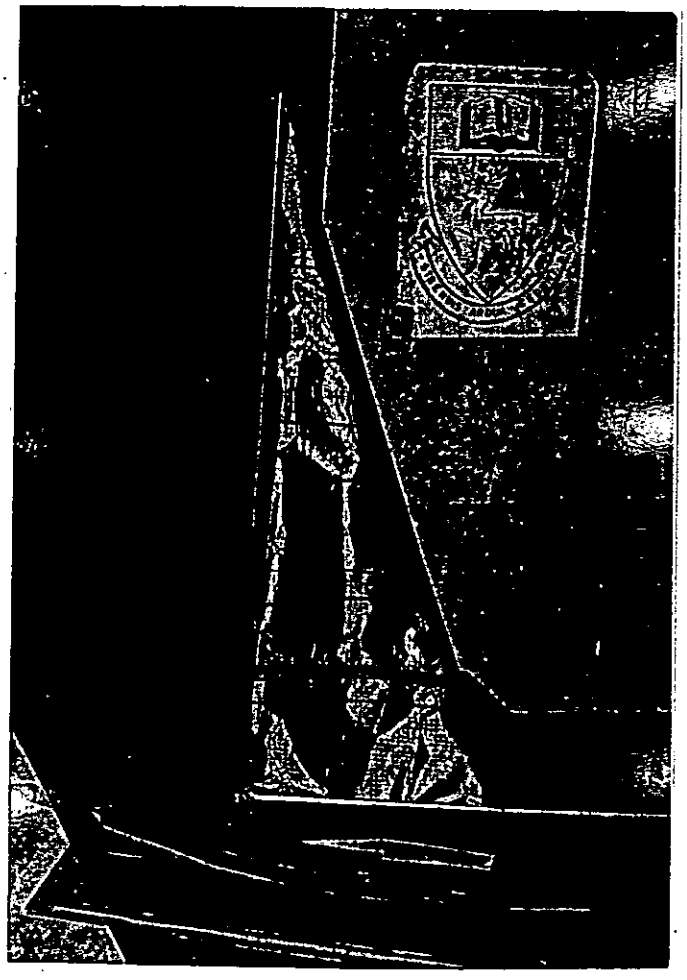

Fig. 2: Model Laser.

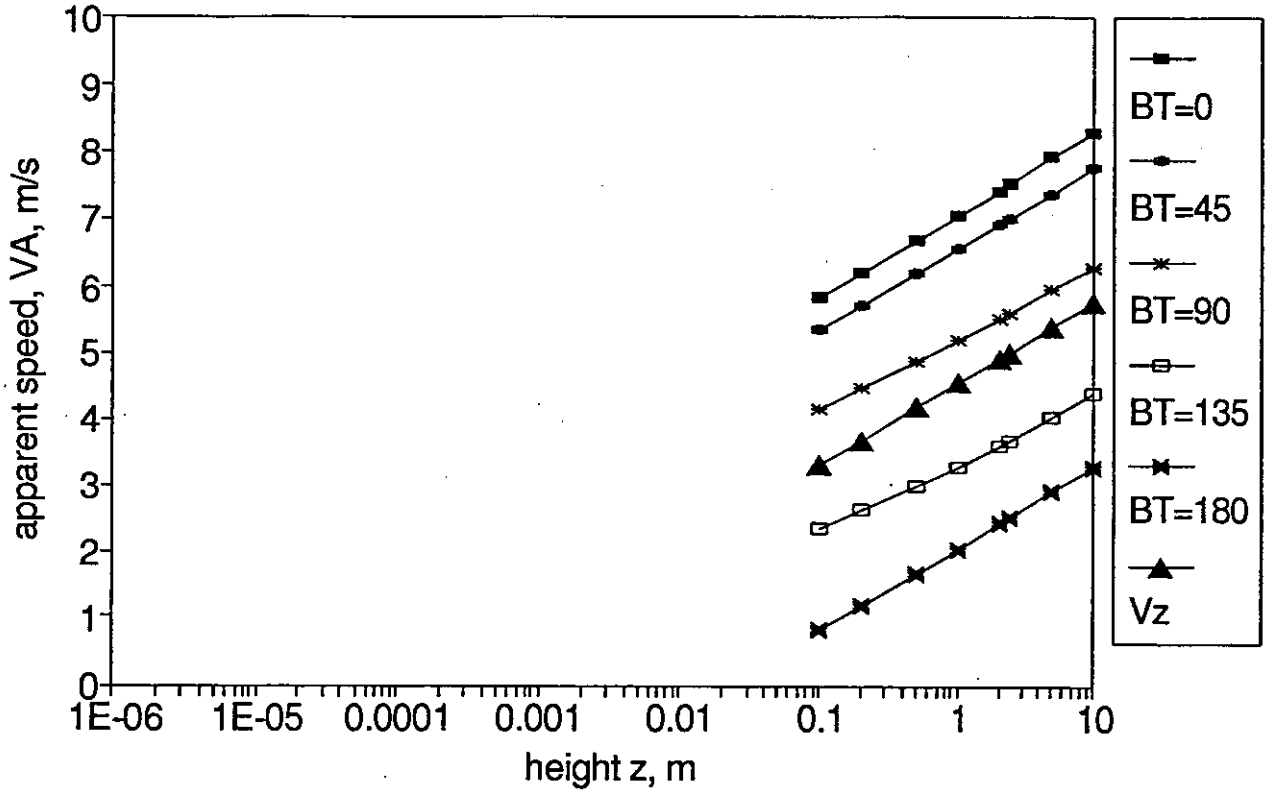

Fig. 3: Apparent speed profiles on semi-log axes.

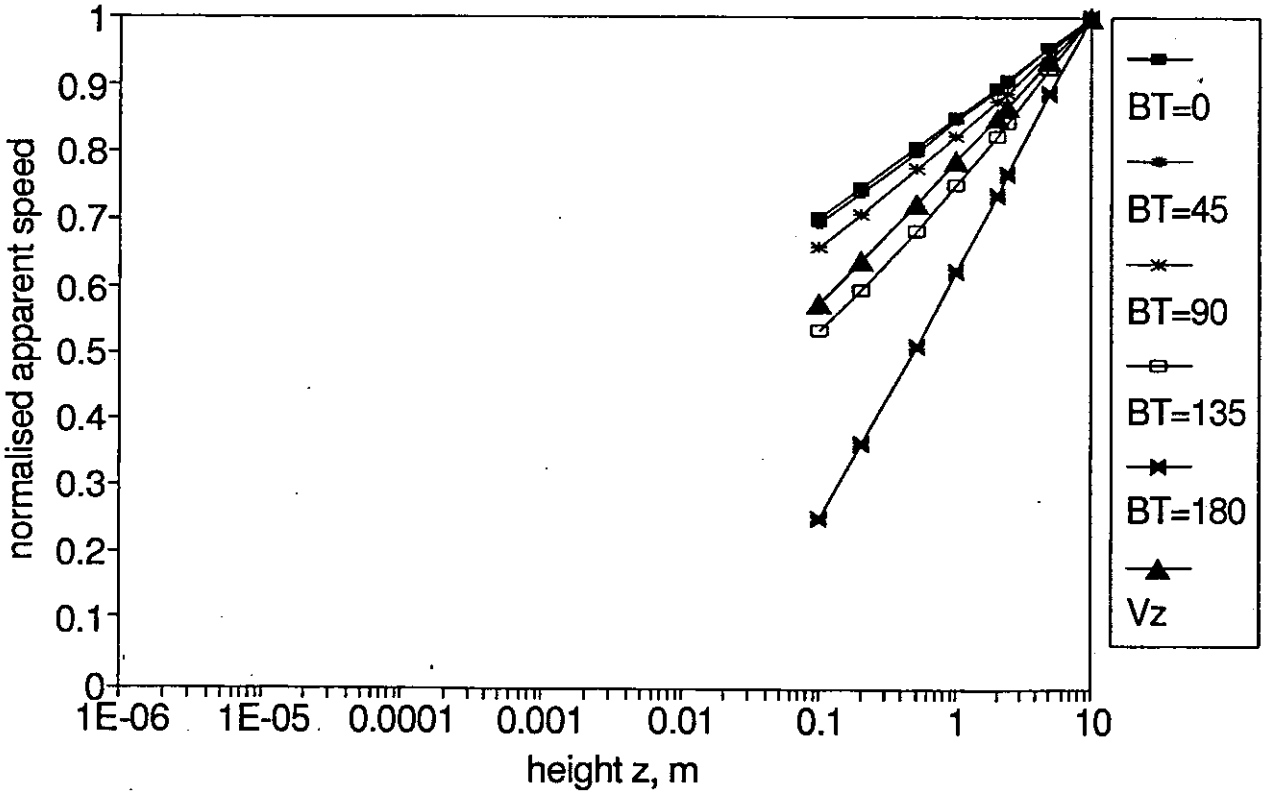

Fig. 4: Normalised apparent speed profiles on semi-log axes.

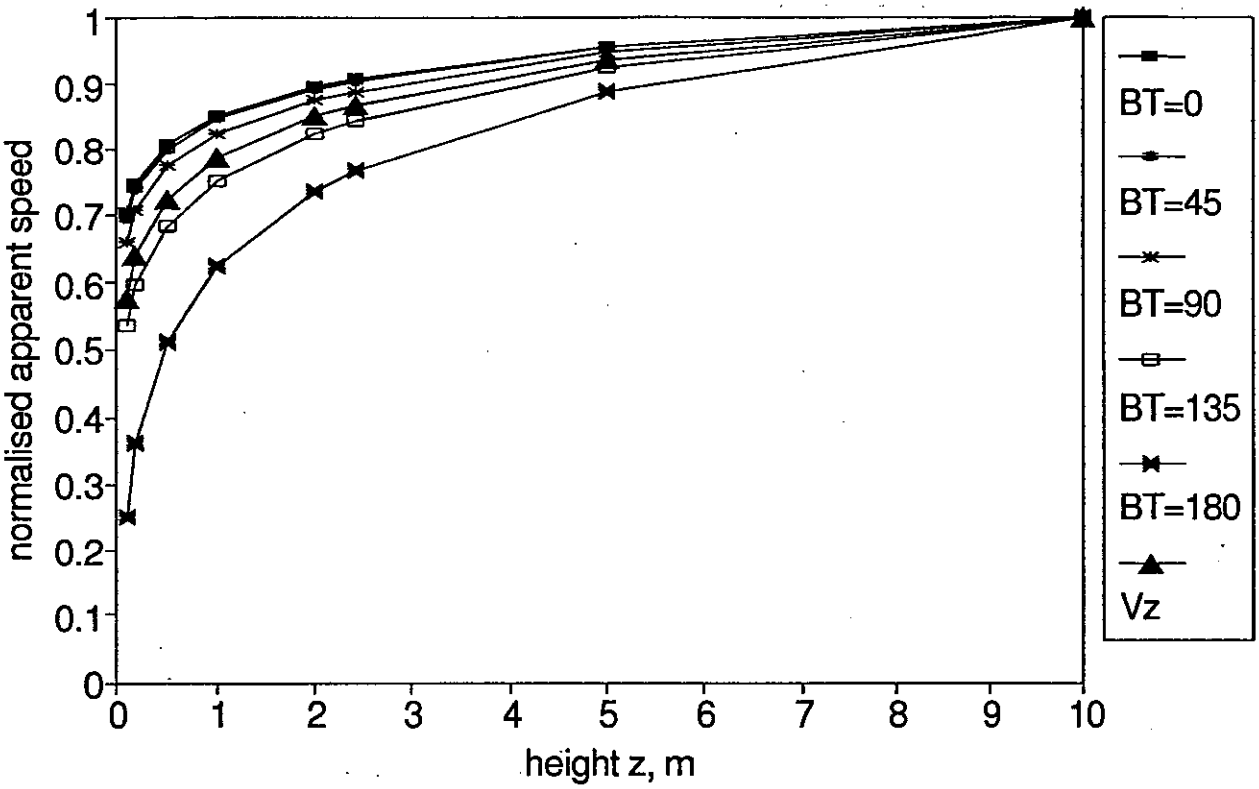

Fig. 5: Normalised apparent speed profiles on linear axes.

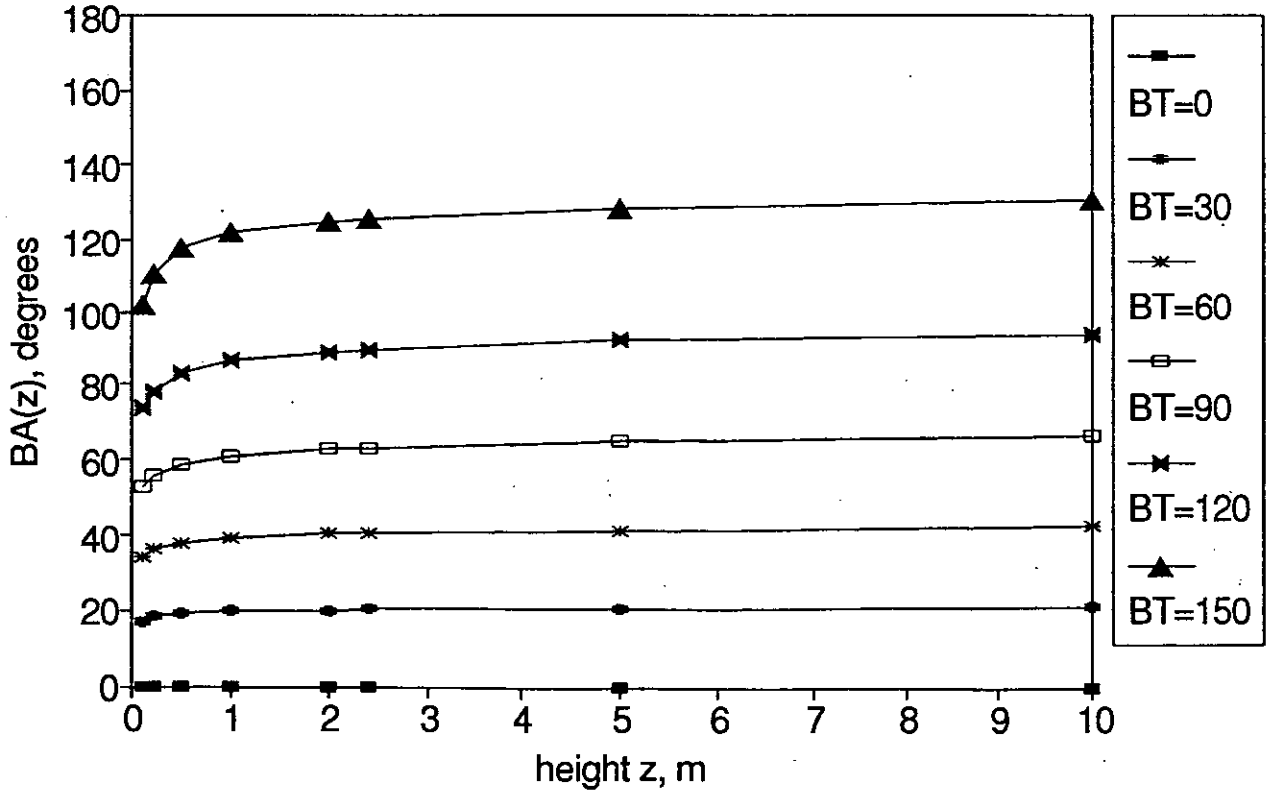

Fig. 6: Variation in apparent wind angle with height and true wind angle.

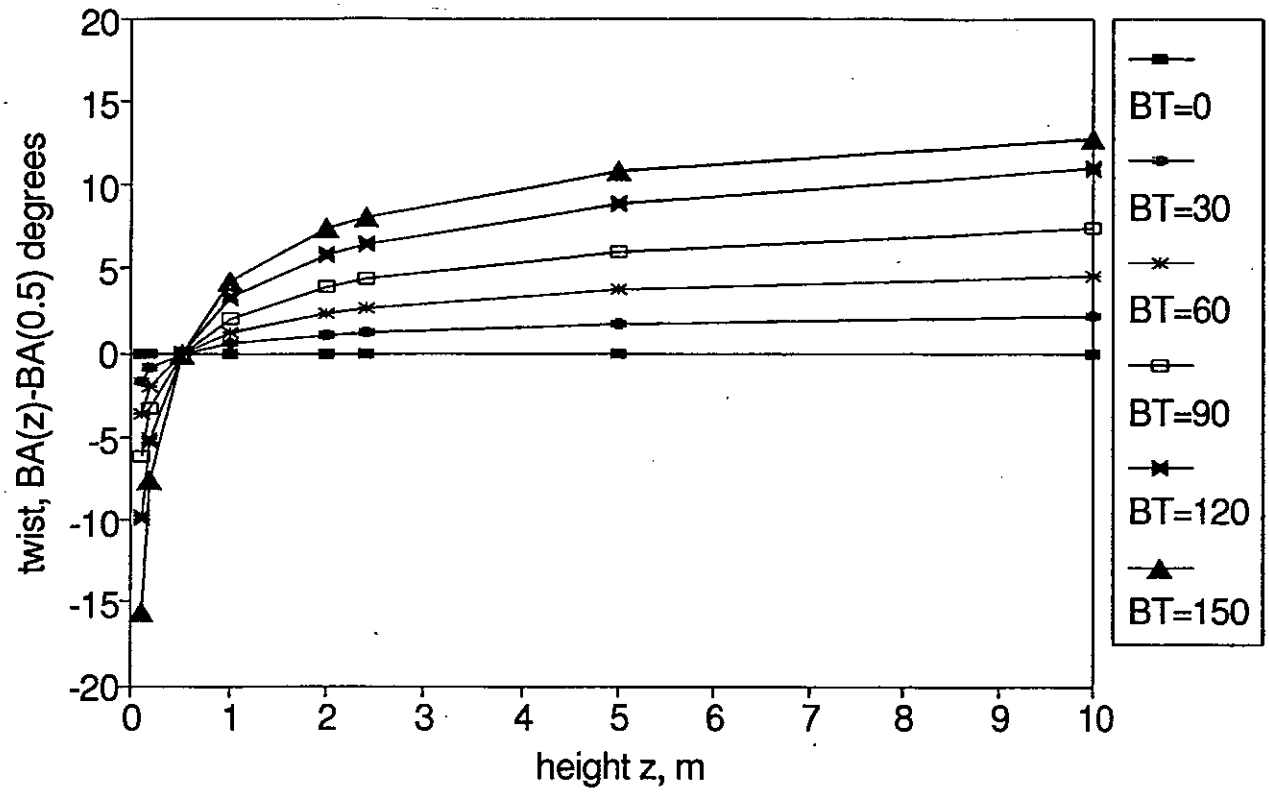

Fig. 7: Variation in apparent wind twist profiles with true wind angle.

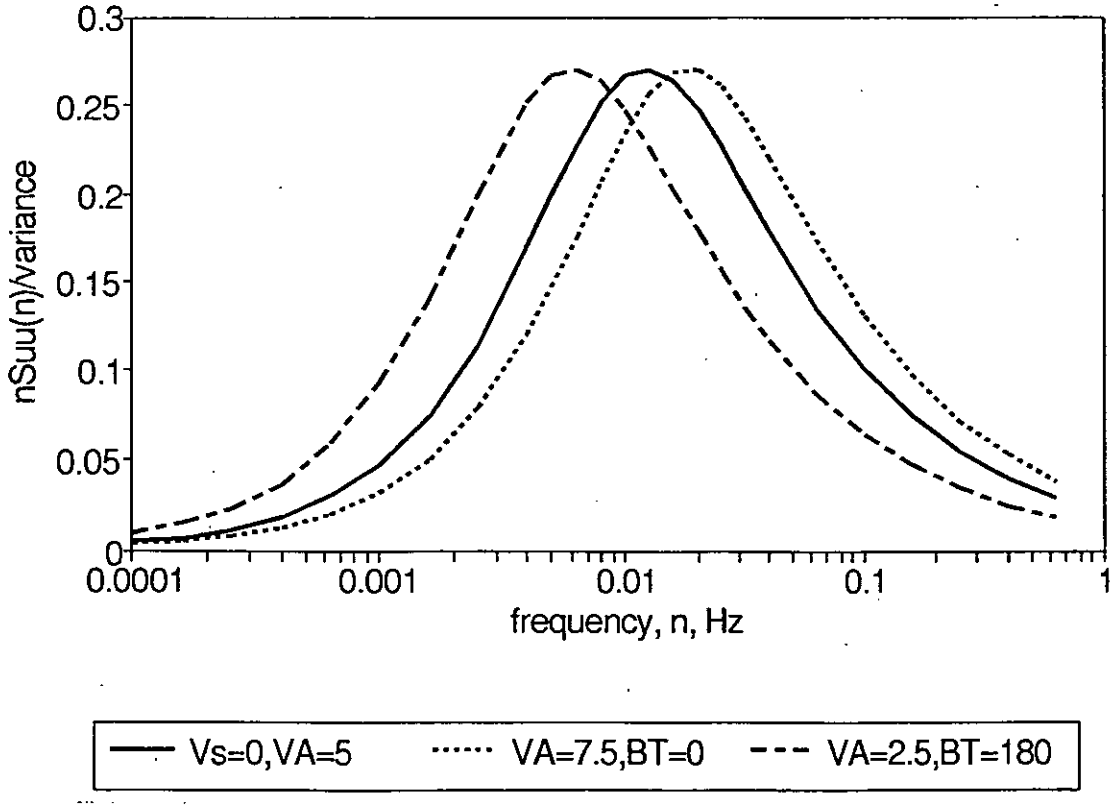

Fig. 8: Apparent wind spectra as seen by a yacht sailing upwind and downwind, and stationary.

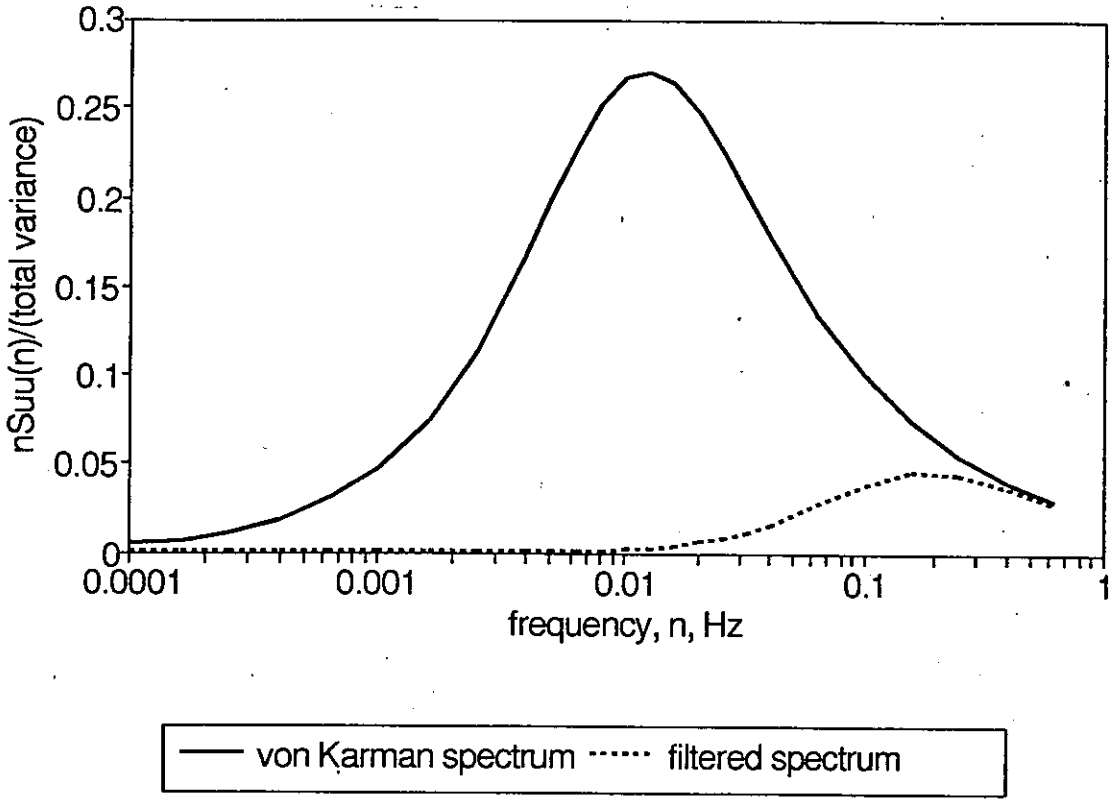

Fig. 9: The effect of high-pass filtering the natural wind spectrum at a cut-off frequency of 0.125 Hz.

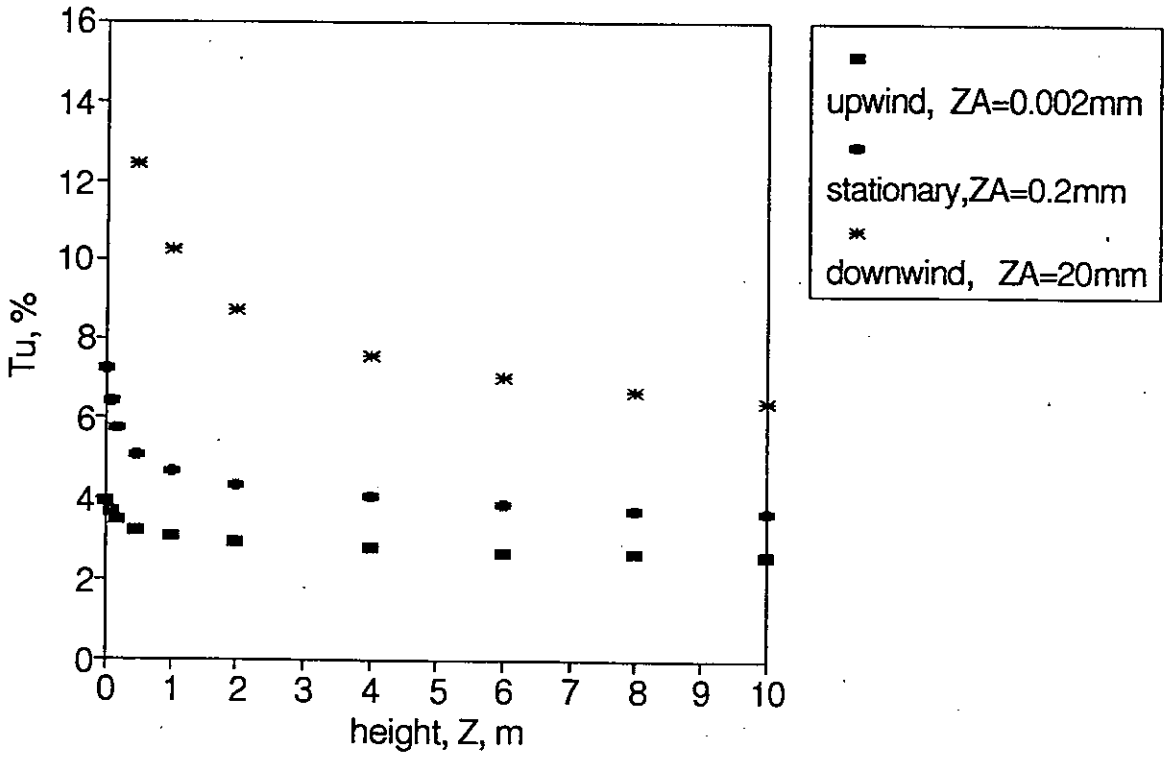

Fig. 10: Idealised turbulence intensity profiles for a yacht sailing upwind and downwind, and stationary.

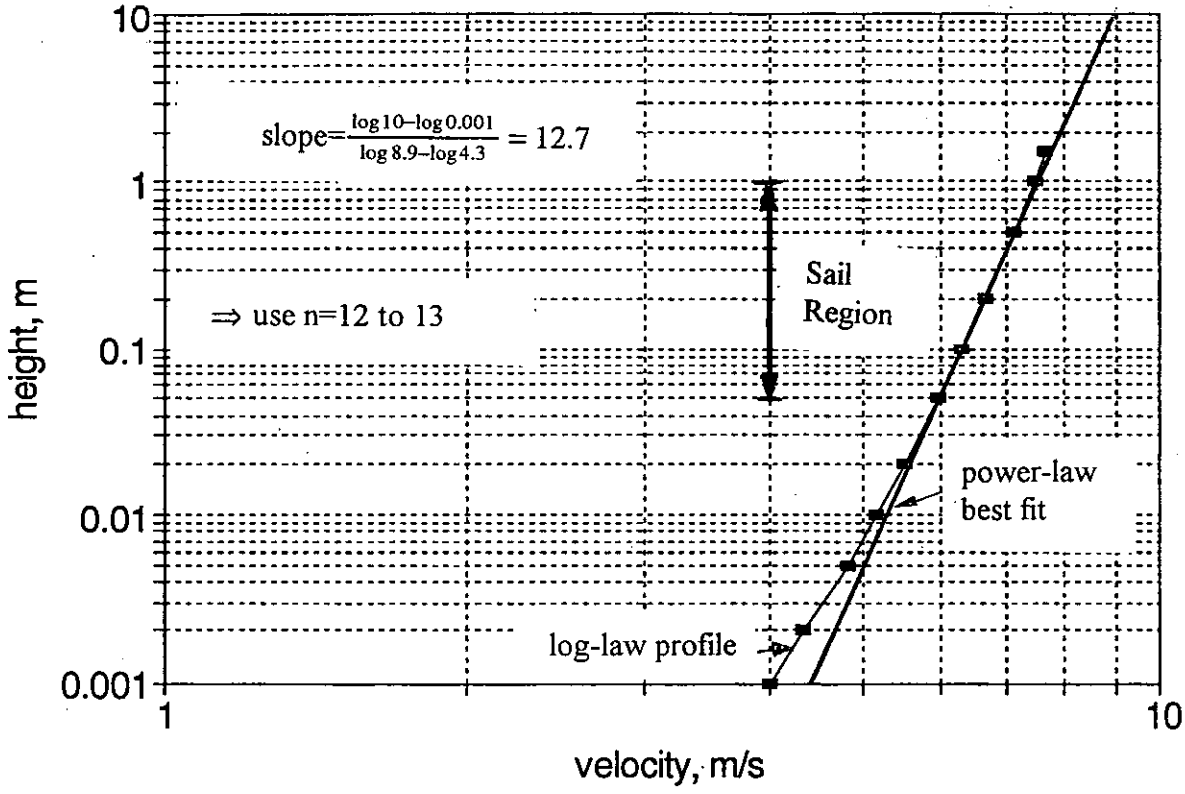

Fig. 11: Comparison of ideal log-law profile with power-law to obtain exponent n in turbulence grid design.

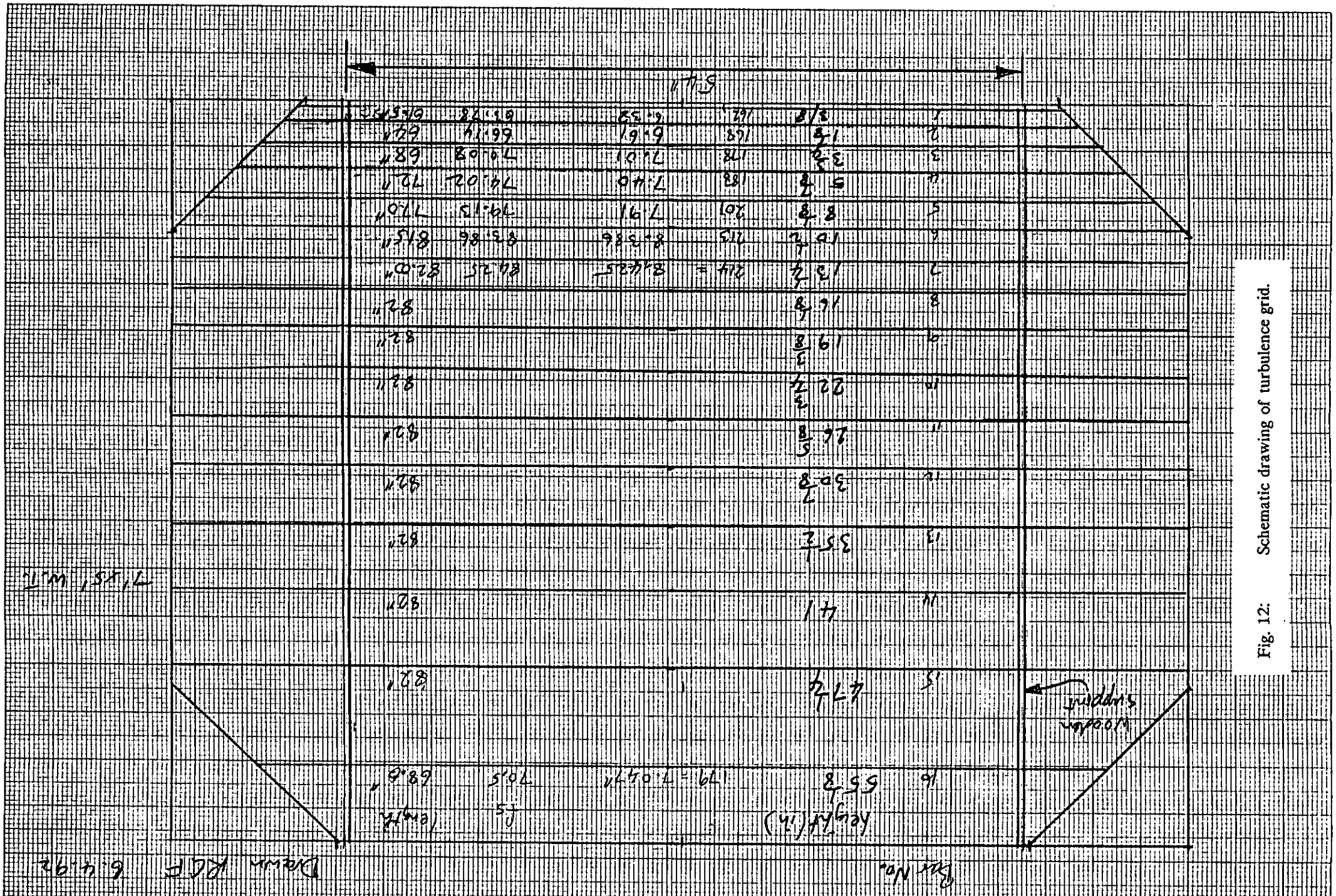

Fig. 12: Schematic drawing of turbulence grid.

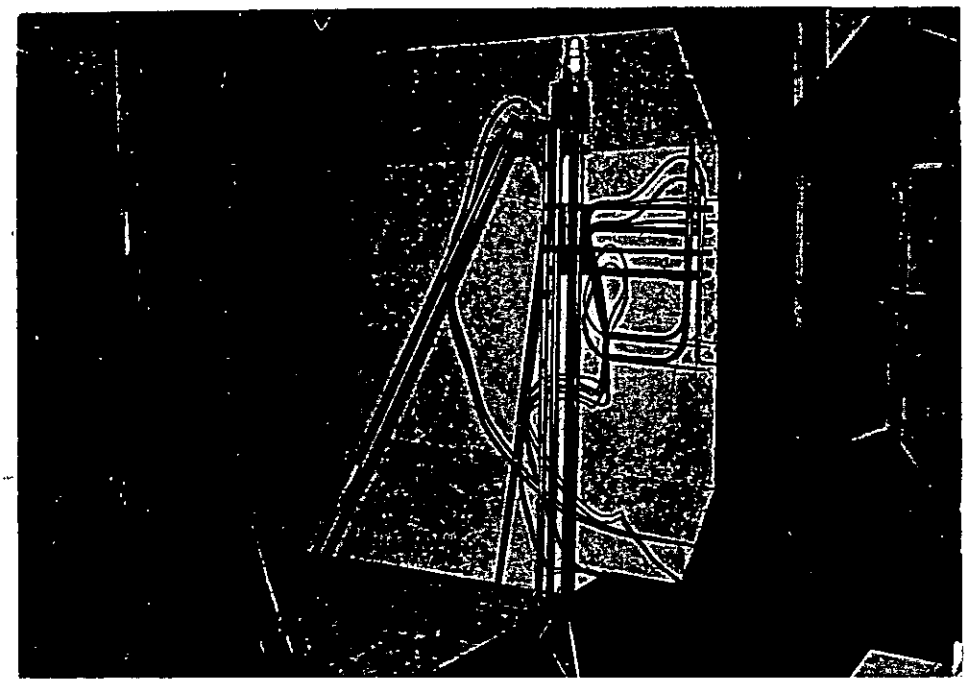

Fig. 13: Photograph of the traversing rig.

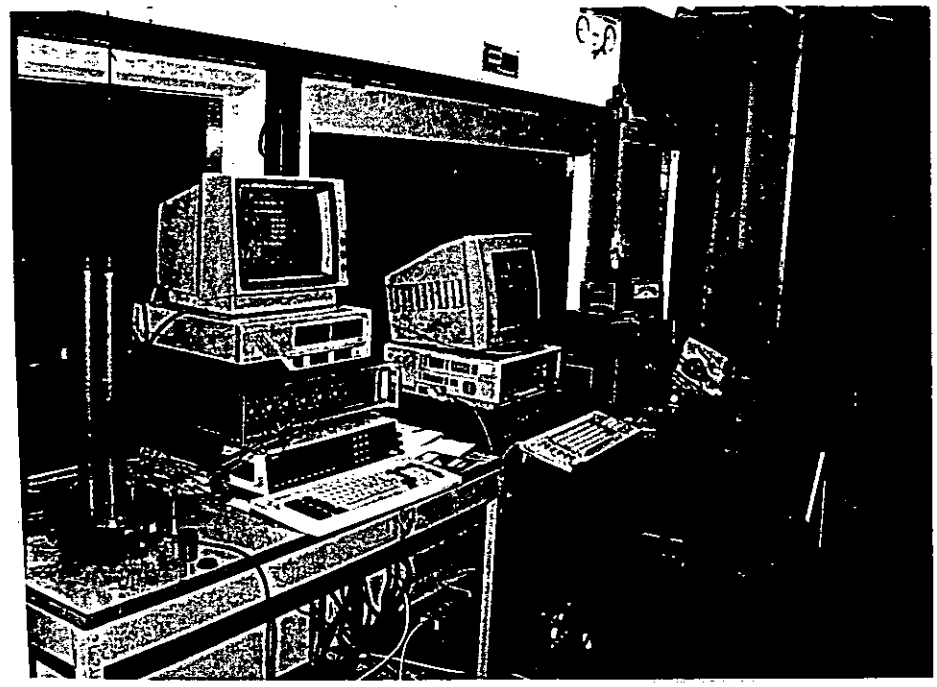

Fig. 14: Photograph of data logging equipment.

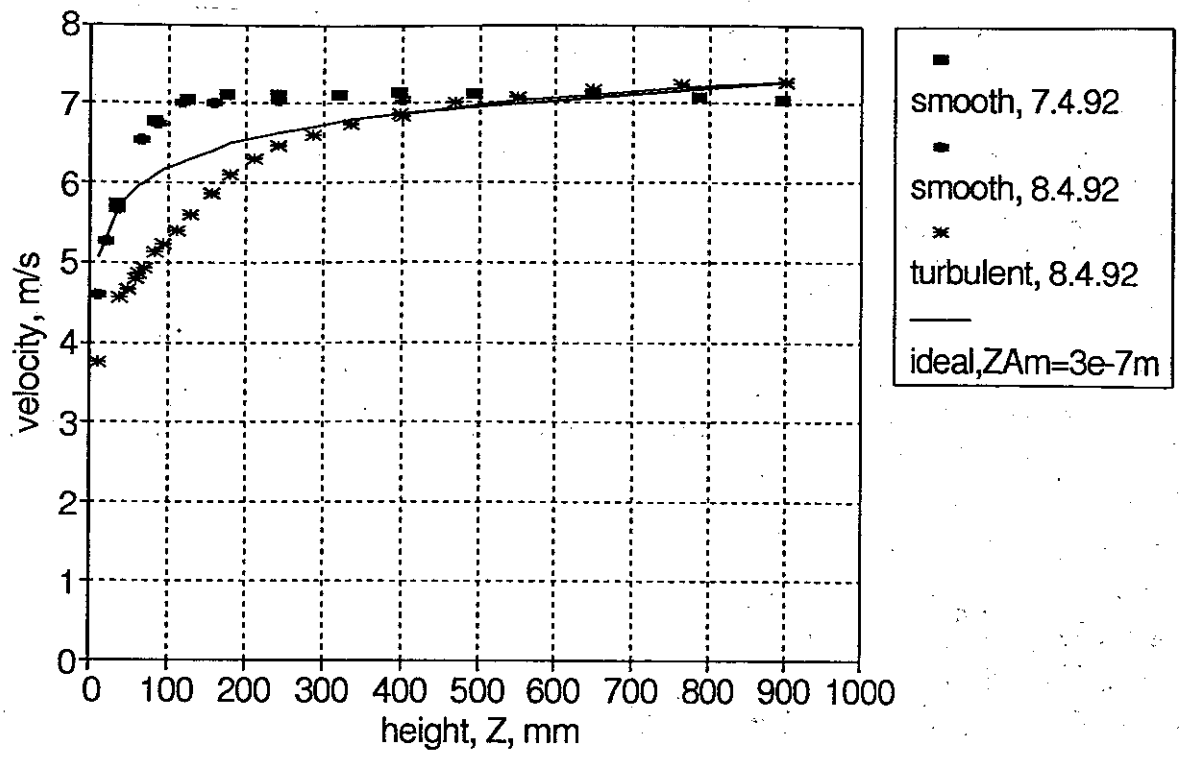

Fig. 15: Ideal and measured velocity profiles, linear axes.

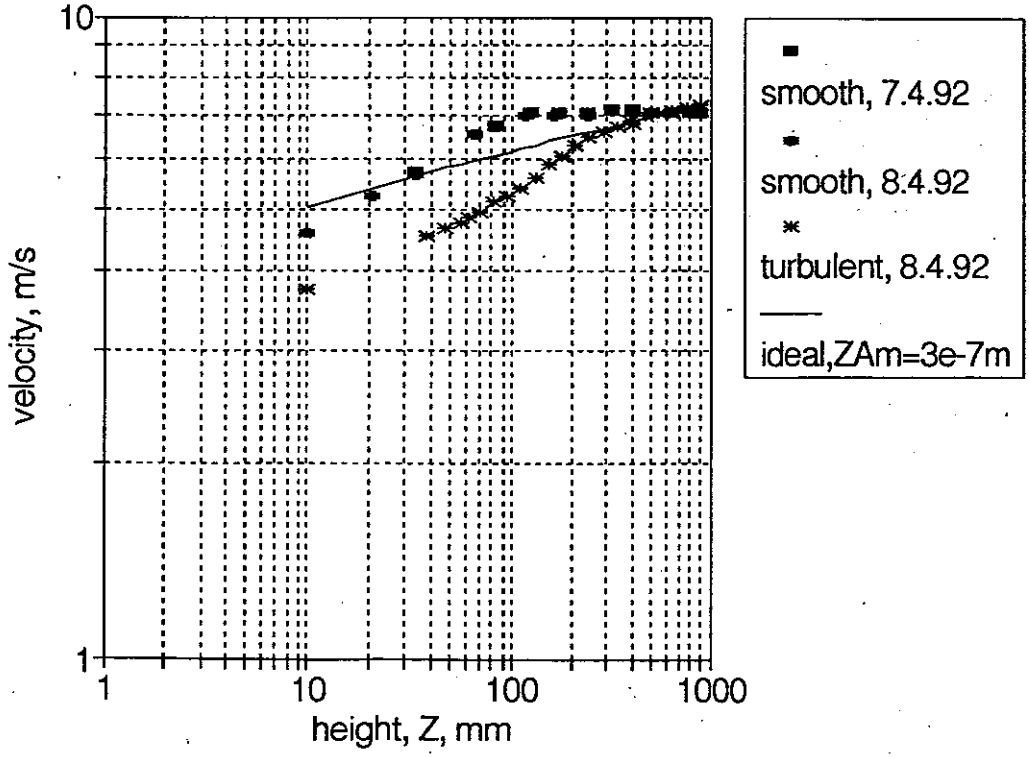

Fig. 16: Ideal and measured velocity profiles, log-log axes.

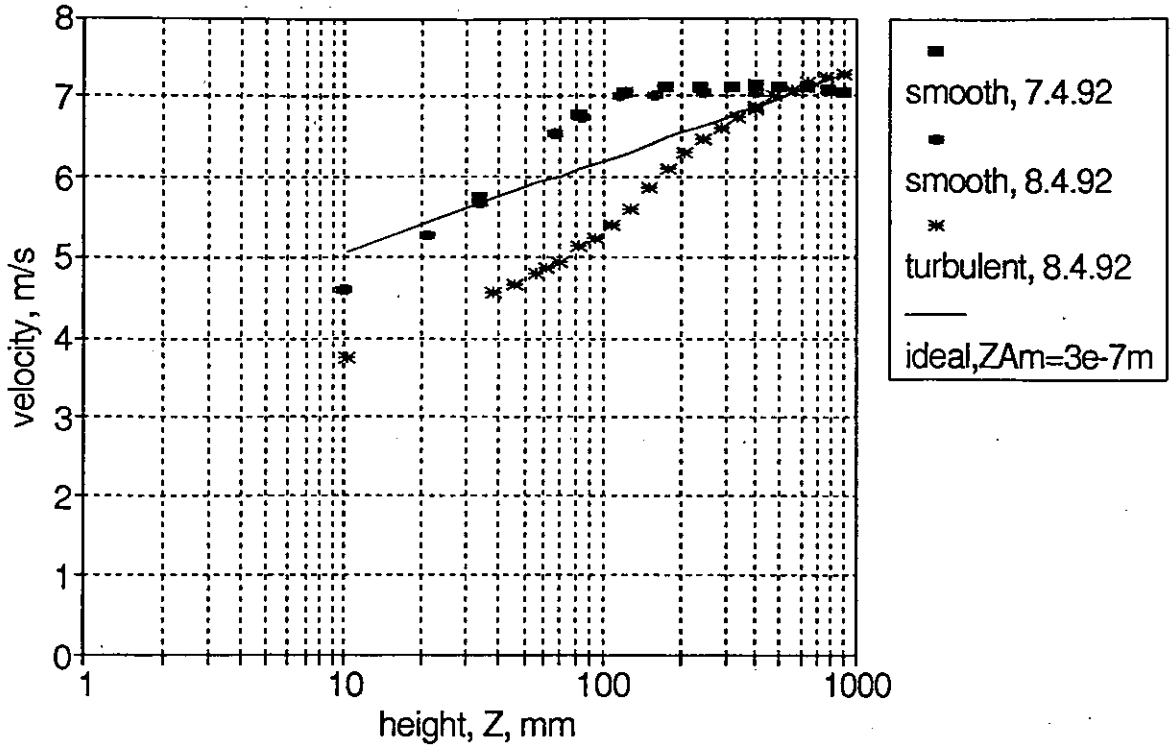

Fig. 17: Ideal and measured velocity profiles, semi-log axes.

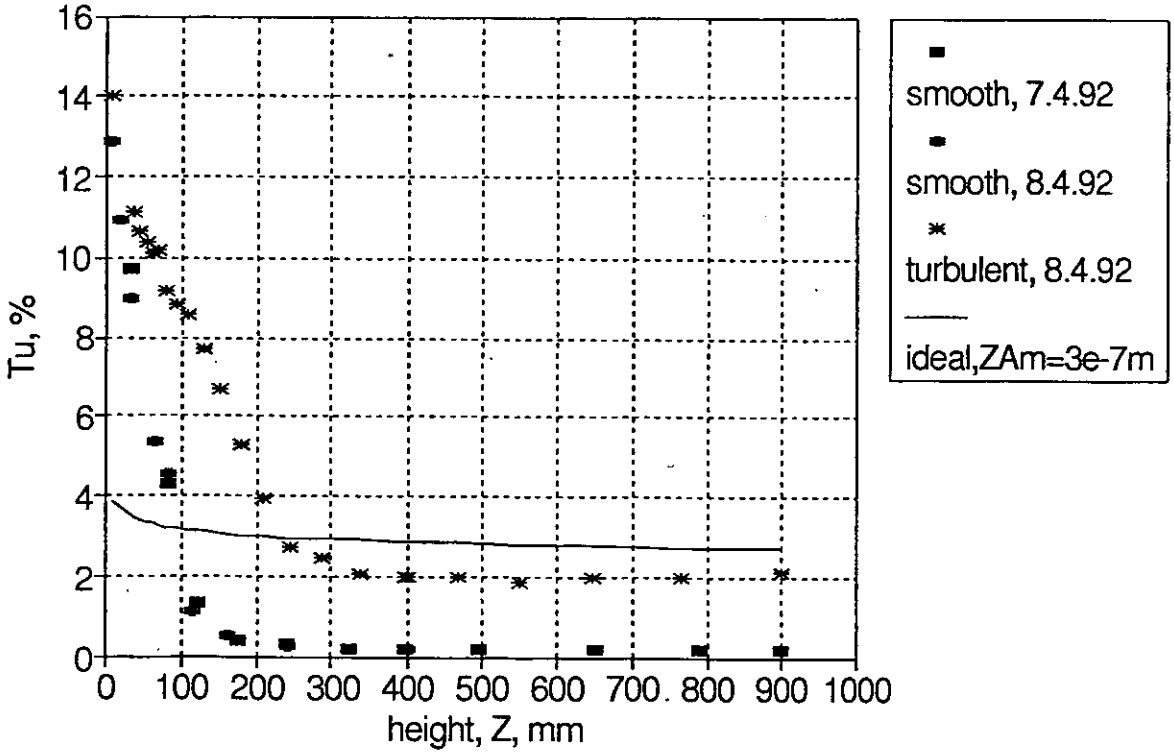

Fig. 18: Ideal and measured turbulence intensity profiles.

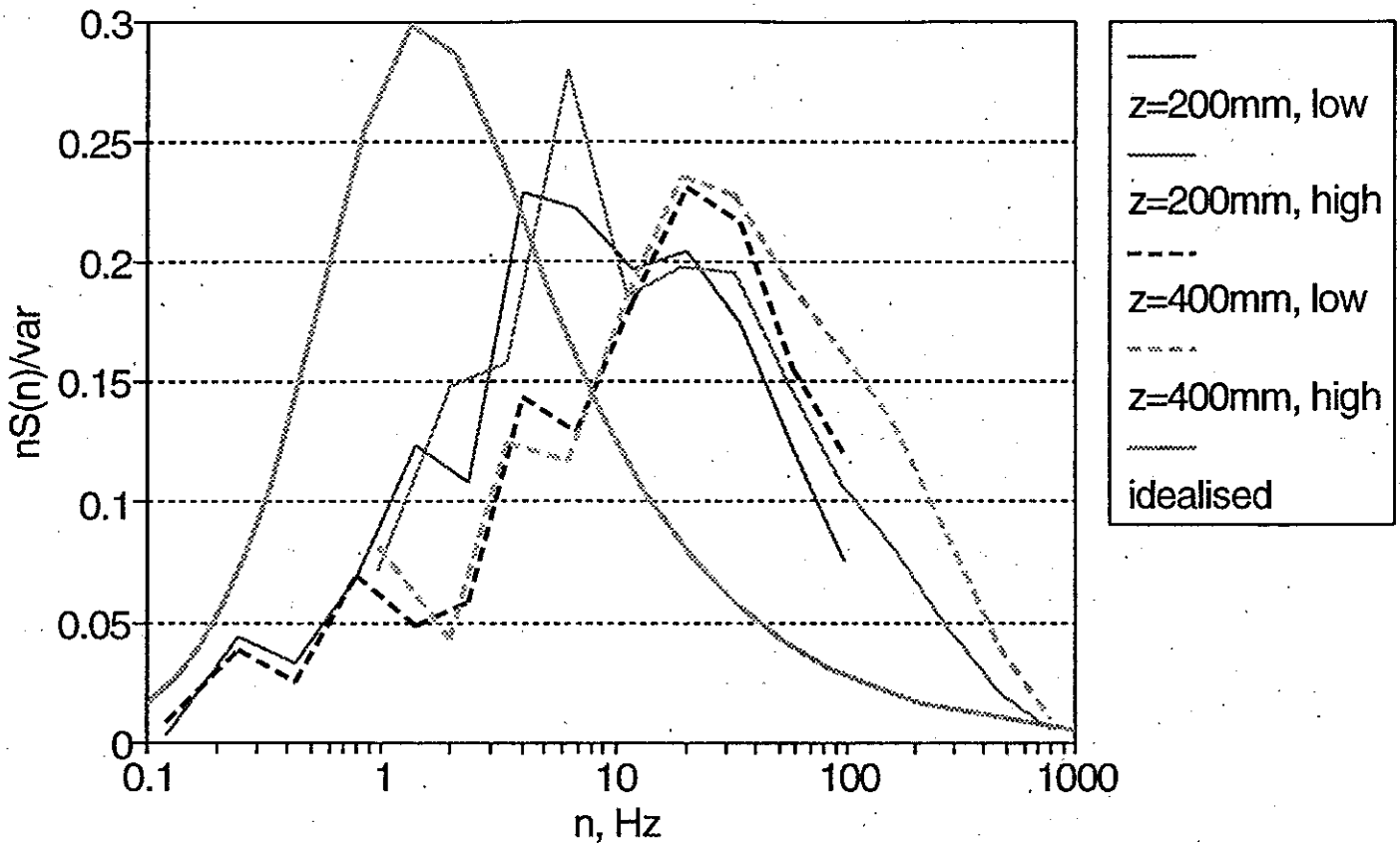

Fig. 19: Ideal and measured turbulence spectra.

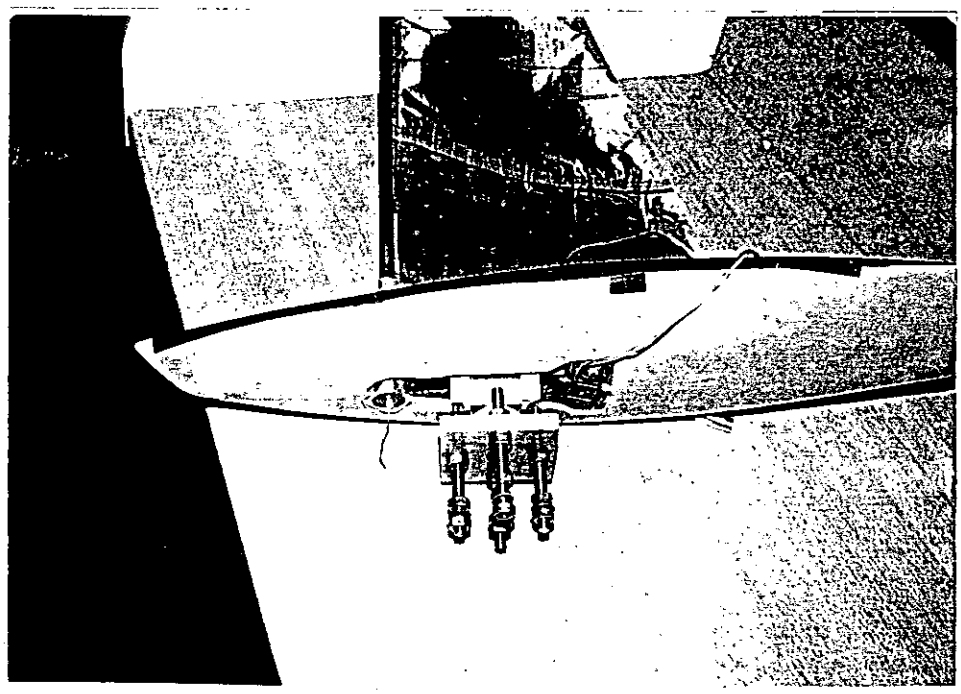

Fig. 20: Photograph of underside of model.

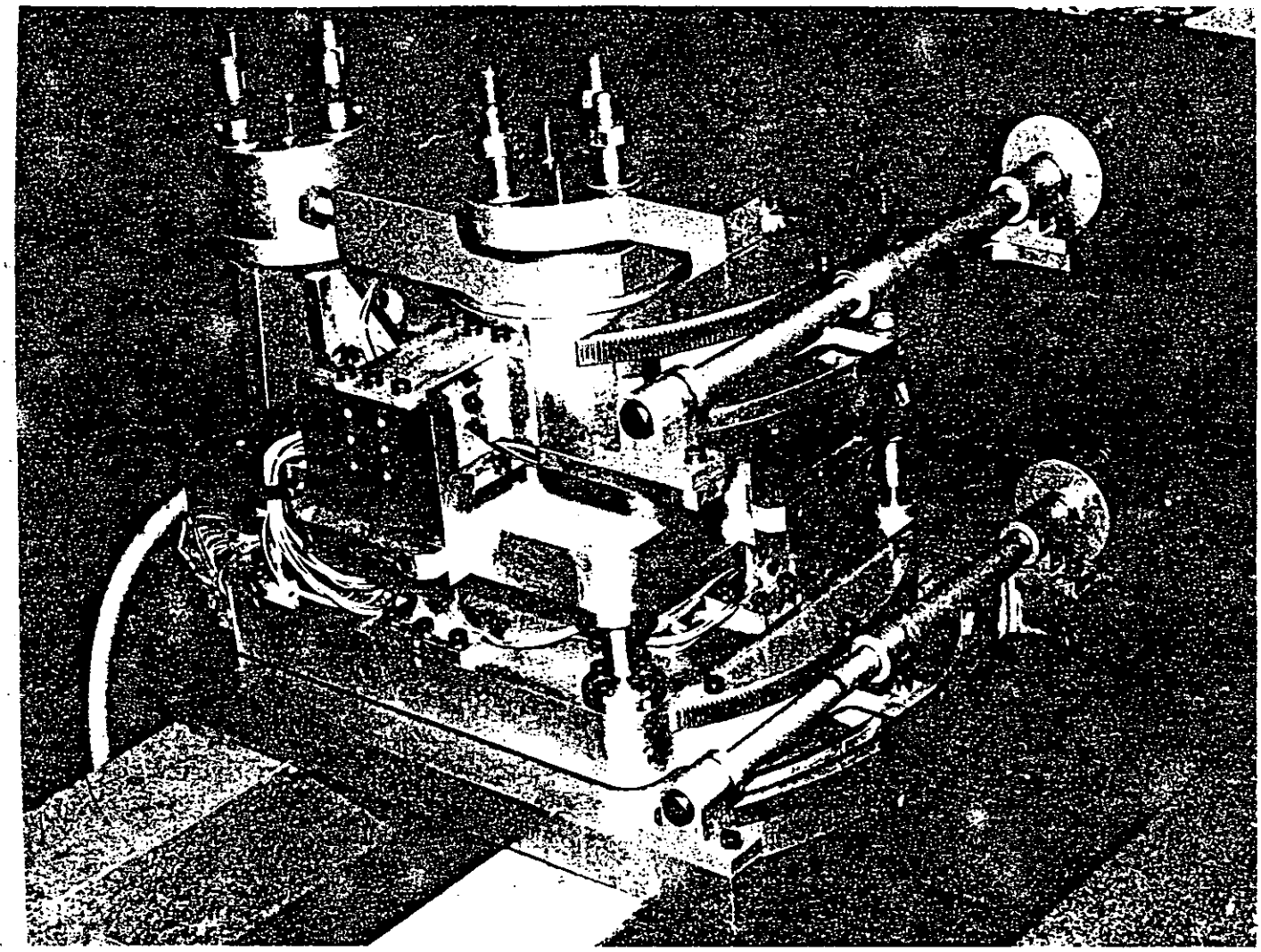

Fig. 21: Dynamometer.

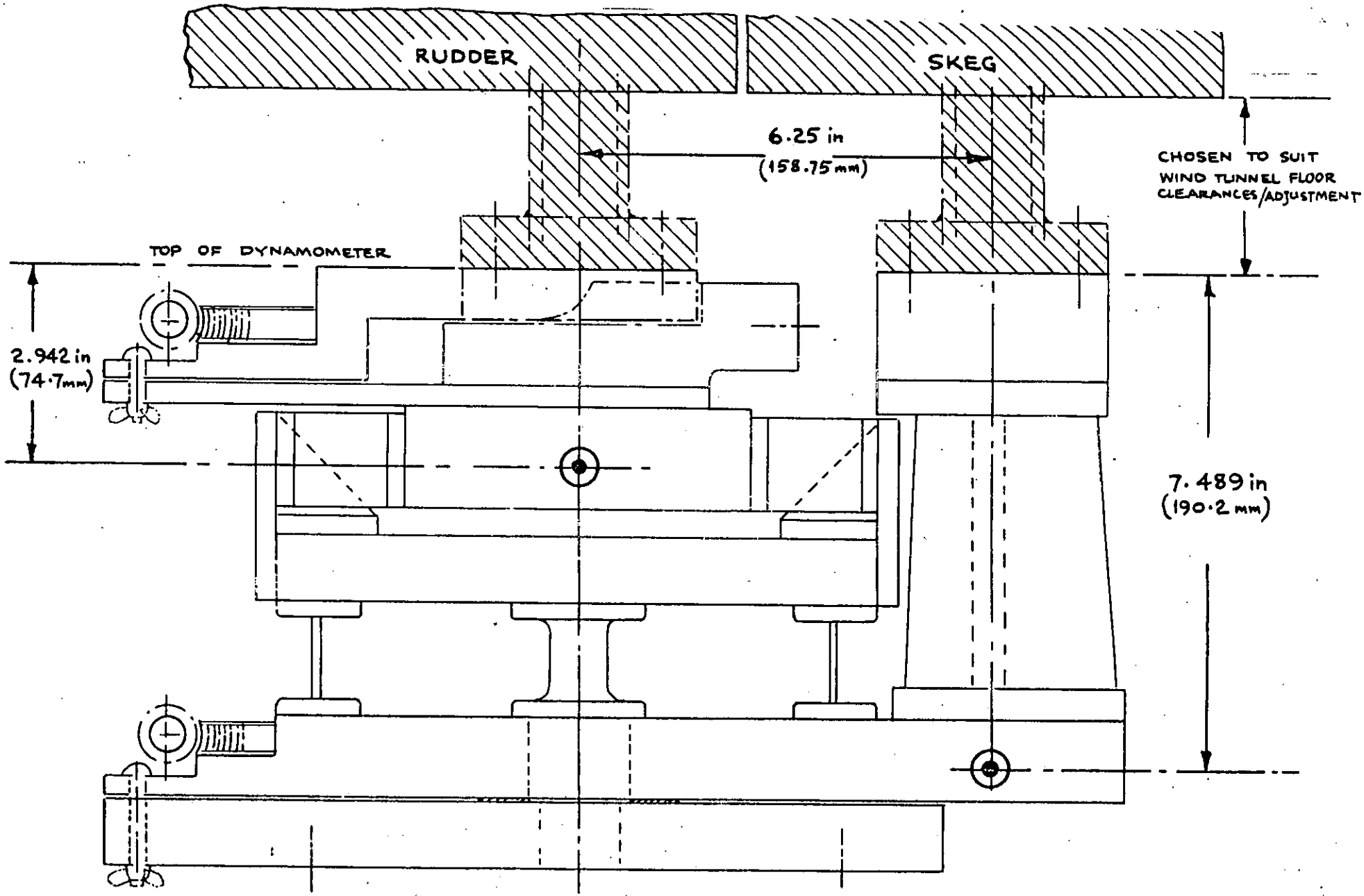

Fig. 22: True roll centres of dynamometer.

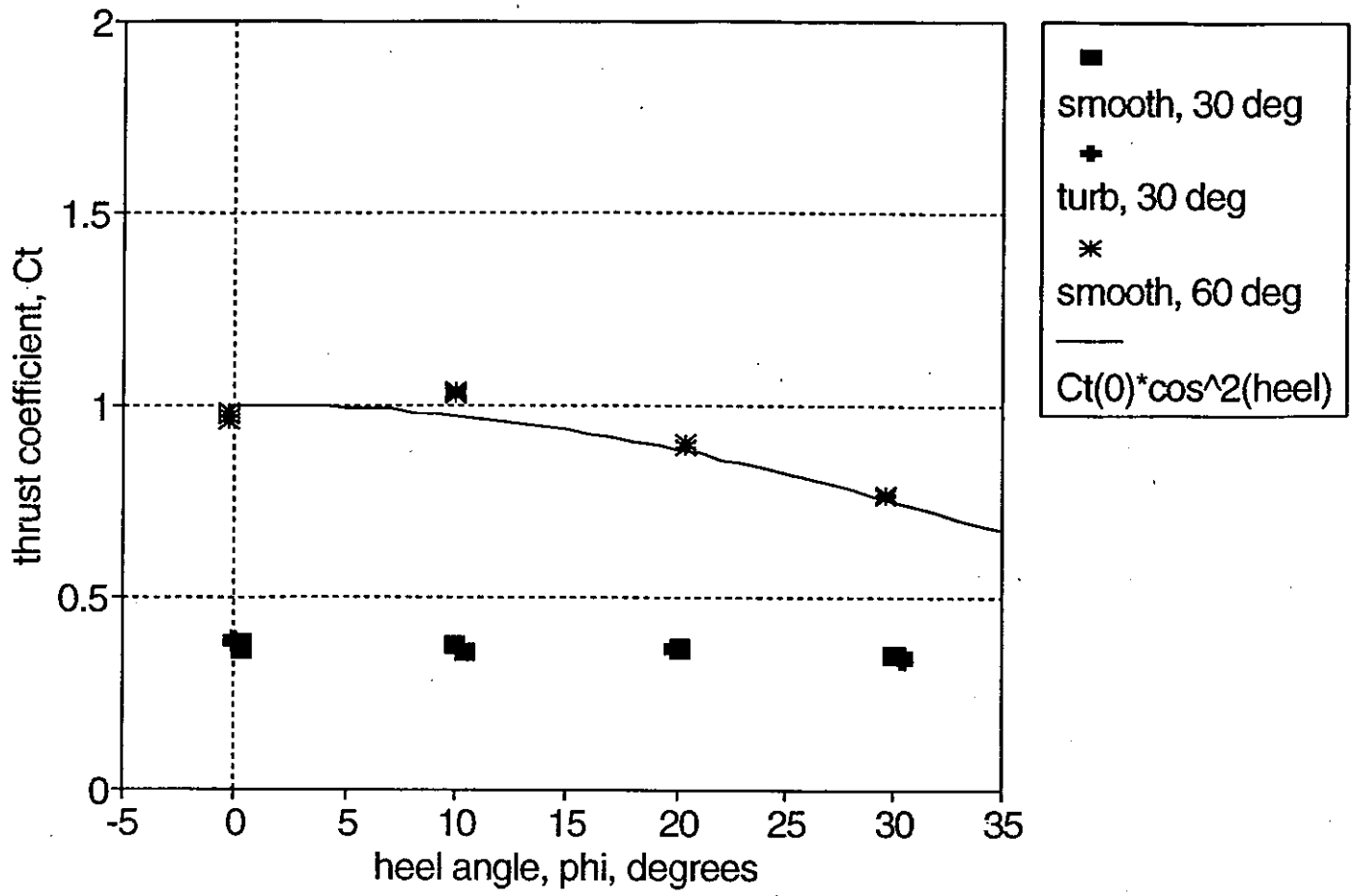

Fig. 23: Thrust coefficient versus heel.

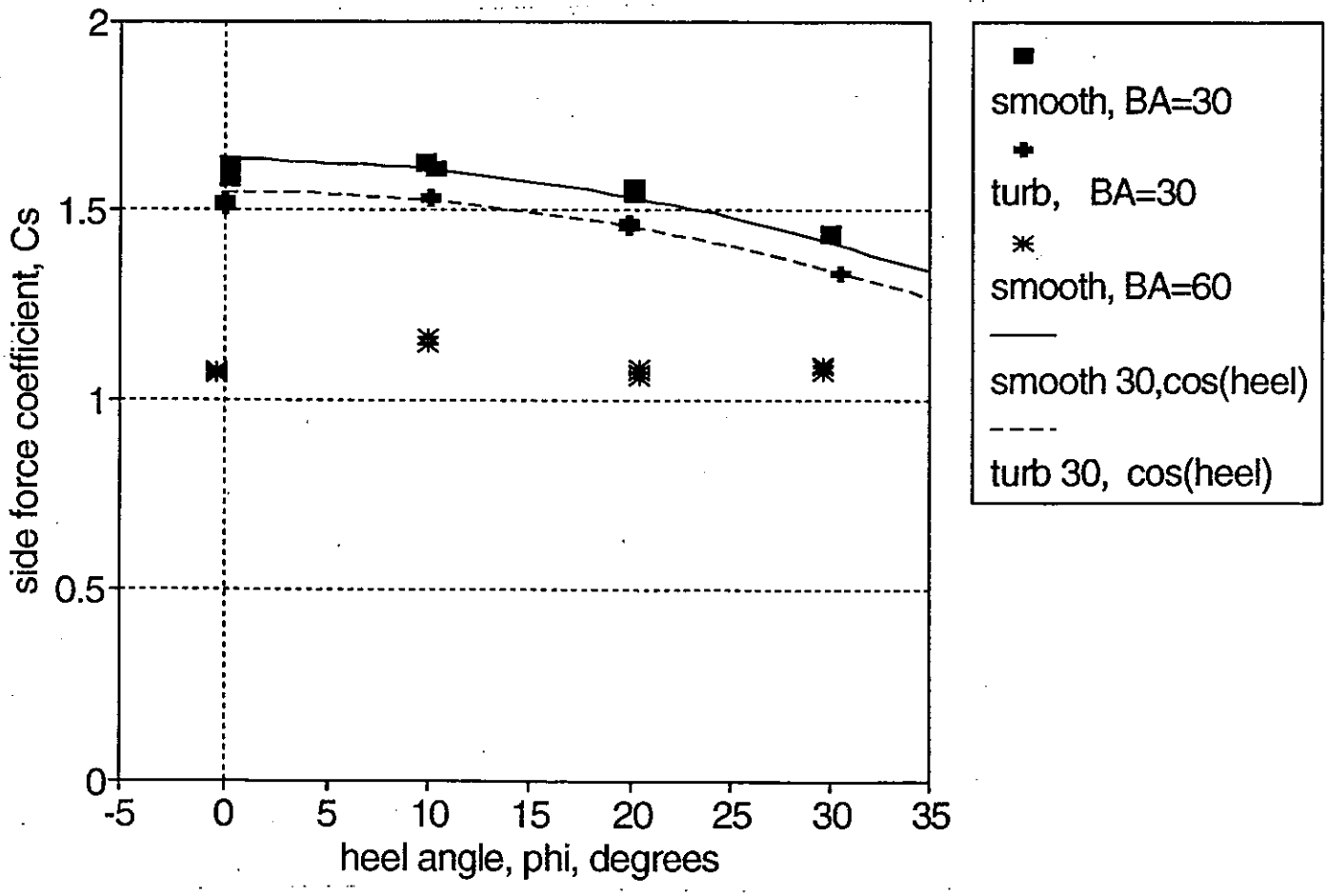

Fig. 24: Horizontal sideforce coefficient versus heel.

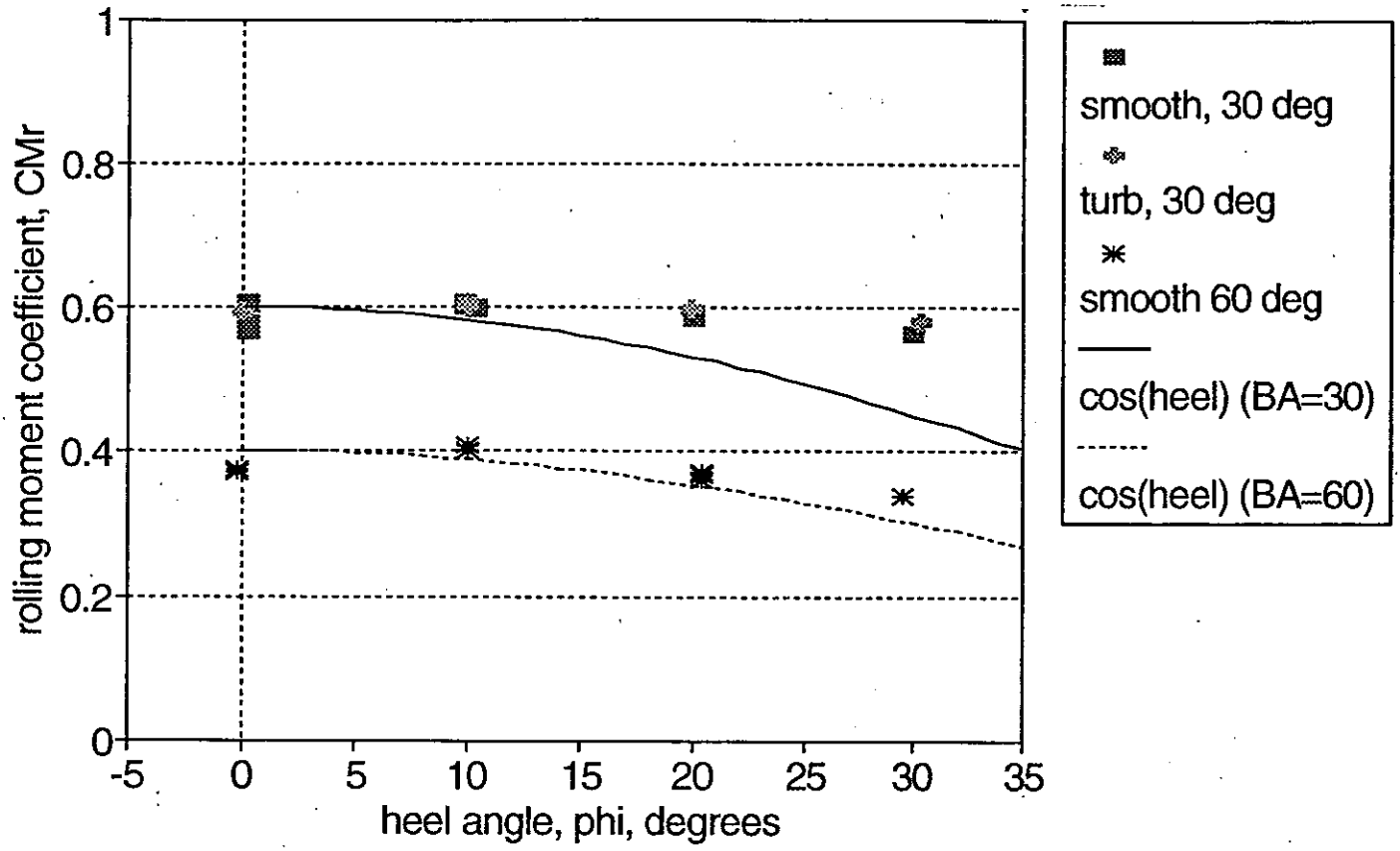

Fig. 25: Rolling moment coefficient versus heel.

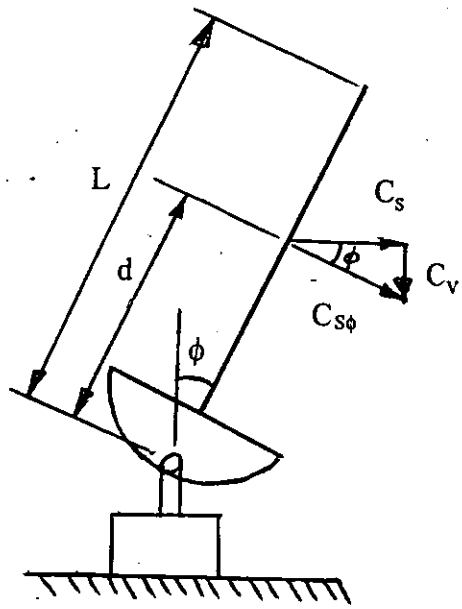

Fig. 26: Sketch showing application of side and vertical forces.

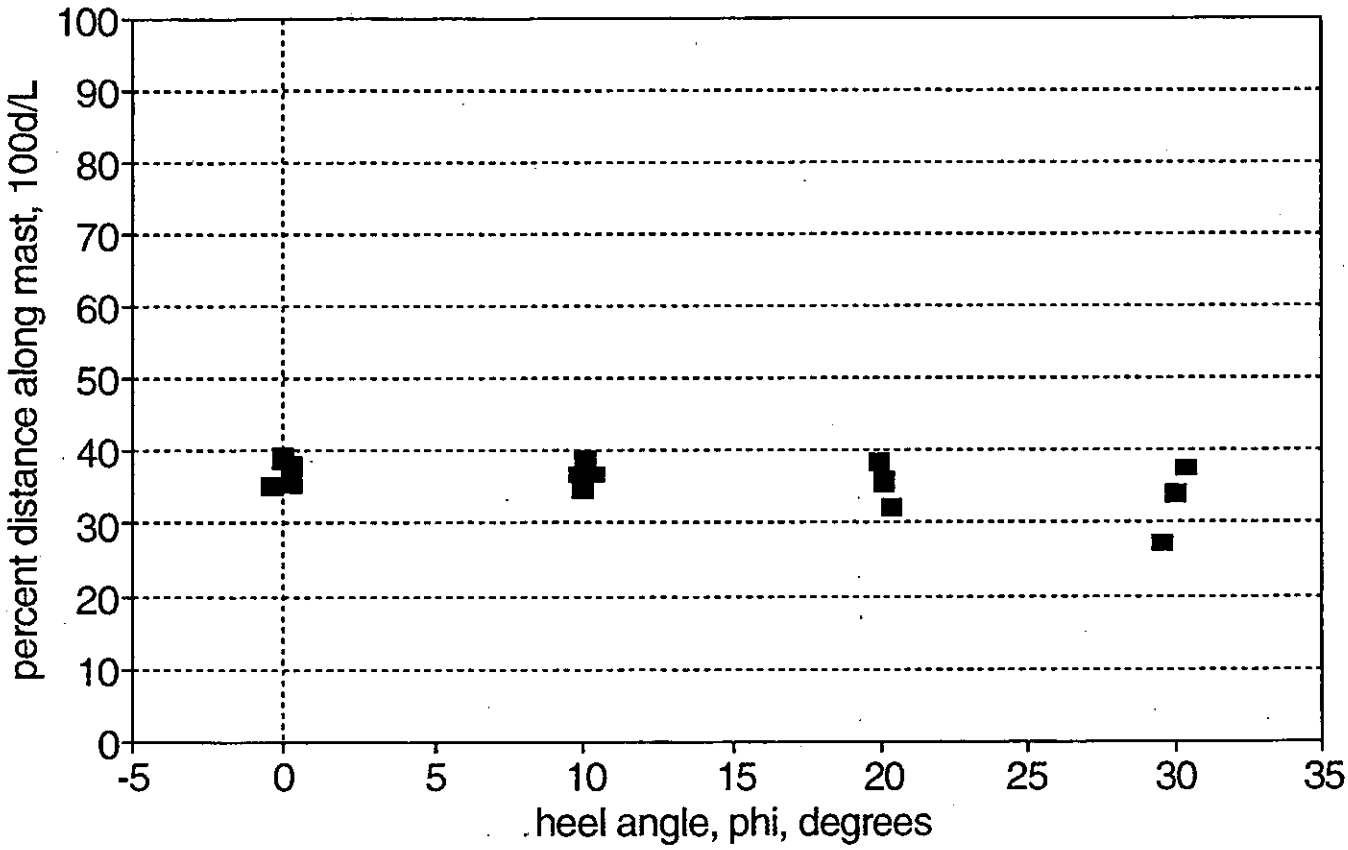

Fig. 27: Effect of heel on the effective height of the sideforce.

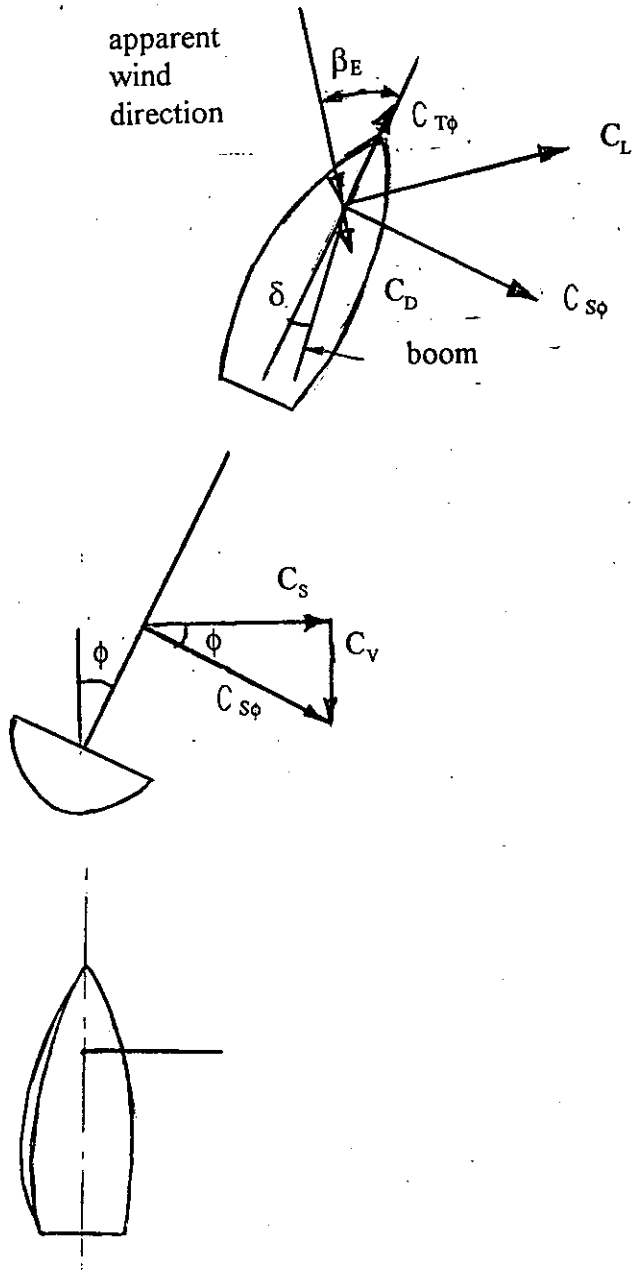

Fig. 28: Sail forces resolved into the plane of the deck.

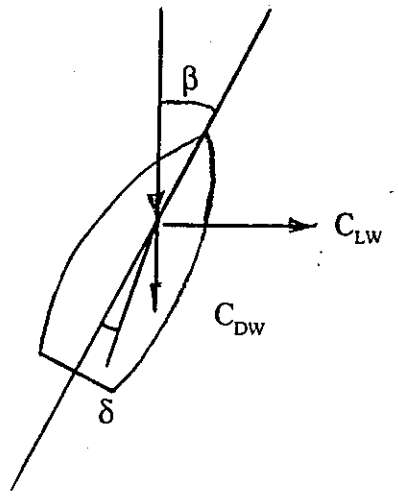

Fig. 29: Resolving forces into wind-tunnel axes.

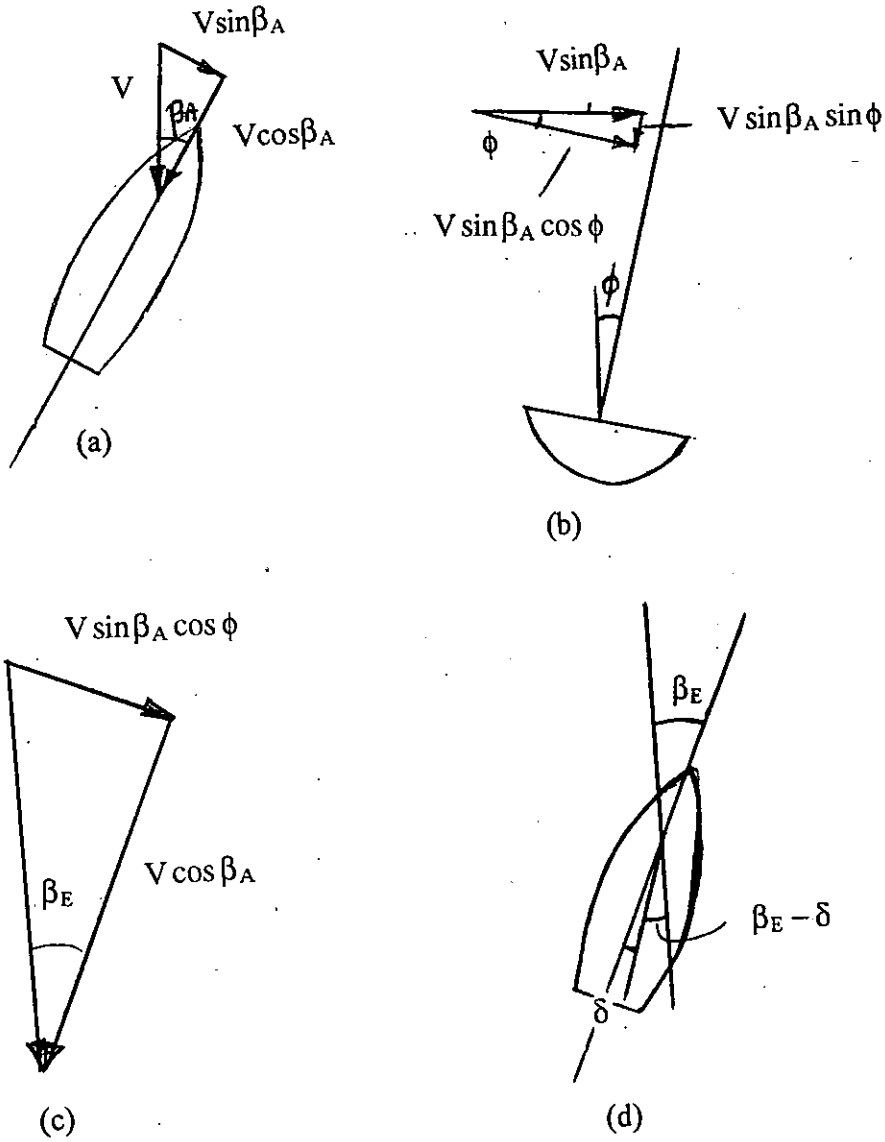

Fig. 30: Definition of the effective wind angle.

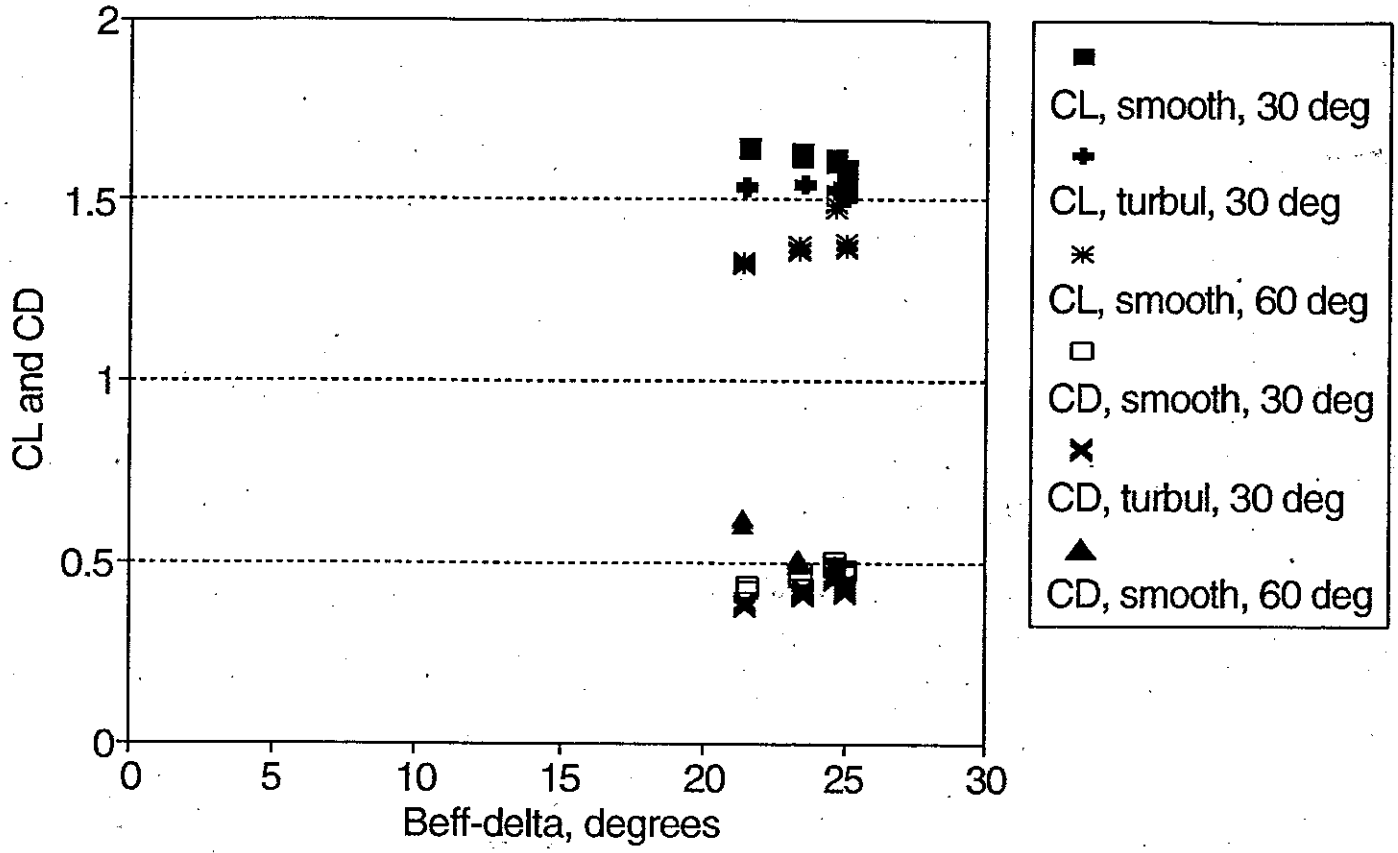

Fig. 31: Lift and drag sail coefficients for $\delta = 5$ and 35°.

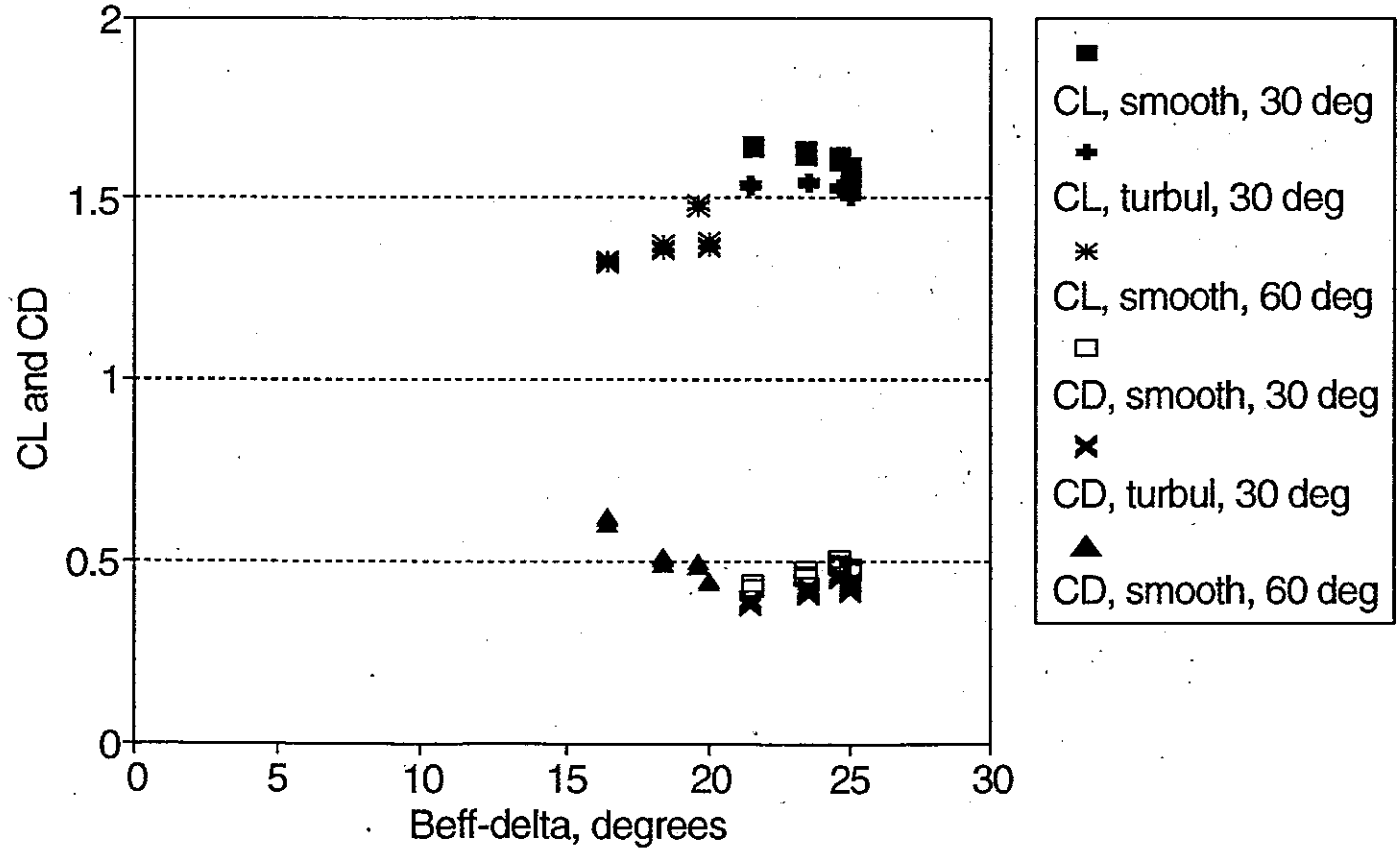

Fig. 32: Lift and drag sail coefficients for $\delta = 5$ and 40°.

APPENDIX 1

COMPUTER PROGRAM FOR TURBULENCE GRID DESIGN AND INPUT AND OUTPUT USED IN THE PRESENT DESIGN

power index = 12.00

tunnel height h = 60.0000

pressure drop coefft k0 = .2500

bar diameter d = .6250

tol = .0020

cowdrey method

no bars = 16

bar no	height(inches)	space
1	.3125	.0000
2	1.8990	1.5865
3	3.7464	1.8474
4	5.8083	2.0619
5	8.0741	2.2658
6	10.5456	2.4714
7	13.2324	2.6868
8	16.1516	2.9192
9	19.3278	3.1762
10	22.7956	3.4678
11	26.6030	3.8074
12	30.8184	4.2154
13	35.5430	4.7246
14	40.9366	5.3936
15	47.2772	6.3406
16	55.1336	7.8563

o and z method

no bars = 16

bar no	height(inches)	space
1	.3125	.0000
2	2.1267	1.8142
3	4.2073	2.0806
4	6.5042	2.2969
5	9.0063	2.5021
6	11.7154	2.7091
7	14.6416	2.9262
8	17.8026	3.1610
9	21.2244	3.4217
10	24.9432	3.7189
11	29.0103	4.0671
12	33.4992	4.4889
13	38.5209	5.0217
14	44.2549	5.7340
15	51.0263	6.7714
16	59.5521	8.5258

```
      real zc,zsc,zoz,zsoz,slast,slost
c     program to calculate grid bar spacing forgiven power
c     law profile using the cowdrey and owenzienkiewicz formulae
      dimension zc(50),zsc(50),zoz(50),zsoz(50),slast(50),slost(50)
      real k,k0,n,h,tol,d,s,x,c,v,q,oldk,a,e,y,b
      integer j,i,m,j0,num1,num2
      open(6,file='prn')
    8 write(*,9)
    9 format(' enter exponent,  tunnel height (in), bar dia (in), dp/q',
     1       ',  tolerance separated by commes')
   10 read(*,11) n,h,d,k0,tol
   11 format(5f7.4)
      if(n.eq.0.)go to 1100
c
c     write input parameters
      write(*,12)n,h,k0,d,tol
   12 format(1H0,4x,'power index = ',f6.2,/1h0,4x,'tunnel height h = ',
     1f8.4,/1h0,4x,'pressure drop coefft k0 = ',f7.4,/1h0,4x,'bar diamet
     2er d = ',f7.4,/1h0,4x,'tol = ',f7.4)
      write(*,7)
    7 format(' type 0 if correct?')
      read(j,6)
    6 format(i1)
      if(j.ne.0) go to 9
      write(6,12)n,h,k0,d,tol
c     set initial conditions
   20 j=1
      s=d
      x=0.
      zsc(j)=0.
      zc(j)=d/2.
      c=h*((n/(n+1.))**n)*((1.+k0)**(n/2.))
c
c     write first bar conditions
      write(*,125)
      write(6,125)
  125 format(1h0,'cowdrey iteration')
      write(*,13)j,j,zsc(j),s,x,zc(j)
      write(6,13)j,j,zsc(j),s,x,zc(j)
   13 format(1h0,2x,'zsc(',i2,')',5x,'s',8x,'x',8x,'zc(',i2')',/1h0,4(2x
     1,f7.4))
c
c     calculations for successive bars
   30 j=j+1
      m=1
      write(*,14)j,j
      write(6,14)j,j
   14 format(1h0,2x,'zsc(',i2,')',6x,'s',8x,'x',8x,'zc(',i2,')')
      zsc(j)=zc(j-1)+s/2.
c
c    iteration cycle
   40 v=(zsc(j)/c)**(2./n)
      if((4.-3.*v).lt.0.) go to 1001
      s=(2.*d*(v-1.))/(v-2.+sqrt((2.-v)**2.-4.*(v-1.)*(v-1.)))
      x=zc(j-1)+s/2.
      write(*,15)zsc(j),s,x
      write(6,15)zsc(j),s,x
   15 format(1h0,2x,f7.3,2x,f8.4,2x,f8.4)
```

```
      x=zc(j-1)+s/2.
      write(*,15)zsc(j),s,x
      write(6,15)zsc(j),s,x
   15 format(1h0,2x,f7.3,2x,f8.4,2x,f8.4)
      if(x.ge.h)go to 200
      j0=j*1000
      if(m.eq.10)go to 1000
      m=m+1
      if(abs((zsc(j)-x)/zsc(j)).lt.tol) go to 50
      zsc(j)=x
      go to 40
c
c     centreline height of bar
   50 zc(j)=zc(j-1)+s
      num1=j
      slast(j)=s
      write(*,16)zc(j)
      write(6,16)zc(j)
   16 format(1h+,32x,f8.4)
      q=s-d
      write(*,17)q
      write(6,17)q
   17 format(1h+,50x,21hseparation of bars = ,f7.4)
      if((zc(j)+s+d).ge.h) go to 200
      go to 30
c
c     repeat for owen and zienkienkiewicz method
  200 write(*,60)
      write(6,60)
   60 format(/,'  owen and zienkiewicz method begins',/)
      j=1
      s=d
      zsoz(j)=0.
      zoz(j)=d/2.
  300 j=j+1
      m=1
      if(slast(j).lt.d) slast(j) =s
      zsoz(j)=zoz(j-1)+slast(j)/2.
      oldk=(d/slast(j))/((1.-d/slast(j))**2.)
      a=1.1
      e=(n+1.)/n
c
c     iteration cycle
   400 b=sqrt(1.+oldk)
   410 k=(((h**(2./n))*(1.+k0)*((a+b)**2.))-((e*e)*((a+b)**(2./e))*(zsoz(
      1j)**(2./n))*((b+a*(h/zsoz(j))**(1./n))**(2./(n+1.)))))/(((zsoz(j)*
      2*(1./n))*e*b+a*(h**(1./n)))**2.)
c
c     calculate spacing s
      s=(2.*k*d)/(1.+2.*k-sqrt(1.+4.*k))
      y=zoz(j-1)+s/2.
      j0=j
      if(m.eq.10) go to 1000
      m=m+1
      if(y.ge.h) go to 600
      if(abs((y-zsoz(j))/y).lt.tol) go to 500
      zsoz(j)=y
      oldk=k
      go to 400
c
c     centreline height of bar
   500 zoz(j)=zoz(j-1)+s
      num2=j
      slost(j) = s
      if((zoz(j)+s+d).ge.h) go to 600
      go to 300
c
c     final layouts
   600 write(6,24)
```

```
c     centreline height of bar
  500 zoz(j)=zoz(j-1)+s
      num2=j
      slost(j) = s
      if((zoz(j)+s+d).ge.h) go to 600
      go to 300
c
c     final layouts
  600 write(6,24)
      write(*,24)
   24 format(1h0,8x,'cowdrey method',30x,'o and z method')
      write(6,18)num1,num2
      write(*,18)num1,num2
   18 format(1h0,4x,'no.bars = ',i2,32x,'no bars = ',i2)
      write(6,19)
      write(*,19)
   19 format(1h0,4x,'bar no',6x,'height(inches)',4x,'space',9x,'bar no',
     16x,'height(inches)',4x,'space')
      if(num1.lt.num2)num1=num2
  650 do 700 i=1,num1
  700 write(6,21) i,zc(i),slast(i),i,zoz(i),slost(i)
   21 format(1h0,6x,i2,12x,f8.4,5x,f7.4,9x,i2,12x,f8.4,5x,f7.4)
      go to 10
 1000 write(6,22)j0
   22 format(1h0,4x,'j0 = ',i5,2x,'convergence too slow')
      go to 1100
 1001 write(6,23)
   23 format(1h0,4x,'v greater than 4/3')
 1100 stop
      end
```

APPENDIX 2

EXTRACT.PAS - PROGRAM USED TO EXTRACT THE INFORMATION FROM THE DATA RECORD, AND PERFORM PRELIMINARY DATA REDUCTION.

EXTRACT.PAS
printed 13 Nov 1992

```
{$R+}    {Range checking on}
{$B+}    {Boolean complete evaluation on}
{$S+}    {Stack checking on}
{$I+}    {I/O checking on}
{$N+}    {Numeric coprocessor (possibly) }
{$E+}    {Emulate coprocessor if not physically present  }
{$M 65500,16384,655360} {Turbo 3 default stack and heap}

PROGRAM EXTRACT;


Uses
  Crt,dos,Printer; {Units found in TURBO.TPL}

var
   infile,outfile,results:text;

   filename,filename1,filename2,
   comment,
   name
                                  :string[20];

  fileend
                  :boolean;
  ch
    :char;
  i,j,MARKER,noofints,noofreals,testno,day,month,year,
  hours,minutes,sailnumber,noofchs,noofreadings,
  windonoff,turbulenceonoff,
  line,lineno,earlierlineno,
  wind,turb,
  count,
  filecounter
                           :integer;
  rudderangle,skegangle,apparentwindangle,heelangle,
  heightaboveref,baropress,temp,dynpress,area,h,
  reflength
                                          :double;
  chan: array [1..30] of integer;
  volt: array [1..30] of double;
  Vs,zeros,Vsz,F,CF,cwa  : array [1..100,1..8] of double;
  Vcal      : array [1..5] of double;
  linenumber,
  reads,
  turbulence
        : array [1..100] of integer;
  apparent,
  heel,
  height,
  temperature,
  q,heightupmast
        : array [1..100] of double;


function tan(angle:double):double;    {  tangent of an angle  }
begin
  tan:=sin(angle)/cos(angle);
end;    {  end of function tan  }


procedure set_up;
begin
  filecounter:=0;
  wind:=0;
  turb:=0;
```

```
    area:=0.16416;
    reflength:=1.0;
    delete(comment,1,length(comment));
    for i:=1 to 5 do
      Vcal[i]:=7.0;
    Vcal[3]:=11.0;
  end;


  procedure zero;   {   beginning of the file   }
  begin
    rewrite(outfile);
    clrscr;
    writeln('beginning of processing of file ',filename1,
            ' containing balance voltages');
    write('MARKER = ',marker:2);
    readln(infile);
    readln(infile,noofints,noofreals);
    if noofints <>7 then writeln('no of integers = ',noofints:4);
    if noofreals <>5 then writeln('no of reals = ',noofreals:4);
    readln(infile,testno);
    readln(infile,day);
    readln(infile,month);
    readln(infile,year);
    readln(infile,hours);
    readln(infile,minutes);
    readln(infile,sailnumber);
    readln(infile,rudderangle);
    readln(infile,skegangle);
    readln(infile,apparentwindangle);
    readln(infile,heelangle);
    readln(infile,heightaboveref);
    write('  test number = ',testno:3);
    writeln('  sail number = ',sailnumber:2);
    write('date of test = ',day:2,'-',month:2,'-',year:4);
    writeln('   time of test = ',hours:2,':',minutes:2);
    write('rudder ang = ',rudderangle:7:2,' deg');
    writeln('   skeg ang = ',skegangle:7:2,' deg (pos clockwise)');
    write('apparent wind angle = ',apparentwindangle:7:2);
    writeln('heel angle = ',heelangle:7:2,' deg, (positive to leeward)');
    writeln('height of model above reference = ',heightaboveref:7:2,' mm');
  {   write data to file  }

    writeln(outfile,'beginning of processing of file ',filename1,
            ' containing balance voltages');
    write(outfile,'MARKER = ',marker:2);
    write(outfile,'  test number = ',testno:3);
    writeln(outfile,'  sail number = ',sailnumber:2);
    write(outfile,'date of test = ',day:2,'-',month:2,'-',year:4);
    writeln(outfile,'   time of test = ',hours:2,':',minutes:2);
    write(outfile,'rudder ang = ',rudderangle:7:2,' deg');
    writeln(outfile,'   skeg ang = ',skegangle:7:2,' deg (pos clockwise)');
    write(outfile,'apparent wind angle = ',apparentwindangle:7:2);
    writeln(outfile,'heel angle = ',heelangle:7:2,
                    ' deg, (positive to leeward)');
    writeln(outfile,'height of model above reference = ',
                     heightaboveref:7:2,' mm');
    writeln(outfile);
  end;  { end of procedure zero }


  procedure one; { barometric pressure, air temperature, dynamic pressure  }
  begin
    readln(infile,baropress);
    readln(infile,temp);
    readln(infile,dynpress);
```

```
end;  { end of procedure one  }


procedure twothreeseven;  {  supply volts, zeros, or actual data  }
begin
  readln(infile,noofchs);
  readln(infile,noofreadings);
  readln(infile);
  for i:=1 to noofchs do
    readln(infile,chan[i],volt[i]);
  gotoXY(1,8);
  writeln('MARKER test sail apparent heel height ',
  'baro temp   q    chans readings turb wind');
  writeln(marker:4,testno:6,sailnumber:5,apparentwindangle:8:2,
  heelangle:7:2,heightaboveref:6:1,baropress:6:1,temp:5:1,
  dynpress:6:2,noofchs:6,noofreadings:6,'   ',turb:6,' ',wind:3);
  gotoXY(1,11);  clreol;
  gotoXY(1,12);  clreol;
  gotoXY(1,13);  clreol;
  gotoXY(1,14);  clreol;
  gotoXY(1,11);
  write('chans ');
  for i:=1 to noofchs do
    write(chan[i]:12);
  writeln;
  write('volts  ');
  for i:=1 to noofchs do
    write(volt[i]:12:7);
{  gotoXY(1,16);
  write('hit any key to continue ');
  ch:=readkey;   }

{  write to file  }
  if marker=3 then
  begin
    write(outfile,'MARKER test sail rudder skeg apparent heel height baro ',
    'temp   q    chans readings turb wind');
    chan[noofchs+1]:=16;
    for i:=1 to noofchs+1 do
      write(outfile,chan[i]:11);
    writeln(outfile);
  end;
  if length(comment)>0 then
  begin
    writeln(outfile,' 9  ',comment);
    delete(comment,1,length(comment));
  end;
  write(outfile,marker:4,testno:6,sailnumber:5,rudderangle:6:1,
  skegangle:6:1,apparentwindangle:8:2,
  heelangle:7:2,heightaboveref:6:1,baropress:6:1,temp:5:1,
  dynpress:6:2,noofchs:6,noofreadings:6,'   ',turb:6,' ',wind:3);
  if marker=2 then
    for i:=1 to 8 do
      write(outfile,'           ');
  for i:=1 to noofchs do
    write(outfile,volt[i]:11:7);
  writeln(outfile);

end;  {  end of procedure twothreeseven  }


procedure four;   {  get new height above reference  }
begin
  readln(infile,heightaboveref);
end;  {  end of procedure heightaboveref  }
```

```
procedure fivesix;
begin
  gotoXY(1,16);
  writeln(lst,'procedure 5 6 used by mistake, Marker = ',marker:3);
end;  { end of procedure fivesix }


procedure eight;   { end of input file has been reached }
begin
  gotoXY(10,24);
  writeln('end of input file ',filename1,' reached properly');
  writeln(lst,'end of input file ',filename1,' reached properly');
  writeln(outfile,'8 end of file');
  close(infile);
  close(outfile);
  fileend:=true;
end;  { end of procedure eight }


procedure nine;   { comment }
begin
  gotoXY(1,18);
  write('comment marker  - ');
  clreol;
  readln(infile,comment);
  writeln(comment);
end;  { end of procedure nine }


procedure ten;  { new heel angle }
begin
  readln(infile,heelangle);
end;  { end of procedure 10 }


procedure eleven;  { new apparent wind angle }
begin
  readln(infile,apparentwindangle);
end;


procedure twelve;   { new temperature }
begin
  readln(infile,temp);
end;  { end of procedure twelve }


procedure thirteen;   { new skeg angle }
begin
  readln(infile,skegangle);
end;  { end of procedure thirteen }


procedure fourteen;  { new dynamic pressure }
begin
  readln(infile,dynpress);
end;  { end of procedure fourteen }


procedure fifteen;  { wind on/off }
begin
  readln(infile,wind);
end;  { end of procedure fifteen }
```

```
procedure sixteen;  {  turbulence on/off  }
begin
  readln(infile,turb);
end;  {  end of procedure sixteen  }


procedure get_file;
begin
  fileend:=false;
  clrscr;
  repeat
    gotoXY(1,10);
    writeln('enter input file name (without extension) ');
    clreol;
    write('              or q to quit                  ');
    readln(filename);
    for i:=1 to length(filename) do
      filename[i]:=upcase(filename[i]);
    if filename='Q' then halt;
    filename1:=filename+'.YRF';
    filename2:=filename+'.VLT';
    assign(infile,filename1);
    {$I-}
    reset(infile);
    {$I+}
    if IOresult<>0 then
       write(filename1,' does not exist - try again');
    {$I-}
    reset(infile);
    {$I+}
  until IOresult=0;
  assign(outfile,filename2);
end;  {  end of procedure get_file  }


procedure extractdata;
begin
  repeat
    readln(infile,marker);
    case marker of
      0: zero;
      1: one;
      2,3,7: twothreeseven;
      4: four;
      5,6: fivesix;
      8: eight;
      9: nine;
      10: ten;
      11: eleven;
      12: twelve;
      13: thirteen;
      14: fourteen;
      15: fifteen;
      16: sixteen;
    else
      writeln(lst,'not in range 0 - 16, MARKER = ',marker:6);
    end;
  until fileend;
end;  {  end of procedure extractdata  }

procedure supplyvoltages;  {  get the supply voltages  }
begin
  reset(outfile);
  for i:= 1 to 7 do
    readln(outfile);
  repeat
```

```
      readln(outfile);
      read(outfile,marker)
    until marker=2;
    lineno:=1;
    earlierlineno:=lineno;
    read(outfile,testno,sailnumber,rudderangle,
    skegangle,apparentwindangle,
    heelangle,heightaboveref,baropress,temp,
    dynpress,noofchs,noofreadings,turb,wind);
    for i:=1 to noofchs do
      read(outfile,Vs[lineno,i]);
    repeat
       repeat
         readln(outfile);
         read(outfile,marker);
         if marker<>9 then lineno:=lineno+1;
       until (marker=2) or (marker=8);
       if marker=2 then
       begin
         read(outfile,testno,sailnumber,rudderangle,
         skegangle,apparentwindangle,
         heelangle,heightaboveref,baropress,temp,
         dynpress,noofchs,noofreadings,turb,wind);
         for i:=1 to noofchs do
           read(outfile,Vs[lineno,i]);
         for line:=earlierlineno+1 to lineno-1 do
           for i:=1 to noofchs do
             Vs[line,i]:=Vs[earlierlineno,i]+(Vs[lineno,i]-
             Vs[earlierlineno,i])*(line-earlierlineno)/(lineno-earlierlineno);
        earlierlineno:=lineno;
      end;
      if marker=8 then
      begin
        lineno:=lineno-1;
        for line:=earlierlineno+1 to lineno do
          for i:= 1 to noofchs do
            Vs[line,i]:=Vs[earlierlineno,i];
      end;
    until marker=8;
    close(outfile);
    writeln(lst);
    writeln(lst,'supply voltages');
    write(lst,'channel ');
    for i:=1 to noofchs do
       write(lst,i:12);
    writeln(lst);
    writeln(lst,'line no.');
    for line:=1 to lineno do
    begin
      write(lst,line:5,'    ');
      for i:=1 to noofchs do
        write(lst,Vs[line,i]:12:7);
      writeln(lst);
    end;
  end;  { end of procedure supplyvoltages }


  procedure findzeros;  { get the windoff balance voltages }
  begin
    reset(outfile);
    for i:= 1 to 7 do
      readln(outfile);
    repeat
      readln(outfile);
      read(outfile,marker)
    until marker=2;
```

```
  lineno:=1;
  earlierlineno:=lineno;
  read(outfile,testno,sailnumber,rudderangle,
  skegangle,apparentwindangle,
  heelangle,heightaboveref,baropress,temp,
  dynpress,noofchs,noofreadings,turb,wind);
  for line:=1 to 100 do zeros[line,noofchs+1]:=0.0;
  repeat
     repeat
       readln(outfile);
       read(outfile,marker);
       if marker<>9 then lineno:=lineno+1;
     until (marker=7) or (marker=8);
     if marker=7 then
     begin
       read(outfile,testno,sailnumber,rudderangle,
       skegangle,apparentwindangle,
       heelangle,heightaboveref,baropress,temp,
       dynpress,noofchs,noofreadings,turb,wind);
       if wind=0 then
       begin
         if dynpress<> 0.0 then
           writeln(lst,'zero block and dynamic pressure = ',dynpress:6:2,
                       '  line number = ',lineno:3);
         for i:=1 to noofchs do
           read(outfile,zeros[lineno,i]);
         if earlierlineno=1 then
           for line:=1 to lineno-1 do
             for i:=1 to noofchs do
               zeros[line,i]:=0.0;
         if earlierlineno<>1 then
           for line:=earlierlineno+1 to lineno-1 do
             for i:=1 to noofchs do
               zeros[line,i]:=zeros[earlierlineno,i]
                           +(zeros[lineno,i]-zeros[earlierlineno,i])
                           *(line-earlierlineno)/(lineno-earlierlineno);
         zeros[lineno,noofchs+1]:=-99.0;
         earlierlineno:=lineno;
       end;
     end;
     if marker=8 then
     begin
       lineno:=lineno-1;
       for line:=earlierlineno+1 to lineno do
         for i:= 1 to noofchs do
           zeros[line,i]:=zeros[earlierlineno,i];
     end;
  until marker=8;
  close(outfile);
  writeln(lst);
  writeln(lst,'zeros');
  write(lst,'channel ');
  for i:=1 to noofchs do
     write(lst,i:12);
  writeln(lst);
  writeln(lst,'line no.');
  for line:=1 to lineno do
  begin
    write(lst,line:5,'    ');
    for i:=1 to noofchs do
      write(lst,zeros[line,i]:12:7);
    if zeros[line,noofchs+1]=-99.0 then write(lst,'  zero');
    writeln(lst);
  end;
end;  { end of procedure zeros }
```

```
procedure balance_matrix;
begin
{  fudge the pitch voltage, which is garbage, measured from the balance
   this is done so that the interactions from pitch will not cause
   incorrect errors                                                  }

  Vsz[count,5]:=0.2525*Vsz[count,2]*(122+height[count]+400*
                    cos(heel[count]*pi/180))/(4.84685e-2*1e3);
{ writeln(lst,'pitch voltage is = ',Vsz[count,5]:11:7);            }

  F[count,1]:= (0.338035   * Vsz[count,1]+
               -1.188100e-3* Vsz[count,2]+
               -3.952000e-4* Vsz[count,3]+
               -1.484800e-3* Vsz[count,4]+
               -3.260500e-3* Vsz[count,5])*1e6;

  F[count,2]:= (2.120000e-5* Vsz[count,1]+
                0.252512   * Vsz[count,2]+
               -6.659000e-4* Vsz[count,3]+
                1.682300e-3* Vsz[count,4]+
               -9.901000e-4* Vsz[count,5])*1e6;

  F[count,3]:=(-0.000182   * Vsz[count,1]+
                2.845000e-4* Vsz[count,2]+
                3.936600e-2* Vsz[count,3]+
                1.344000e-4* Vsz[count,4]+
                0.00032    * Vsz[count,5])*1e6;

  F[count,4]:= (7.002000e-4* Vsz[count,1]+
               -2.370000e-5* Vsz[count,2]+
               -3.403600e-3* Vsz[count,3]+
                6.349250e-2* Vsz[count,4]+
                2.049000e-4* Vsz[count,5])*1e6;

  F[count,5]:=(-3.300000e-6* Vsz[count,1]+
                6.333000e-4* Vsz[count,2]+
                1.470000e-5* Vsz[count,3]+
               -3.008000e-4* Vsz[count,4]+
                4.846850e-2* Vsz[count,5])*1e6;

{  estimate vertical force assuming that the sideforce acts perpindicular
   to the mast }
   F[count,6]:=F[count,1]*tan(heelangle*pi/180.0);

end;  {  end of procedure balance_matrix  }


procedure moveMRC;
begin

   F[count,3]:=F[count,3]+0.085*F[count,1];
   F[count,4]:=F[count,4]-F[count,1]*(0.122+height[count]/1000.0);
   F[count,5]:=F[count,5]-F[count,2]*(0.122+height[count]/1000.0)
                         -F[count,6]*0.085;

  if F[count,1]<>0.0 then
    heightupmast[count]:=F[count,4]*cos(heelangle*pi/180.0)*1000/F[count,1]
  else
    heightupmast[count]:=0.0;

end;   {   end of procedure moveMRC    }


procedure coefficients;
begin
```

```
    h:=400.0*cos(heelangle*pi/180.0)+heightaboveref-115.0+5.0;
    if turb=1 then
      q[count]:=3*9.81*(0.76239+0.0005326*h)
    else
      q[count]:=3*9.81*1.03;
    for i:=1 to 2 do
      CF[count,i]:=F[count,i]/(area*q[count]);
    for i:=3 to 5 do
      CF[count,i]:=F[count,i]/(area*reflength*q[count]);
    CF[count,6]:=F[count,6]/(area*q[count]);
  end;   {   end of procedure coefficients   }


  procedure wind_axes;
  begin

    cwa[count,1]:=CF[count,2]*sin(apparent[count]*pi/180.0)
                  +CF[count,1]*cos(apparent[count]*pi/180.0);
    cwa[count,2]:=CF[count,1]*sin(apparent[count]*pi/180.0)
                  -CF[count,2]*cos(apparent[count]*pi/180.0);
    cwa[count,3]:=CF[count,3];
    cwa[count,4]:=CF[count,4]*cos(apparent[count]*pi/180.0)
                  +CF[count,5]*sin(apparent[count]*pi/180.0);
    cwa[count,5]:=CF[count,5]*cos(apparent[count]*pi/180.0)
                  -CF[count,4]*sin(apparent[count]*pi/180.0);
    cwa[count,6]:=CF[count,6];
  end;   {   end of procedure wind_axes   }


  procedure correctdata;
  begin
    reset(outfile);
    for i:= 1 to 7 do
      readln(outfile);
    repeat
      readln(outfile);
      read(outfile,marker)
    until marker=2;
    lineno:=1;
    count:=0;
    read(outfile,testno,sailnumber,rudderangle,
    skegangle,apparentwindangle,
    heelangle,heightaboveref,baropress,temp,
    dynpress,noofchs,noofreadings,turb,wind);
    repeat
       repeat
         readln(outfile);
         read(outfile,marker);
         if marker<>9 then lineno:=lineno+1;
       until (marker=7) or (marker=8);
       if marker=7 then
       begin
         read(outfile,testno,sailnumber,rudderangle,
         skegangle,apparentwindangle,
         heelangle,heightaboveref,baropress,temp,
         dynpress,noofchs,noofreadings,turb,wind);
         if wind=1 then
         begin
           if dynpress<>3.0 then
             writeln(lst,'data block and dynamic pressure = ',dynpress:6:2,
                         '  line number = ',lineno:3);
           count:=count+1;
           linenumber[count]:=lineno;
           apparent[count]:=apparentwindangle;
           heel[count]:=heelangle;
```

```
          height[count]:=heightaboveref;
          temperature[count]:=temp;
          q[count]:=dynpress;
          reads[count]:=noofreadings;
          turbulence[count]:=turb;
          for i:=1 to noofchs do
            read(outfile,Vsz[count,i]);
          for i:=1 to noofchs do
            Vsz[count,i]:=(Vsz[count,i]-zeros[lineno,i])*Vcal[i]/Vs[lineno,i];
          balance_matrix;
          moveMRC;
          coefficients;
{          wind_axes;                    }
        end;
      end;
  until marker=8;
  close(outfile);
  writeln(lst);
  writeln(lst,'voltages corrected for supply and zero offsets');
  write(lst,'channel  ');
  for i:=1 to noofchs do
     write(lst,i:12);
  writeln(lst);
  writeln(lst,'count  line no.');
  for line:=1 to count do
  begin
    write(lst,line:3,'    ',linenumber[line]:3,'  ');
    for i:=1 to noofchs do
      write(lst,Vsz[line,i]:12:7);
    writeln(lst);
  end;
  writeln(lst);
  writeln(lst,'balance matrix applied and MRC moved to boat');
  write(lst,'channel  ');
     write(lst,'       sideforce     thrust    yaw moment   roll momt',
                    '  pitch momt');
  writeln(lst);
  writeln(lst,'count  line no.');
  for line:=1 to count do
  begin
    write(lst,line:3,'    ',linenumber[line]:3,'  ');
    for i:=1 to noofchs do
      write(lst,F[line,i]:12:7);
    writeln(lst);
  end;
  writeln(lst);
  writeln(lst,'                                                    COEFFICIENTS');
  write(lst,'channel  ');
     write(lst,'                              side  thrust yaw mom',
               '  roll pitch   Fv  hupmst');
  writeln(lst);
  writeln(lst,'     line height  heel tu apprnt');
  for line:=1 to count do
  begin
    write(lst,line:2,'    ',linenumber[line]:2,'  ',height[line]:6:1,
    heel[line]:6:1,turbulence[line]:2,apparent[line]:6:1);
    for i:=1 to noofchs do
      write(lst,CF[line,i]:7:3);
    write(lst,CF[line,6]:7:3,heightupmast[line]:6:1);
    writeln(lst);
  end;
  writeln(lst);
{  writeln(lst);
  writeln(lst,'                                        WIND AXIS     COEFFICIENTS');
  write(lst,'channel  ');
     write(lst,'                           lift  drag   yaw ',
```

```
                ' roll   pitch   Fv   hupmst');
    writeln(lst);
    writeln(lst,'     line  height heel tu apprnt');
    for line:=1 to count do
    begin
      write(lst,line:2,'    ',linenumber[line]:2,'  ',height[line]:6:1,
      heel[line]:6:1,turbulence[line]:2,apparent[line]:6:1);
      for i:=1 to noofchs do
        write(lst,cwa[line,i]:7:3);
      write(lst,cwa[line,6]:7:3,heightupmast[line]:6:1);
      writeln(lst);
    end;
    writeln(lst);                                                    }
    writeln(lst);
  end;  {  end of procedure correctdata  }


  procedure saveresultsinafile;
  begin
    if filecounter=0 then
      begin
        writeln;
        write('enter results file name (without extension) ');
        readln(name);
        for i:=1 to length(name) do
          name[i]:=upcase(name[i]);
        name:=name+'.CPS';
        assign(results,name);
        rewrite(results);
       end
       else
        append(results);
    writeln(results,'0  processed results from ',filename1,' and ',filename2);
    writeln(results,'test no. date    time    sail no. baro press');
    writeln(results,testno:3,'    ',day:2,'-',month:2,'-',year:4,'  ',
                  hours:2,':',minutes:2,'  ',sailnumber:3,'    ',baropress:7:3);
    write(results,'      line  apprnt heel height',
                    '  temp  q  reads turb hupmast');
{     write(results,' Vsz                                              ',
      '            ');
      write(results,' F                                                ',
      '            ');
}     write(results,' CF                                               ',
      '            ');
{     write(results,' cwa');        }
      writeln(results);
    for i:=1 to count do
    begin
      write(results,i:3,linenumber[i]:6,apparent[i]:8:2,heel[i]:6:1,
            height[i]:7:2,temperature[i]:6:1,q[i]:5:1,reads[i]:3,
            turbulence[i]:5,heightupmast[i]:7:1);
{     for j:=1 to noofchs do
        write(results,Vsz[i,j]:11:7);
      for j:=1 to noofchs do
        write(results,F[i,j]:11:7);
}     for j:=1 to noofchs+1 do
        write(results,CF[i,j]:11:7);
{     for j:=1 to noofchs+1 do
        write(results,cwa[i,j]:11:7);                                }
      writeln(results);
    end;
    close(results);
  end;  {  end of procedure saveresultsinafile  }


  function finished:boolean;   {  finished all files?  }
```

```
begin
  write('process another file (y/n) ? ');
  repeat
    ch:=upcase(readkey);
  until ch in ['Y','N'];
  finished:=(ch='N');
end;

{  main  }

begin
  set_up;
  repeat
    get_file;
    extractdata;
    supplyvoltages;
    findzeros;
    correctdata;
    saveresultsinafile;
    filecounter:=filecounter+1;
  until finished;
end.
```

SSSU 55
ISSN 0140 3818

UNIVERSITY OF SOUTHAMPTON

DEPARTMENT OF SHIP SCIENCE

FACULTY OF ENGINEERING AND APPLIED SCIENCE

WIND TUNNEL TESTS ON A 1/16TH-SCALE LASER MODEL

by

Dr. R.G.J. Flay
Visiting Senior Lecturer

Ship Science Report No. 55

June 1992

WIND TUNNEL TESTS ON A 1/6th-SCALE LASER MODEL

By Dr. R.G.J. Flay
Visiting Senior Lecturer*

Ship Science Report No. 55

* On Sabbatical leave at Department of Ship Science from The University of Auckland, New Zealand, January - June 1992.

SUMMARY

An analysis of full-scale wind structure relevant to sailing yachts is carried out in order to develop a target model for wind-tunnel simulations. Unavoidable differences between real onset yacht flows and idealised wind-tunnel simulations are pointed out. Detailed measurements of the actual wind-tunnel flows developed for the present tests are discussed in depth, and are compared to idealised cases, concluding that although the simulations are not as good as physically possible, they are perfectly adequate for the present test programme.

Measurements of the forces and moments acting on a 1/6th scale model of a Laser yacht for apparent wind directions of 30 and 60 degrees, for heel angles of 0, 10, 20, and 30 degrees, and for smooth and turbulent sheared flow are presented. The results are discussed in terms of sail aerodynamics, and a transformation procedure is developed which leads to an excellent collapse of the measured results on the basis of calculated sail lift and drag coefficients.

ACKNOWLEDGEMENTS

I should like to thank Professor W.G. Price, Head of the Department of Ship Science for his support and encouragement, and for making the facilities of the Department available to me during my January to June 1992 Sabbatical Leave in the Department of Ship Science.

At the inception stage of the test programme reported herein, the help of Dr. A.F. Molland was invaluable in sorting out various pieces of hardware, especially a suitable balance (dynamometer). Mr. S.R. Turnock contributed significantly by writing a data acquisition program to drive the balance voltmeter, and then by actually running the program during the testing phase. Thanks also to Mr. G. Baldwin for operating the wind-tunnel throughout the tests and for making the many adjustments to the model setup.

The discussions with Dr. J.F. Wellicome and Mr. I.M.C. Campbell concerning model yacht-sail wind-tunnel testing procedures, and sail aerodynamics were of much interest, and very helpful. The data analysis could not have advanced without the help of Mr. P.A. Wilson in sorting out my various problems in learning to operate the Departmental computers.

I should like to thank Mrs. Sue Garside for typing this report, and for carrying out the necessary tasks for its completion after the end of my Sabbatical Leave in the Department.

Finally, I should like to thank my wife Linda for taking on the lion's share of looking after our young family away from home during my Sabbatical Leave.

CONTENTS

1. INTRODUCTION

The wind tunnel is a very useful tool for carrying out tests on yacht models to enable predictions of full-scale performance to be made. However, aerodynamically yachts are very complicated devices and there is not necessarily a one to one correspondence between wind tunnel performance measures and real performance of the full-scale prototype. This arises through a variety of reasons, but is mainly due to the difficulty of adequately simulating the full-scale onset flow to the yacht in the wind tunnel where the model is stationary. Other difficulties arise such as getting adequate sail shapes when the models are too small.

A practical difficulty when undertaking wind tunnel tests is deciding on appropriate sail configurations to test. A sail requires a minimum of say 10 variables to specify its shape, and to cover various ranges of heel angle and apparent wind angle, as well as wind speed requires an inordinate number of individual tests unless simplifications are made.

One outcome of the Conference on The Science of Sail Design at the University of Western Ontario, in June 1982 (Ref. 1) was that it was agreed that a "standard" sail should be selected and tested to enable comparisons to be made among the results from different facilities. This is done in calibrating Aeronautical wind-tunnels (standard AGARD models) and Wind Engineering wind-tunnels (CAARC model). The laser yacht (Fig. 1) was selected as the standard because it simply has a single mainsail, and it is a very common design worldwide.

Following on from some earlier wind-tunnel investigations where America's Cup designs had been tested by the Mechanical Engineering Department at the University of Auckland, (12 metre and K class designs), it was decided that a detailed study of various shapes of mainsails flying on a Laser model would be carried out. This study was carried out as a Master of Engineering research project (Ref. 2), and involved the systematic testing of a large number of different sails in different configurations on a 6th scale model Laser yacht, with a stiff cantilevered mast (Fig. 2). It was felt that it would be useful to continue the tests on this model, concentrating in particular on the effects of heel. Thus the present studies of the effects of heel, and also the effects of testing in smooth and a turbulent shear flow, were carried out at the University of Southampton in the 7'x5' wind-tunnel while the author was there during part of his Sabbatical leave, January - June 1992.

The test programme on which this report was based was carried out during the 7th, 8th and 9th of April, and although it would have been desirable to have had a longer test period, this was not possible due to the pressure of wind-tunnel bookings for commercial testing.

The report describes the apparent wind structure of the onset flow in full scale and points out the simplifications which have to be made in practical wind-tunnel tests. It then presents the actual wind-tunnel flow, and discusses how this differs from the flow which was ideally desired. The results are then presented and analysed and compared to relevant results in the literature. The effectiveness of the method used to non-dimensionalise and collapse the results is discussed.

2. APPARENT WIND STRUCTURE

2.1 Velocity Profile

The apparent wind structure seen by the sailing laser depends on the true wind speed, and the direction the yacht is heading. This study will be confined to the upwind sailing case, and it will be assumed that the true wind speed, V_S = 5 m/s = 9.7 knots, a fairly pleasant wind speed for sailing. Furthermore, it will be assumed that this speed

applies at a reference height of 40% of the mast height of 6m, or 2.4m, as it has been found previously that the centre of pressure of sails is around this height. Assuming that the true wind angle β_T is 45° and the boat to true wind speed ratio,

$$\frac{V_s}{V_T} = 0.5 \tag{1}$$

gives the velocity triangle shown.

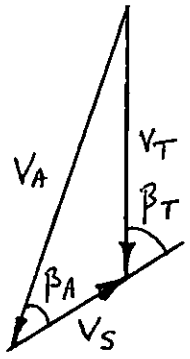

$$V_A = (V_s^2 + V_T^2 + 2V_s V_T \cos\beta_T)^{1/2} \tag{2}$$

$$\beta_A = \sin^{-1}\left(\frac{V_T}{V_A}\sin\beta_T\right) \tag{3}$$

Thus the apparent wind speed is

$$V_A = (5^2 (0.5^2 + 1) + 2 \times 0.5 \times 5^2 \cos 45)^{1/2}$$

$$V_A = 6.995 \text{ m/s}$$

and

$$\beta_A = \sin^{-1}\left(\frac{5}{6.995}\sin 45\right)$$

$$\beta_A = 30.4°$$

The drag coefficient of the water surface, and consequently the roughness length, Z_o, depends on the mean wind speed, as increased wind speed (and fetch) increases the height of the waves, and consequently the surface roughness. However, aerodynamically waves turn out to be very smooth, probably because they are rounded, and in general are translating in the mean wind direction. One correlation for roughness length as a function of the mean wind speed at a height of 10m, V_{10} is available in Cook (Ref. 3) and is

$$Z_o = 5\text{x}10^{-5} V_{10}^2/g \tag{4}$$

At elevations below about 50-100m, in the absence of thermal effects, the true wind velocity profile is described by the simple log-law

$$\bar{V} = \frac{U^*}{0.4} \ln \frac{Z}{Z_o} \tag{5}$$

Guessing that Z_o = 0.2mm allows the speed at 10m height to be estimated

$$\frac{\bar{V}_{10}}{5} = \frac{\ln \frac{10}{0.0002}}{\ln \frac{2.4}{0.0002}}$$

giving $\bar{V}_{10} = 5.76$ m/s

and hence $Z_o = 5x10^{-5} (5.76)^2/9.81$

$= 0.17$mm

which is close enough, so we shall assume $Z_o = 0.2$mm for subsequent calculations.

The motion of the yacht affects the "apparent" roughness length Z_A, as the sails are of course sensitive only to the apparent wind formed by the vector sum of the boat speed and true wind speed. Sailing upwind tends to flatten the velocity profile as far as the yacht is concerned, whereas sailing downwind tends to make it more non-uniform. For the rather contrived cases of sailing directly upwind or downwind ($\beta_T = 0$ and 180° respectively) the effect of hull motion on the incident wind is simply to modify the actual roughness length Z_o to an apparent roughness:

$$\frac{Z_A}{Z_o} = \frac{1}{f} \text{ (upwind)} \quad ; \quad = f \text{ (downwind), where } f = (\frac{h}{Z_o}) \frac{Vs}{V_T} \qquad (6)$$

where h is the reference height, in this case 2.4m.

For the present case, if β_T were 0°, the apparent roughness length would be

$$Z_A = 0.2/(\frac{2.4}{0.0002})^{0.5}$$

$$= 0.002\text{mm}$$

or reduced by a factor of about 100. If β_T were 180°, Z_A would be increased to about 20mm.

For the real upwind case the situation is more complicated, and the apparent wind varies in speed and direction with height so that the velocity profile appears twisted. The variation of apparent wind speed with height is given by

$$V_A(Z) = (V_s^2 + V_T(Z)^2 + 2V_s\, V_T(Z) \cos\beta_T)^{1/2} \qquad (7)$$

where from (5)

$$V_T(Z) = \frac{0.213}{0.4} \ln \frac{Z}{0.0002} \qquad (8)$$

and

$$\beta_A(Z) = \sin^{-1} (\frac{V_T(Z)}{V_A} \sin \beta_T) \qquad (9)$$

Apparent speed profiles for various values of β_T, and $V_S/V_T = 0.5$ are given in

Fig. 3, in conjunction with the true wind velocity variation with height. When extrapolated to zero speed, it is clear how the apparent roughness length is diminished for upwind cases, and increased for downwind cases. When the speed profiles are normalised by the speed at a height of 10m, the differences are more apparent (Fig. 4). The real upwind case where β_T = 45° has quite a similar velocity profile to the contrived case where β_T = 0. The biggest changes occur for downwind cases, and this can be seen more clearly in Fig. 5 where the height axis is linear, and the speed is dimensionless.

The variation of apparent wind direction (ideally) is shown in Fig. 6. For upwind cases the variation in direction is small, but it increases as β_T increases. The difference in wind direction with height (i.e. twist) with respect to the wind direction at 0.5m height (near boom) is shown in Fig. 7. Here, the angle scale has amplified the change in direction compared to the previous figure, and whereas for β_T = 30° the change in direction over the sail is only a few degrees (2), when β_T is 150° it is increased to almost 13° twist. In practice, wind twist may be less than indicated here for the upwind case and more for the downwind case, due to the flow tending to accelerate at low levels as it rises to pass over the hull. In so doing, the velocity component perpendicular to the hull centreline is increased which causes this effect. (Ref. 4).

The preceding comments illustrate that there is some legitimacy in conducting wind tunnel tests of yachts sailing upwind as far as the velocity profile is concerned, but that for the downwind case, the compromises required will be more severe.

For the present example where it is desired to simulate the flow for a yacht sailing upwind with (say) β_T = 45°, the speed profile should be based on a log-law distribution, with Z_o around 0.002mm in full-scale. Since the test model is one-sixth of full-scale, this means that Z_o in the wind-tunnel should be 0.002/6 $\simeq$ 0.0003mm, a very small value. The wind speed variation over the height of the sail is thus relatively small, but is nonetheless still significant.

2.2 Turbulence Intensity

The wind engineering community accepts (Ref. 5) that it is essential to model the spectrum of turbulence (Ref. 6) accurately in building aerodynamic studies in order for the model flow field to truly represent full-scale. This is because turbulence in flow has two aerodynamic effects. It promotes early transition of laminar boundary-layers (Ref. 7), and it must therefore be modelled correctly to reproduce boundary layer behaviour in attached flow, and the associated pressure distributions and occurrence of separation. Turbulence also increases the rate of entertainment in shed shear layers in separated flows, thus reducing their radius of curvature (Ref. 8). In turn this affects the pressure in the wake, or base pressure, which can increase or decrease depending on the afterbody shape and can even change the direction of lift on certain bluff bodies by promoting reattachment and thus altering the direction of the wake. In wind tunnel studies of buildings, the state of the boundary layers on the model is not usually significant in determining the loads, except in certain cases where the shapes are very rounded, and the main function of turbulence modelling in the wind tunnel flow is to reproduce wakes and separation bubbles which mimic full-scale behaviour.

Surprisingly, most vehicle aerodynamic studies have been done in relatively low turbulence wind tunnels (Ref. 9), when one would expect from wind engineering studies that the turbulence generally present in flows onset to vehicles (except for the case of no traffic and no wind) would affect the aerodynamic behaviour. Recently some analysis of the turbulence relevant to vehicles has been carried out (Ref. 10), and it is likely that this point will receive more attention in the future with the drive towards cars with good handling and low drag in the normal situation of turbulent onset flow.

Yachts can only sail when it is windy, and since they operate at the bottom of the earth's boundary layer, they always operate in a turbulent shear flow. As shown in the

previous section, the sea is aerodynamically quite smooth, and this means that over the range of typical mast heights, the turbulence intensity will be of the order of 10%, much less the 15-40% typical for buildings.

The effect of atmospheric turbulence on full-scale sails is not known with certainty, and indications in the literature are confusing. For example, in Ref. 11 it was found that the critical Reynolds number for the drag of a sphere was not affected by atmospheric turbulence whereas in wind tunnels it was found that a small amount of fine scale turbulence had a major effect on the resulting coefficients. Since it is not known what effect it really has on yacht sails, it is difficult to say whether it is important to model it accurately in wind tunnel simulations.

In the author's work, a pragmatic approach has been taken where it has been attempted to model as well as possible the approach turbulence as seen by the moving yacht in full-scale. Since to the author's knowledge there are no published data of turbulence measured by a sensor attached to a sailing yacht, it is useful to try to deduce what the appropriate turbulence level is to give guidance on what it should be in the wind tunnel. The following analysis for the Laser yacht under consideration follows the method developed in Ref. 12.

The turbulence has to be considered with respect to a moving reference frame attached to the yacht. This is similar to the approach taken in Ref. 13 concerning turbulence with respect to moving ground vehicles. The yacht motion, however, can be considered as consisting of two parts, a mean part, plus a dynamic part. The dynamic part occurs because the yacht *reacts* to turbulence, particularly large low frequency gusts, and thus it performs a filtering function.

Rectilinear translation of a vessel through the boundary layer does not alter variance of the turbulence, provided that the relative velocity of the vessel to the wind is not less than one third of the mean wind speed. This assumption is therefore valid for a vessel speed of half the mean wind speed, except at very low heights when sailing downwind where the relative wind speed becomes very small (Ref. 14). It does change the apparent frequency of the turbulence however. Using the analysis of Ref. 13, it can be seen in Fig. 8 that for sailing upwind ($\beta_T = 0°$) the apparent frequency is increased and vice versa for downwind ($\beta_T = 180°$) compared with the stationary yacht case.

These atmospheric wind spectra illustrate that most of the turbulence is at relatively low frequencies, in the region of 0.01 Hz or 1 cycle in about 2 minutes. For a Laser yacht, which reacts quickly to "gusts" this is a very low frequency. The helmsman continually alters the orientation of the Laser to generally keep the heel angle roughly constant, and he would see a gust at this low frequency as simply a variation in the mean wind speed. A cut-off frequency between high frequency turbulence likely to be important in sail aerodynamics, and low frequency turbulence can be deduced if, for example, it is assumed that gusts with wavelengths greater than say 10 boat lengths are simply changes in the same wind speed. For a yacht length of say 4m, this is $\lambda = 40$m, and for an apparent wind speed of say 5m/s, a gust of this wavelength would take 8 seconds to pass the boat. Changes in the boat's heading will filter out changes in wind direction, whereas low frequency changes in speed are not really filtered out, just assumed to manifest themselves as changes in mean wind speed. Furthermore, rather surprisingly, it was found in Ref. 8 that the wake behaviour behind bluff models in turbulent flows could be reproduced by introducing a wire upstream of the model on the stagnation streamline. From this it would also appear that fine-scale turbulence is also the key in controlling wake behaviour.

Based on the aforementioned arguments, we shall then deduce the relevant part of the turbulence spectrum as far as the yacht is concerned, on the premise that the high frequency part is the most important. If we suppose that the yacht acts like a first-order high-pass filter, with a half-power point at n_c, then the effect on the wind spectrum is as

illustrated for the stationary yacht case in Fig. 9. Here it has been assumed that $n_c = 1/8 = 0.125$ Hz, but this was a somewhat arbitrary selection.

This means that much of the turbulence in the normal atmospheric wind spectrum can be omitted, as frequencies less than about 0.03 Hz are not that important, leaving only the high frequency part. This is an enormous help, because it is the large low frequency eddies which are most difficult to generate in wind tunnel simulations, usually requiring rather lengthy test sections. We need only generate some suitable fine scale turbulence, and this can be done using bars and grids in a relatively short test section.

It can be shown by integration of the filtered spectrum in Fig. 9 that the contribution to the turbulence variance is reduced to about

$$\sigma_{uf}^2 = 0.16\, \sigma_u^2, \tag{10a}$$

so,

$$\sigma_{uf} = 0.4\, \sigma_u \tag{10b}$$

It turns out that the turbulence variance is not affected by apparent wind direction (unless the relative wind speed becomes too small, as mentioned earlier), but the apparent turbulence intensity $T_{uf} = \sigma_{uf}/V_A$ *is* affected by translation of the yacht because this changes the apparent wind speed in the denominator.

If it is assumed that the apparent velocity profile can be described by a log-law with suitable choice of apparent roughness length, i.e.

$$\frac{V_A}{u_*} = \frac{1}{k} \ln \frac{Z}{Z_A}, \tag{11}$$

(where k is von Karman's constant = 0.4).

and further, if it is assumed that

$$\sigma_u = 2.5\, u_* \tag{12}$$

as observed by measurement (Ref. 15), then the apparent turbulence intensity for a yacht, as a function of height, is given by

$$Tu_{Z,\,A} = \frac{0.4}{\ln \frac{Z}{Z_A}} \tag{13}$$

Turbulence intensity profiles for upwind, downwind and yacht stationary conditions are plotted in Fig. 10. For the upwind case, it can be seen that the idealised turbulence intensity should be about 3%.

3. TURBULENCE GRID DESIGN

The normal procedure at the University of Auckland for creating a sheared, turbulent onset flow for yacht studies is to generate it with a grid of appropriately spaced circular bars spanning the test section upstream of the model. A computer program from Ref. 16 using methods based on theories by Cowdrey, and Owen and Zienkiewicz was used for this purpose. A listing is given in Appendix 1, along with input and output from the present run.

The program requires the user to input a power index n to describe the velocity profile shape, i.e.

$$\frac{u}{u_{ref}} = \left(\frac{Z}{Z_{ref}}\right)^{1/n} \tag{14}$$

the test section height in inches, h, a value for the pressure drop coefficient k0, the bar diameter in inches, and an error tolerance.

In the present design 5/8" diameter aluminium alloy tubes were used as they were readily available. By curve fitting a power-law profile to the ideal log-law profile in the sail region (Fig. 11) a value n=12 was selected. For the 7'x5' test section, h=60, and by trial and error it was found that k0=0.25 and tol=0.002 gave 16 bars which appeared to offer reasonable blockage. A schematic drawing of the grid is shown in Fig. 12.

It needs to be noted at this point that the grid design method does not consider turbulence, and the selection of the pressure drop coefficient, and tube diameter has to be done on the basis of experience in order to attempt to get the correct turbulence levels.

4. THE FLOW SIMULATION

4.1 Data Acquisition and Analysis

The flow simulation was measured by attaching a hot-wire and pitot-static probe to a traversing rig borrowed from Wolfson MTIA as shown in Fig. 13. The pitot-static probe was connected to a Betz manometer and pressures recorded manually, whereas the hot-wire output was connected to an analogue to digital input channel on a CED 1401, an Intelligent Interface, manufactured by Cambridge Electronic Design Ltd., Science Park, Milton Road, Cambridge CB4 4FE. The voltage output from a potentiometer on the traverse, attached to the screw thread, and giving a signal proportional to height above the floor was also connected to a CED A/D analogue input channel. The CED was driven by a program called TURBOAD written by Wolfson MTIA staff.

After appropriate calibration, text-files of heights and corresponding means and standard deviations of the hot-wire voltages were created. Each data point corresponded to measurements at 100 Hz for 20 seconds. This process allowed velocity and turbulence intensity profiles for the smooth flow (grid out) and turbulent flow (grid in) cases to be obtained at the model test position near the downstream end of the test section (see Fig. 13). The manually tabulated pitot-static probe readings confirmed the accuracy of the hot-wire for the mean velocity measurements.

In addition, at heights above the floor of 200, 400 and 800mm, 16384 samples were saved in separate files to enable the power spectral densities to be evaluated. These data were obtained at a sampling frequency of 2000 Hz with a low pass filter setting of 1000 Hz

4.2 Velocity and Turbulence Profiles

In Section 2.1, it was argued that Z_A for the upwind sailing case should be about $2x10^{-6}$m. At 1/6th-scale in the wind tunnel, this gives

$$Z_{Am} \simeq 3x10^{-7}m.$$

The vertical profile measurements were taken when the reference pitot-static probe (mounted upstream of the turbulence grid about 200mm from the wall, 1m above the floor, on the left hand side looking upstream) measured a pressure difference of 3mm of water. At the test position reference height of 40% of mast height, taken as 400mm above the floor, this gave a velocity of about 7m/s. This can be seen in Fig. 15 which shows the 2 sets of smooth flow results, and one set of turbulent flow measurements. A curve corresponding to the ideal case is also shown ($Z_{Am} = 3x10^{-7}$m) which has been matched to the measured turbulent profile at 400mm height. The agreement is good for the height range 200 - 900mm, but is poor at lower heights. The same results are shown in Fig. 16 with power-law axes, and in Fig. 17 with log-law axes.

Since they both have log height axes, Figs. 16 and 17 expand the graphs at lower heights, exaggerating the differences between ideal and measured. Clearly the measured profiles are not as good as they might be, although in Fig. 17, extrapolating the velocity profile curve downwards from readings about Z = 200mm would give an estimate for Z_{Am} close to that actually desired.

It is clear that the velocity profiles are all too low at low levels. There is even quite a boundary layer for the smooth flow case as well. The reason for the discrepancy in the turbulent flow case probably lies partly with the grid design program which assumes uniform onset flow to the grid. The distance from the grid to model was 3.5m, which also gives the boundary layer plenty of fetch to thicken. A step in the floor height of around 100mm at the front of the moving belt ground plane could have also produced a separation bubble, thus thickening the boundary layer as well. The suction system to bleed off this boundary layer was not used in the present tests.

The measured turbulence intensity profiles are compared with the ideal upwind profile in Fig. 18. This figure shows the good flow quality of the test section in the smooth flow case away from the floor, where the turbulence intensity is typically about 0.2%. As for the velocity profile, the idealised and measured turbulent profiles agree quite well at heights above about 200mm, but at lower heights the actual flow is far too turbulent. This applies to the grid out results too, for heights below about 100mm.

These results indicate that the grid tube density was too high near the ground, and that the model was placed too far downstream in the test-section. Unfortunately, it was not possible within the test programme to right these two problems. There was no time available to re-test with a different turbulence grid, and the model had to be located at the downstream end of the test section because the moving belt ground plane was installed in the test section floor and was not able to be removed for these two tests. Thus measurements of forces and moments on the Laser model were taken with the onset flow as it is shown here.

4.3 Wind Spectra

The turbulence grid design method does not consider turbulence at all, just the velocity profiles. Spectra at heights of 200, 400 and 800mm above the floor were therefore measured at the model test location to see if they had any resemblance at all to the desired shapes developed in Section 2.2.

16384 samples were obtained at 2000 Hz at each height, and these were then analysed as 8 blocks of 2048 samples. A fast Fourier transform was run on each of the 8

blocks. The 8 spectral estimates at each frequency were then averaged to reduce the standard error. In addition, the samples were averaged over frequency as well, over 13 equal log-frequency bands, to finally give 13 spectral estimates. Since there are more samples in each band at higher frequencies, the statistical reliability of the estimates improves as frequency increases. These spectra had a bandwidth from f_1 = 2000/2048 = 0.977 Hz to f_2 = 2000/2 = 1000 Hz.

In order to improve the statistical reliability of the results at frequencies around 1 Hz, it was decided to digitally filter the raw samples by simply adding each eight consecutive samples up to obtain new samples approximately equivalent to sampling at 1000/8 - 125 Hz, resulting in one block of 2048 samples for each height. Spectral estimates were therefore also obtained for these lower frequency samples over the bandwidth f_3 = 125/2048 = 0.06104 Hz to f_4 = 125/2 = 62.5 Hz. Block averaging obviously could not be carried out, but frequency averaging over 13 equally spaced log-frequency bands was carried out as before.

The resulting smoothed spectra can be seen in Fig. 19. Pairs of full and dotted lines correspond to the measured spectra. There is reasonable agreement where each set overlaps, which confirms that the averaging process used to obtain the larger bandwidth overlapped spectra behaved properly. Spectra at 800mm height were very similar to the 400mm curves, so are not shown to improve readability. It can be seen that the peak of the 200mm height spectrum is at around 6 Hz, and the peak of the 400mm spectrum is at around 20 Hz, some 3 times higher. However, the idealised spectrum has a peak at around 1-3 Hz which is much lower. This curve is the same one as the dotted curve in Fig. 9 except that it has been normalised so that the area under it is unity, and it has been shifted on the frequency axis to preserve the correct reduced frequency, i.e.

$$\left(\frac{nL}{V}\right)_{model} = \left(\frac{nL}{V}\right)_{full\text{-}scale}$$

$$n_m = n_{fs}\left(\frac{V_m}{V_{fs}}\right)\left(\frac{L_{fs}}{L_m}\right)$$

Thus, $n_m \simeq n_{fs}\,(1)\,(6)$

$$n_m \simeq 6n_{fs}$$

It is clear that the bar grid generates turbulence at too high a frequency by a factor of about 8. The vortex shedding frequency of the bar can be found from the Strouhal number, giving

$$n_s = 0.2\,\frac{V}{D}$$

For V = 7m/s and D = 5/8" = 15.87mm

$$n_s = 0.2 \times 7/0.016$$

$$= 88 \text{ Hz.}$$

It is interesting, and perhaps rather surprising that there is no evidence of the bar

vortex shedding frequency in the spectra. This is probably because the measurements were taken some 220 bar diameters downstream of the turbulence grid.

To summarise, it can be seen that the turbulence simulation is not particularly good as far as its spectral content is concerned, and that larger bars, or possibly some other method is required to generate turbulence spectra which resemble the desired shapes more exactly. However, the variance of the turbulence is only slightly less than that desired ideally.

5. MODEL AND SAIL DETAILS

The model used in this, and the earlier study (Ref. 2) at the University of Auckland was a simplified 1/6th scale model of a Laser sailing dinghy. A rigid mast made of a uniform 11mm OD steel tube was used rather than a scaled down version of the flexible prototype. The mainsail was attached with a bolt-rope to a thin slot cut in the mast. It was cantilevered in two deep-groove roller bearings located inside the hull, and was thus able to rotate freely. The model mast height was 1m (measured from heel axis near the hull bottom to the top of the tested sail).

Sail trim was adjusted using electric winches located inside the hull which controlled mainsheet and boom vang tension. During testing it was found that the boom vang winch was not powerful enough, and it was difficult at times to get enough leach tension. The mainsheet winch worked well. The mainsail foot was attached to the boom by an outhaul at the clew only. No gap between the sail and boom resulted from this means of attachment.

The test rig was attached to the balance as shown in Fig. 20 by an arrangement which allowed vertical height adjustment, and rotation about the heel axis fitting near the bottom of the hull. The hull could be separated to give access to the winches and heeling mechanism. During testing the model was located in a circular cutout in the test section floor. A cardboard surround was taped over most of this, leaving a vertical gap of less than 5mm between the hull and surround. When the hull was heeled to 20 and 30°, it was raised on the 4 threaded studs as required so that there was no contact between it and the test-section floor. This vertical height shift was measured so that the actual distance between the balance horizontal axis and the reference axis (taken as the heel axis near the hull bottom) could be used in subsequent moment calculations.

The mainsail was constructed from the lightest grade of Mylar sail cloth obtainable at the time. Initially the Sailmaker (TM) sail mould development program was set up to plot the required panels on sail cloth, however, as the seam shape was so small, the plotted panels were not of sufficient accuracy. Thus based on the advice of a local NZ sailmaker, a more old fashioned method was adopted, as described below.

The approximate outline of the complete mainsail was marked out on a single sheet of sailcloth. Using cross-cut panels, the seam shape (curve) and taper were marked out at various luff heights. Seam shape was drawn using a flexible metal strip that formed the required curve across the chord. Keeping the curvature of the strip constant, the same form of seam curve could be drawn at various luff heights. By increasing the curvature, the camber (draught) could be increased, and by moving the location fore and aft, its chord-wise location could be shifted.

Individual panels were cut and joined. The curved panel edge was placed onto the straight panel edge of the adjacent panel which had double-sided tape attached. After the panels were joined, the correct luff curve for the mast was drawn on the developed mainsail. Finally, the leech curve was drawn to form the final planform of the mainsail.

The sail used in the present tests had a 913mm luff, a 360mm foot, a luff/foot ratio of 2.5 and a maximum camber of about 13% at 50% of the chord at a height of

about 33% up the luff. A reference area of 0.1642 m^2 was used for the tests. For moment coefficients a reference length of 1m was used, the distance between the heel axis fitting and the sail head.

6. BALANCE DETAILS

There was some difficulty in obtaining a suitable balance for the sail tests at the University of Southampton, as the low test speed required of around 7 m/s meant that the loads were much smaller than normally obtained in common wind tunnel tests there. Dynamometers used for keel tank tests were available, but could measure lift and drag only, whereas it was desired to measure heeling moment as well. In the end a compromise solution was reached whereby a 5-component (vertical force not measured) dynamometer developed especially for wind tunnel tests of rudders (Ref. 17) was used. It is a very strong and stiff dynamometer (hereafter referred to as balance), and is capable of measuring loads of about 100lbs. The rudder and skeg can be mounted and rotated independently on it. The overall balance can be seen in Fig. 21, and a cross-section showing the roll centres in Fig. 22.

The model yacht was mounted where the rudder is shown in Fig. 22, and the lower handwheel was used to alter the direction of the model (to obtain the desired test apparent wind angles) so that the yacht and balance axes were always parallel. In other words body, not wind axes were used. The top handwheel was used once only to centre the top balance plate for the tests.

The balance was extensively calibrated around 1977, and has not been recalibrated since. A check calibration was carried out to verify the repeatability and linearity of the balance for the rather small anticipated loads, and this was found to be good for lift, drag, and heeling moment, but the pitching moment output was clearly erroneous. This didn't matter, as measurements of pitching moment were regarded as of secondary importance.

The balance was repeatable to about $\pm 0.3\mu V$, and signals during testing of about $20\mu V$ were expected, giving an accuracy of about $\pm 2\%$.

7. DATA PROCESSING

7.1 Data Acquisition

The balance strain gauges were connected directly to a strain gauge amplifier and power supply (Manufactured by Fylde) by purpose built cables and plugs. This was connected to a very accurate Schlumberger voltmeter (Model No. 7061) which used a special patented averaging method to give average voltages from each channel to $0.1\mu V$. This unit was controlled from software written by Stephen Turnock, a Research Fellow in the Department of Ship Science. This software scanned through each of the 5 data channels or the supply voltage channels the number of times specified (usually 10) and recorded the resulting voltages, averaged over the (say) 10 consecutive scans to 7 decimal places in an ASCII text file. In addition, information concerning the test was added as needed, such as heel angle, wind on or off, turbulence grid in or out etc.

A separate file was obtained for each test, (eg for a particular apparent wind angle), where each file simply contained the unprocessed voltages and experiment information as described above. This hard copy allowed "by hand" verification to be made of the software used to analyse the test data files.

7.2 Preliminary Data Reduction

The data acquisition program had been adapted from a version used for rudder tests, and as such, it actually recorded some additional extranious information which was

not required in the present work. A program called EXTRACT was developed by the writer to extract only the pertinent mean results for the present tests, and the experiment information, and to write them to a file. The data were then scaled for variation in the supply voltages V_s, and zero offset voltages V_o in all channels, assuming a linear variation in these values with scan number between measurements of them. Thus the recorded bridge voltage V_T was scaled to give a voltage V proportional to the applied force at the original calibrated voltage V_c:

$$V = (V_T - V_o) \times V_c/V_s$$

The original calibration of the balance in Ref. 16 quantified the interaction between the five components of the balance. The matrix expression given below uses the interaction matrix and incorporates the calibration constants to give the sideforce, thrust, yaw, roll and pitch (F_1 through F_5 respectively) in N and Nm.

$$\begin{bmatrix} F_1 \\ F_2 \\ F_3 \\ F_4 \\ F_5 \end{bmatrix} = \begin{bmatrix} 0.338035 & -1.1881\times10^{-03} & -3.952\times10^{-04} & -1.4848\times10^{-03} & -3.2605\times10^{-03} \\ 2.12\times10^{-05} & 0.252512 & -6.659\times10^{-04} & 1.6823\times10^{-03} & -9.901\times10^{-04} \\ -1.82\times10^{-04} & 2.845\times10^{-04} & 3.9366\times10^{-02} & 1.344\times10^{-04} & 3.2\times10^{-04} \\ 7.002\times10^{-04} & -2.37\times10^{-05} & -3.4036\times10^{-03} & 6.34925\times10^{-02} & 2.049\times10^{-04} \\ -3.3\times10^{-06} & 6.333\times10^{-04} & 1.47\times10^{-05} & -3.008\times10^{-04} & 4.8468\times10^{-02} \end{bmatrix} \begin{bmatrix} V_1 \\ V_2 \\ V_3 \\ V_4 \\ V_5 \end{bmatrix}$$

where V_1 - V_5 are the corrected balance voltages in μV.

However, there was one "fiddle" done in the application of the interaction matrix. As noted previously, the pitching moment voltage V_5 was incorrect, and it was felt that this incorrect voltage would generate errors in the other channels through the interaction matrix. To eliminate the source of error, an estimate of what V_5 should have been was made, based on the thrust voltage V_2 by assuming that the pitching moment was due entirely to the thrust force acting at 40% of the mast height.

$$V_5 = 0.2525 \times V_2 \times h/4.84685 \times 10^{-2}$$

where h is the vertical height above the balance axis of a point 400mm along the mast. V_5 was estimated as shown before the balance matrix was applied to each set of corrected balance voltages.

The next manipulation to the data was to move the moment centre from the balance to the reference centre in the boat. This was defined to be the point corresponding to the intersection of the mast and the heel axis. This point was 0.085m in front of the vertical axis of the balance, and 0.122+h above the balance axis, where h is a variable distance which depended on heel, and was measured at each test. Moments based on the yacht reference centre were calculated as follows from the forces and moments (F_1 - F_5) resulting from application of the interaction matrix.

$$M_3 = F_3 + 0.085 \times F_1 \text{ (yaw)}$$
$$M_4 = F_4 - F_1 \times (0.122 + h) \text{ (roll)}$$
$$M_5 = F_5 - F_2 \times (0.122 + h) - F_6 \times 0.085 \text{ (pitch).}$$

F_6 is the estimated vertical force (positive downwards) assuming that the sideforce acts perpendicular to the mast, i.e.

$$F_6 = F_1 \times \tan \phi$$

where ϕ is heel angle.

M_3 and M_5 are of no real interest; indeed pitch was measured incorrectly, but

they were processed in any event for completeness.

The final part of the preliminary data reduction was to convert the measured forces and moments into coefficients. Since all tests were done with the wind tunnel pitot-static probe measuring 3mm of water, this was done with the following set of equations:

$$
\begin{aligned}
C_s &= F_1/3 \times 9.81 \times A \times r \\
C_t &= F_2/3 \times 9.81 \times A \times r \\
C_{ym} &= M_3/3 \times 9.81 \times A \times r \times L \\
C_{rm} &= M_4/3 \times 9.81 \times A \times r \times L \\
C_{pm} &= M_5/3 \times 9.81 \times A \times r \times L \\
C_v &= F_6/3 \times 9.81 \times A \times r
\end{aligned}
$$

where the reference area A = 0.1642 m^2 and the reference length for moments L = 1m. r is the ratio of the dynamic pressure at a point 400m along the mast from the heel axis to the dynamic pressure on the wind tunnel probe. For smooth flow r = 1.03. For turbulent flow r varies with height above the wind tunnel floor, h. Curve fitting the turbulent flow calibration velocity profile in the region h = 400mm gave the following empirical expression for r:

$$r = 0.76239 + 0.0005326 \times h$$

where h here is height above the floor in mm.

The preliminary data reduction process described above resulted in force and moment coefficients based on the boat moment reference centre, where all the force and moment coefficients are in horizontal and vertical directions. These basic coefficients are manipulated in the following sections in order to collapse the data in a meaningful way.

8. MEASURED DATA

The preliminary data reduction process described in the foregoing results in the following coefficients of particular interest = C_t (thrust) and C_s (sideforce) in the horizontal plane, and C_{mh} (heeling moment). These are plotted as a function of heel in Figs. 23, 24 and 25.

The thrust coefficient in Fig. 23 for an apparent wind angle of 30° shows almost no variation with the range of heel angles tested from 0 to 30°. The coefficients for both the smooth and turbulent flow case also for this apparent wind angle show amazingly good agreement, and in all cases are about 0.4, with a slight drop to 0.3 for ϕ = 30°. Clearly the use of the dynamic pressure at 40% mast height works well. For the β_A = 60° results (smooth flow only measured) the coefficients are higher (around 1.0) and show a more significant drop for ϕ = 20 and 30°, which is well fitted by a cosine heel squared function.

The sideforce coefficients results in Fig. 24 do not show such a perfect collapse of the smooth and turbulent results for β_A = 30° as for thrust, but nonetheless, it is still good. The reduction in C_s with heel is fitted well by a cosine heel function. The C_s results for β_A = 60° show no consistent variation with heel. Not surprisingly, because the sail has been let out further, C_s for β_A = 60° is much less (about 2/3) of the β_A = 30° values.

The rolling moment coefficient (or heel coefficient) is due to the sideforce acting part way up the mast (about 40%), and to the vertical force acting out at some distance horizontally from the heel axis. Because it arises mainly from the sideforce, it can be seen that the variation of C_{rm} with ϕ (Fig. 25) is somewhat similar to the variation of C_s with ϕ (Fig. 24) although smaller. Note that Deakin (18) found that C_{rm} reduced

with ϕ according to $\cos^{1.3}\phi$. If it is assumed that the side and vertical force components act in such a way that the net force is perpendicular to the mast, then the height of application of this force can be estimated.

Referring to Fig. 26 we have:

$$C_{rm}\, L = C_S d\cos\phi + C_V d\sin\phi$$

and by assuming that

$$\frac{C_V}{C_S} = \tan\phi$$

it follows that

$$\frac{d}{L} = \frac{C_{rm}}{C_S(\cos\phi + \frac{\sin^2\phi}{\cos\phi})} = \frac{C_{rm}\cos\phi}{C_S}$$

The result of this calculation is shown in Fig. 27 for all test cases. Heel angle clearly has little effect apart from increasing the scatter at 30° heel and, on average, the force acts about 37% of the way along the mast, close to the 40% reported by many workers.

A similar kind of analysis cannot be applied to the thrust results to get its height of application because the balance measurements of pitching moment were in error.

9. SAIL AERODYNAMICS

The foregoing section merely discussed the display of the measured data, the only assumption being in Fig. 26 where it was assumed that the side component of the sail force acted perpendicular to the mast. The results verified that the dynamic pressure at 40% mast height gives a good collapse of the coefficients, and indeed, the results verified that the sideforce does in fact act near that height. However, one would really like to be able to predict the various coefficients at various heel angles and so on, based on a knowledge of the sail aerodynamics. In other words, it would be very convenient to be able to predict the performance of the sail rig at various heel angles from the results of measurements at a single heel angle.

In this section we will suppose that a yacht sail of given shape produces an aerodynamic force which can be described by conventional lift and drag coefficients which are a function of the angle of attack between a reference chord line on the sail, and the component of the wind resolved in a plane which is horizontal in the fore and aft direction, and inclined at the heel angle ϕ in the beam direction. It can be loosely described as the plane of the deck. It is convenient to sub-divide this angle of attack into two further angles, the effective wind angle, β_E which is the angle between the wind component and the centreline of the yacht, and the sail sheeting angle, δ, the angle between the yacht centreline and a reference sail chord line which we will take as the boom direction, measured in the deck plane. These angles are shown in Fig. 28.

In this inclined plane, and for a particular sail shape, we have

$$C_L = C_L(\beta_E - \delta)$$
$$C_D = C_D(\beta_E - \delta)$$

and from Fig. 28 it can be seen that the thrust (horizontal), and sideforce (inclined at ϕ) coefficients are related to the sail coefficients by

$$C_{T\phi} = C_L \sin \beta_E - C_D \cos \beta_E$$
$$C_{s\phi} = C_L \cos \beta_E + C_D \sin \beta_E$$

Resolving these into the horizontal plane gives

$$C_T = C_{T\phi} \text{ is already horizontal)}$$

$$\text{so} \quad C_T = C_L (\beta_E - \delta) \sin \beta_E - C_D (\beta_E - \delta) \cos \beta_E \qquad (1)$$

and since $C_s = C_{s\phi} \cos\phi$, it follows that

$$C_s = [C_L \cos \beta_E + C_D \sin \beta_E] \cos\phi \qquad (2)$$

Equations (1) and (2) enable the sail lift and drag coefficients to be deduced from measurements of C_s and C_T in the horizontal plane by the balance.

$$C_T = C_L (\beta_E - \delta) \sin \beta_E - C_D (\beta_E - \delta) \cos \beta_E \qquad (1)$$

$$C_s/\cos\phi = C_L (\beta_E - \delta) \cos \beta_E + C_D (\beta_E - \delta) \sin \beta E \qquad (2)$$

Re-arranging leads to

$$C_L (\beta_E - \delta) = \frac{C_s}{\cos\phi} \cos \beta_E + C_T \sin \beta_E \qquad (3)$$

$$C_D (\beta_E - \delta) = \frac{C_s}{\cos\phi} \sin \beta_E - C_T \cos \beta_E \qquad (4)$$

Further, by assuming that the heeling moment arises wholly from the elevated action of the sideforce, we get

$$C_{rm} L = C_{s\phi} h = \frac{C_s}{\cos\phi} h$$

where L is the reference length, and h is the height of application of the sideforce. Hence,

$$C_{rm} = \frac{h}{L} \frac{C_s}{\cos\phi} = \frac{h}{L} \left[C_L (\beta_E - \delta) \cos \beta_E + C_D (\beta_E - \delta) \sin \beta_E \right]$$

Finally, if the lift and drag coefficients in the wind tunnel axes are required, the following pair of equations carry out the rotation necessary (see Fig. 29):

$$C_{LW} = C_s \cos \beta_A + C_T \cos \beta_A$$

$$C_{DW} = C_s \sin\beta_A - C_T \cos \beta_A$$

The Effective Wind Angle, β_E

This angle was introduced above. We now consider its geometrical interpretation. We take the case of a yacht at an apparent wind angle β_A, apparent wind speed V_A heeled at an angle ϕ (see Fig. 30). The apparent wind velocity component parallel to the yacht centreline is $V_A\cos\beta_A$, and the component perpendicular to the centreline, and in a plane inclined at the heel angle ϕ is $V_A\sin\beta_A\cos\phi$. These two components form a right-angled triangle in the deck plane, and the effective wind angle, β_E, is given by

$$\tan\beta_E = \frac{V_A \sin\beta_A \cos\phi}{V_A \cos\beta_A}$$

whence $\beta_E = \tan^{-1}(\tan\beta_A \cos\phi)$

For β_A and $\phi < \sim 30°$ this can be approximated to

$$\beta_E = \beta_A \cos\phi$$

When the boom is out to leeward from the yacht centreline an angle δ, then the sail angle of attack is

$$\beta_S = \beta_E - \delta = \tan^{-1}(\tan\beta_A \cos\phi) - \delta$$

We now have a set of equations which enable the sail coefficients to be obtained from the balance measurements and presented as functions of $\beta_S = \beta_E - \delta$. If for a given sail shape the sail coefficients can be described by $C_L(\beta_S)$ and $C_D(\beta_S)$, then universal curves corresponding to these functions should be able to be obtained from wind tunnel measurements at various values of β_A, ϕ and δ. If a good collapse can be obtained, then this means that such results can be used in a predictive manner.

10. RESULTS AND DISCUSSION

As mentioned previously, the sail test programme involved two apparent wind angles β_A = 30 and 60°, 4 heel angles - 0, 10, 20 and 30°, and tests in both smooth and sheared turbulent flow. For each test case corresponding to a particular flow type and apparent wind angle the sail was set by adjusting the mainsheet and boom vang to get maximum thrust at nominally zero heel. The sail controls were not altered as the heel was changed, and the luff and foot tensions were not altered at all t hroughout the test programme. It was also found that in all cases the boom vang tension needed to be as tight as possible - the winch was driven until it stalled. In the β_A = 30° tests the boom was pulled in over the deck and the vertical component of the sheet tension tended to keep the sail leech tighter than for the β_A = 60° test cases where it had less effect and the leech twisted away more noticeably.

The model design used a rotating straight mast cantilevered from within the hull which was perpendicular to the heel axes. This means that, in theory, for a constant boom vang tension, altering the sheet tension (changing δ) should not alter the sail shape significantly - it should simply rotate with the mast. This was not quite the case in the present test arrangement because of the reduction in the vertical component of the sheet tension as δ increased, but nonetheless, it was decided to compare the β_A = 30 and 60° results as if they resulted from the same sail shape.

The sail lift and drag coefficients were calculated for all test cases and are shown plotted in Fig. 31. When β_A = 30°, the angle δ from the centreline to the boom was 5°, and when β_A = 60° it increased to 35°. Thus it can be seen that all results lie in the

relatively small sail angle range 20 to 25°. The lift coefficient is about 1.5 and the drag coefficient about 0.5. The smooth and turbulent flow results are in relatively good agreement which is somewhat surprising given the substantial differences between the flows. The β_A = 60° results show lower lift and higher drag coefficients.

The comparison between the two apparent wind angle results is not entirely fair because of the increased sail twist at β_A = 60° noted already. Some allowance for this can be made by simply setting δ to some larger effective angle. The effect of setting δ = 40° is illustrated in Fig. 32. This figure shows C_L reducing in a somewhat linear fashion towards 0 as β_E-δ is decreased, and the trend of C_D is now to increase at the same time.

It is clear now that the tests have been completed that it would have been useful to have had data for a range of smaller values of β_E-δ as well. To discover whether there are universal functions $C_L(\beta_S)$ and $C_D(\beta_S)$ for a particular sail shape for various values of ϕ, β_A and δ requires that the sail shape be maintained in all cases. For a Laser with a cantilevered mast this should be able to be achieved by keeping the boom vang tension constant. However, although such tests are interesting aerodynamically they are not particularly relevant to sailing where the sails are always adjusted for a given apparent wind angle to maximise thrust, providing the heeling moment is not too large. In fact, one can argue that the sails should be adjusted to maximise the ratio thrust/sideforce, corresponding to the low windspeed sailing condition, and to maximise thrust for a given sideforce (or heeling moment) in the case of the high windspeed sailing condition.

Nonetheless, the present results have illustrated that for β_A = 30° the sail coefficients, as defined herein, are virtually identical for the smooth and turbulent cases, and the β_A = 60° results show lower lift and higher drag, as could be expected from the somewhat more twisted shape in this test case.

11. CONCLUSIONS

The ideas of wind engineering and mechanics can be used to develop models of onset flow to sailing yachts. Such models show that it is more legitimate to wind-tunnel test yachts sailing upwind than downwind because in the former case wind twist is smaller and the velocity profile is more uniform than in the latter case.

An analysis of wind turbulence has shown that only the high frequency end of the atmospheric wind spectrum is important as far as yacht sail aerodynamics is concerned, and thus only this part needs to be modelled in wind-tunnel simulations.

A grid of horizontal bars can be used to generate velocity and turbulence intensity profiles which simulate these parameters quite well, but the spectrum of turbulence generated this way shows that the turbulence length scale is really too low, and in the present case the turbulence spectrum was energetic at frequencies which were too high by a factor of about eight.

The simplified yacht model was adequate for the test programme apart from the boom vang winch which was under-powered so that it proved difficult to get sufficient leach tension. The high capacity, stiff dynamometer (balance) used in the tests had acceptable accuracy for thrust, sideforce, and heeling moment, but it would have been interesting to have had measurements of pitching moment and vertical force as well.

The 30 deg apparent results showed essentially constant thrust and effective-height-of-sideforce with change in heel angle, but the sideforce reduced according to cos(heel) and the associated rolling moment coefficient showed little change with heel. This was the same for both the turbulent and smooth results.

The 60 deg apparent results were somewhat different. The sideforce, and rolling moment coefficient were all essentially invariant with change in heel angle, but the

effective-height-of-sideforce showed a small reduction with heel and the thrust coefficient showed a reduction proportional to $\cos^2$ heel).

When the measured forces and moments were converted to lift and drag coefficients based on a wind axis system in a plane perpendicular to the mast, the collapse of the data was quite spectacular. The angle between the apparent wind direction and the boom was about 23 deg in all test cases, and gave a mean lift coefficient of about 1.5, and a mean drag coefficient of about 0.5. By making some allowance for sail twist, and increasing β_E - δ by 5 deg for the 60 deg apparent results, C_L showed a reduction as β_E - δ reduced. It was also clear that the 60 deg results had a higher drag coefficient than the 30 deg results, probably resulting from the more twisted sail shape in the former case. It would thus appear that this method of collapsing wind-tunnel data is a worthy candidate for further study.

12. REFERENCES

1. Jackson, P.S. The science of sail design. Proc. of a Conf. held at the Boundary Layer Wind Tunnel Laboratory, University of Western Ontario, London, Ontario, Canada, June 21-22 1982.

2. Shaw, D.A. Yacht mainsail aerodynamics. M.E. Thesis, Mechanical Engineering Dept, University of Auckland, Private Bag 92019, Auckland, New Zealand, 1991.

3. Cook, N.J. The designer's guide to wind loading of building structures. Part 1, Butterworths, 1985.

4. Wellicome, J.F. Private communication. Dept. of Ship Science, University of Southampton.

5. Aerodynamics Committee of the American Society of Civil Engineers, Manual of practice for wind-tunnel testing of buildings and structures. January 1986.

6. Engineering Sciences Data Unit, Characteristics of the atmospheric environment near the ground. Part 2, single point data for strong winds (neutral atmosphere), ESDU 85020, ESDU International plc, London, UK, 1985.

7. Mueller, T.J., Pohlen, L.J., Congigliano, P.E., Jansen, B.J. The influence of freestream disturbances on low Reynolds number airfoil experiments. Experiments in fluids, 1, 3-14, 1983.

8. Gartshore, I.S. The effects of freestream turbulence on the drag of rectangular two-dimensional prisms, University of Western Ontario, Canada, BLWT-4-73, 1973.

9. Waudly-Smith, P.M. and Rainbird, W.J. Some principles of automotive aerodynamic testing in wind tunnels with examples from slotted wall test section facilities, Paper 850284, SAE Intl. Congr. and Exp., Detroit, Michigan, USA, February-March 1985.

10. Cooper, K.R. The wind tunnel simulation of wind turbulence for surface vehicle testing. J.W.E. and IA, 38, 71-81, 1991.

11. Millikan, C.B., Klein, A.L. The effect of turbulence: an investigation of the maximum lift coefficient and turbulence in wind tunnels and in flight. Aircraft Engineering, August, pp169-174, August 1933.

12. Flay, R.G.J. and Jackson, P.S. Flow simulation for wind-tunnel studies of sail aerodynamics. Eighth International Conf. on Wind Engineering, London, Ontario,

Canada, July 1991.

13. Cooper, R.K. Atmospheric turbulence with respect to moving ground vehicles. Aerodynamics of Transportation - II. The winter annual meeting ASME, Boston, Mass., pp53-63, 13-18 November 1983.

14. Teunissen, H.W. Characteristics of the mean wind and turbulence in the planetary boundary layer, UTIAS Review 32, Institute for Aerospace Studies, University of Toronto, Toronto, Canada, 1970.

15. Flay, R.G.J. Structure of a rural atmospheric boundary layer near the ground. Mechanical Engineering Department, University of Canterbury, New Zealand, Ph.D. Thesis, 1978.

16. Raine, J.K. Modelling the natural wind: Wind protection by fences. Vol. II, Ph.D. Thesis, University of Canterbury, NZ, October 1974.

17. Molland, A.F. The design, construction and calibration of a five component strain gauge wind tunnel dynamometer. SSSU 1/77, ISSN 0140-3818.

18. Deakin, B. The development of stability standards for UK sailing vessels. RINA Meeting, 23rd April 1990, London

Fig. 21: Dynamometer.

Fig. 22: True roll centres of dynamometer.

Fig. 23: Thrust coefficient versus heel.

Fig. 24: Horizontal sideforce coefficient versus heel.

Fig. 25: Rolling moment coefficient versus heel.

Fig. 26: Sketch showing application of side and vertical forces.

Fig. 27: Effect of heel on the effective height of the sideforce.

Fig. 28: Sail forces resolved into the plane of the deck.

Fig. 29: Resolving forces into wind-tunnel axes.

Fig. 30: Definition of the effective wind angle.

Fig. 31: Lift and drag sail coefficients for δ = 5 and 35°.

Fig. 32: Lift and drag sail coefficients for δ = 5 and 40°.

Fig. 1: Full-scale Laser yacht.

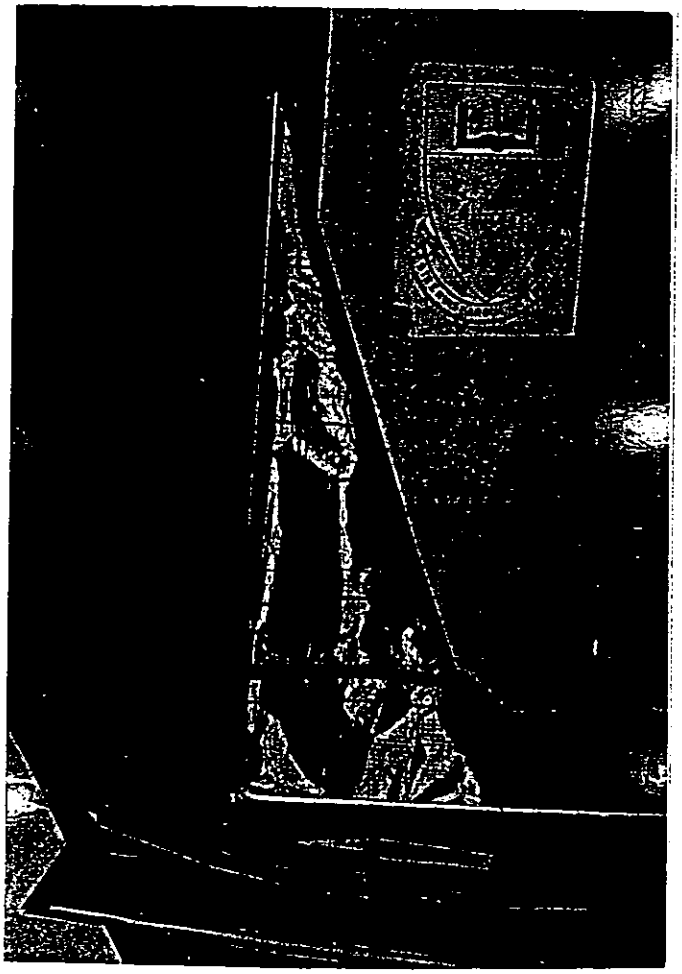

Fig. 2: Model Laser.

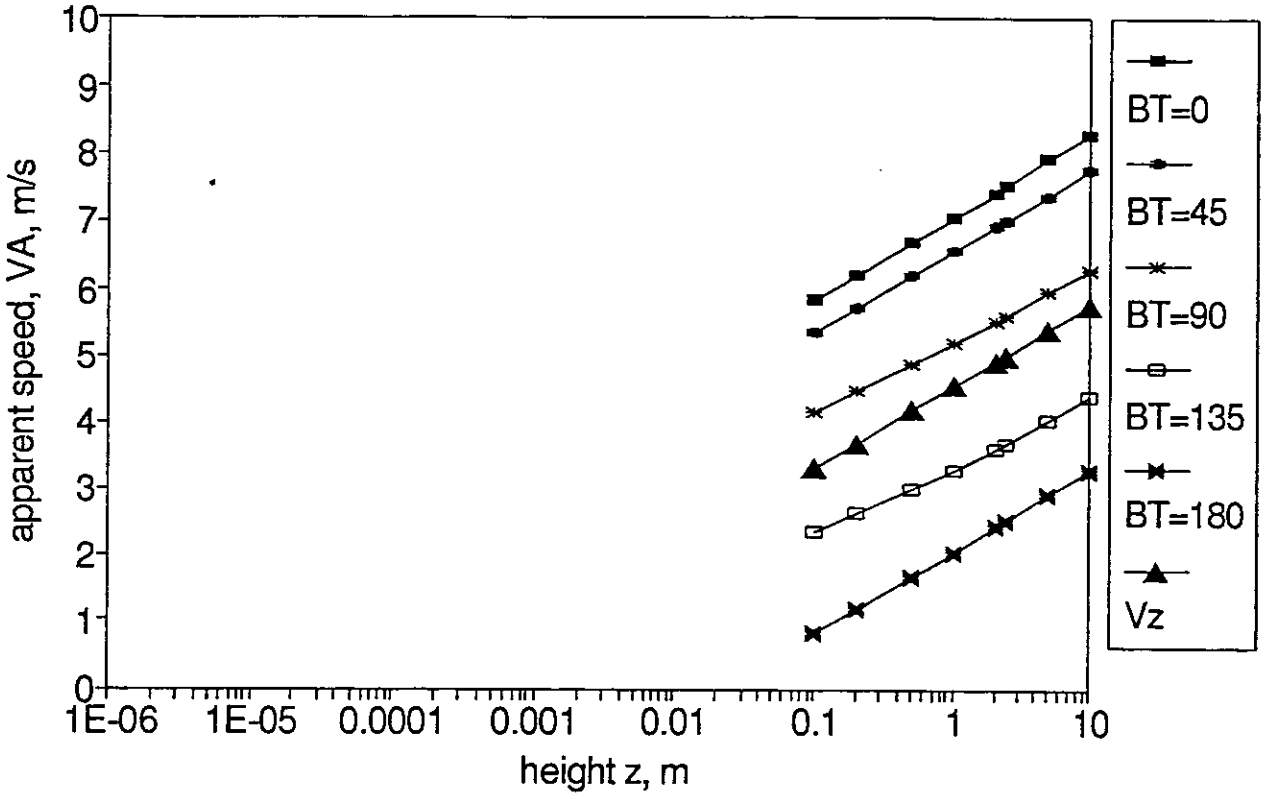

Fig. 3: Apparent speed profiles on semi-log axes.

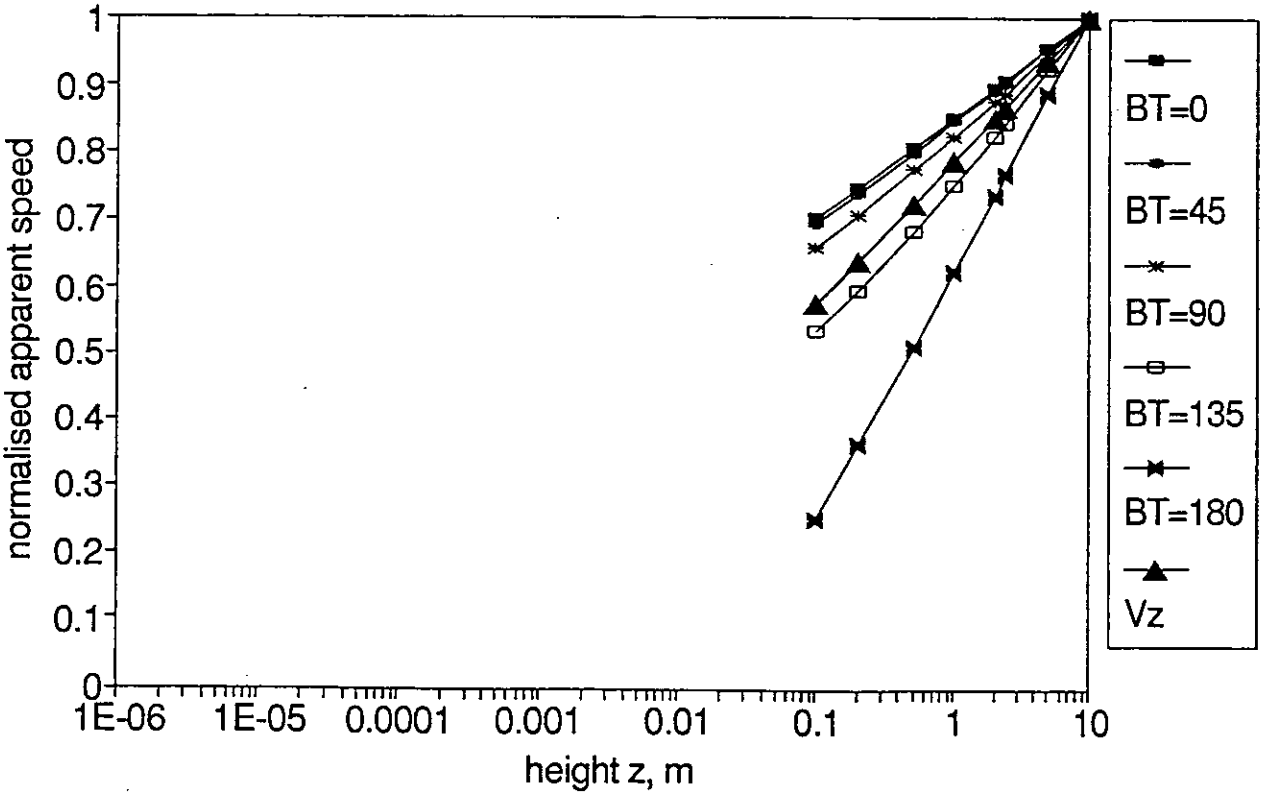

Fig. 4: Normalised apparent speed profiles on semi-log axes.

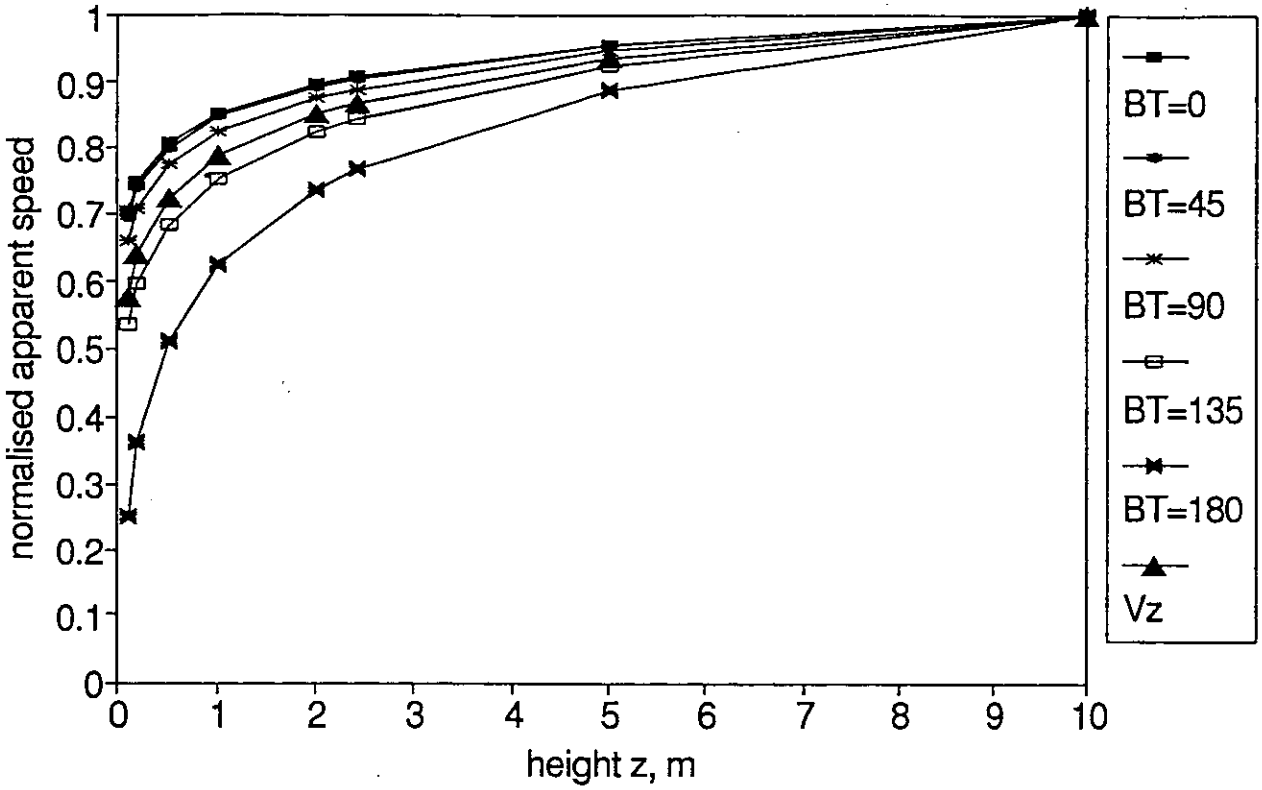

Fig. 5: Normalised apparent speed profiles on linear axes.

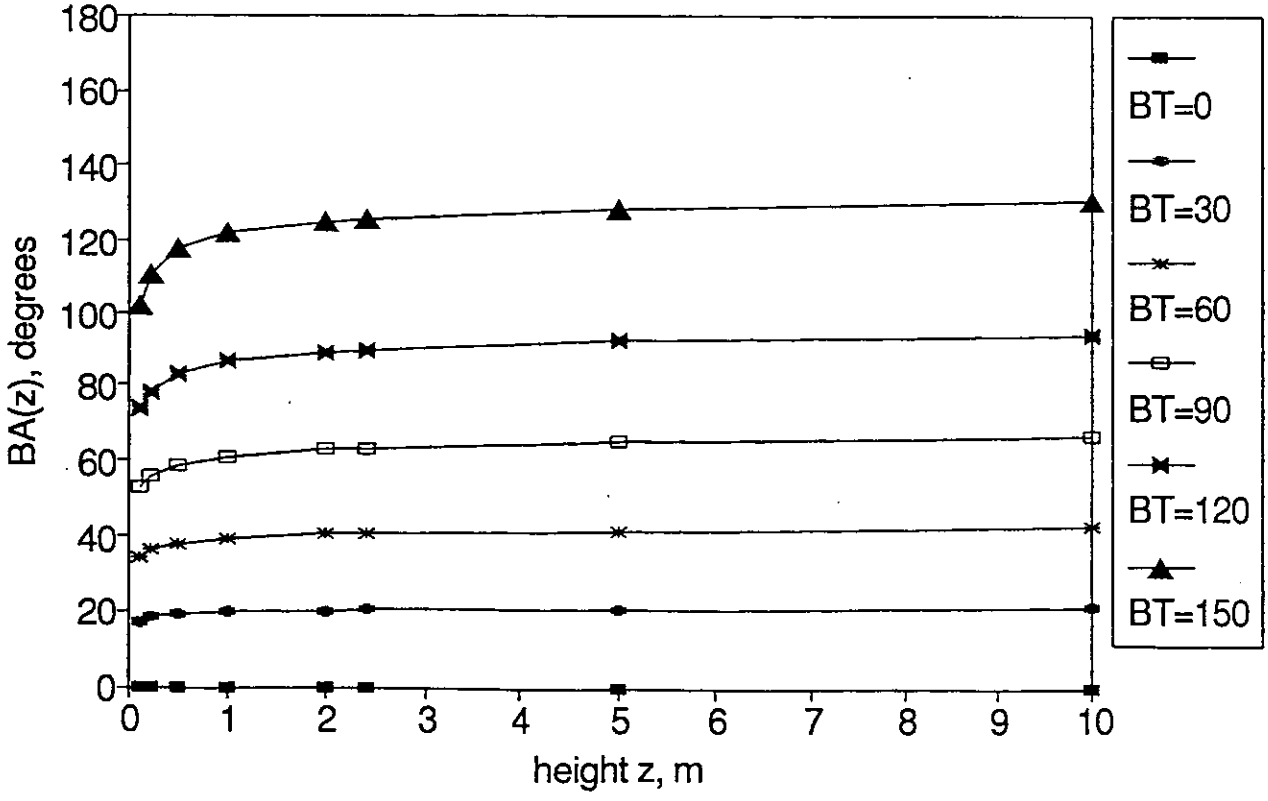

Fig. 6: Variation in apparent wind angle with height and true wind angle.

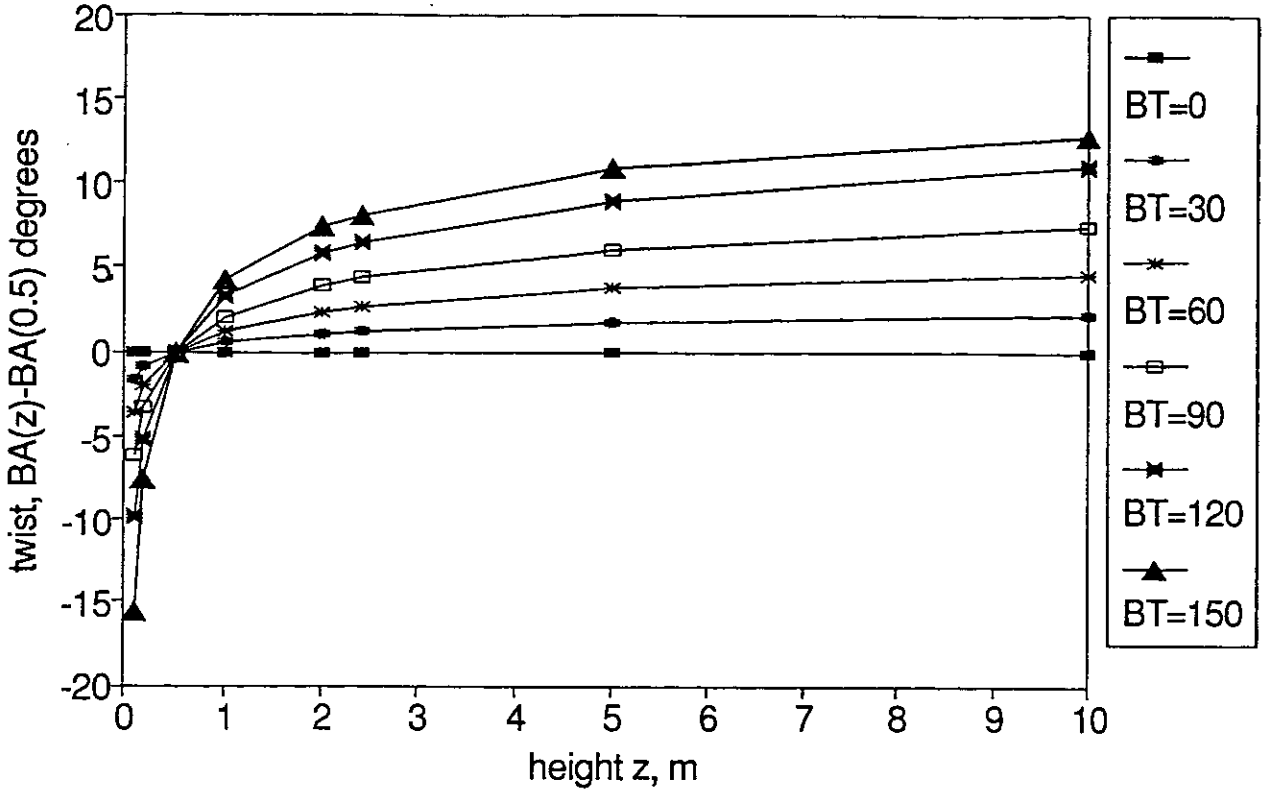

Fig. 7: Variation in apparent wind twist profiles with true wind angle.

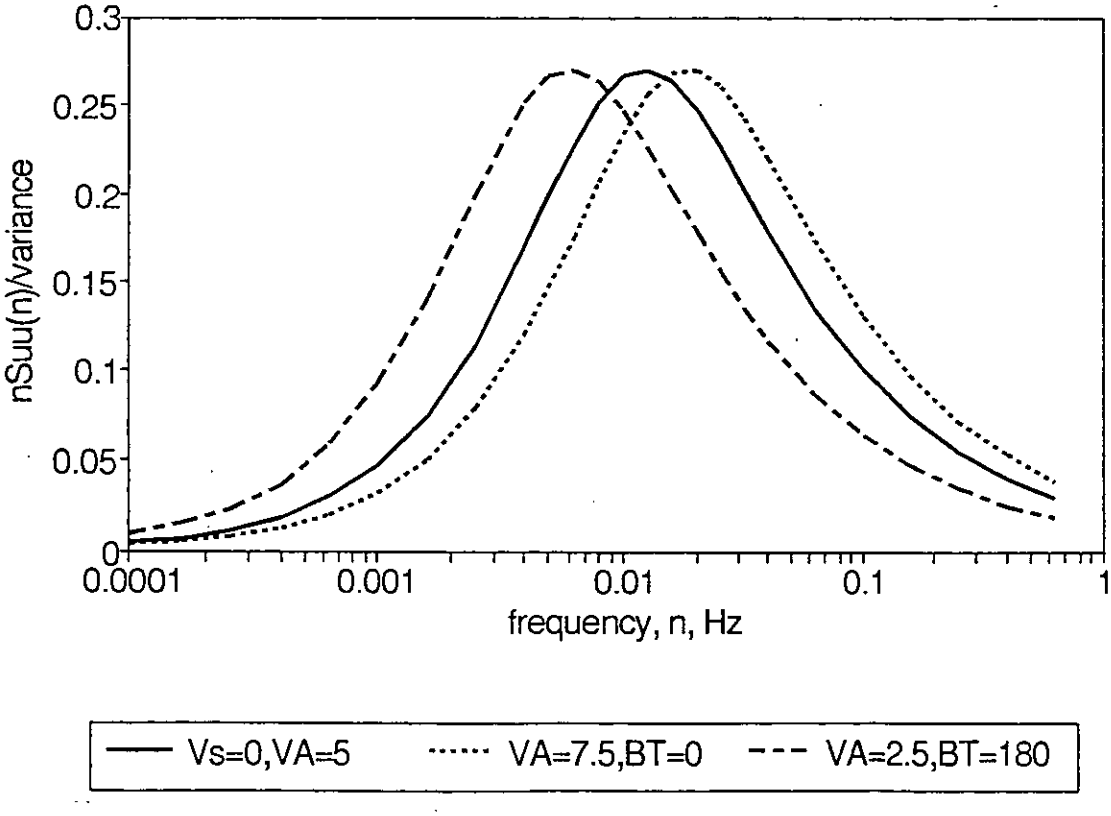

Fig. 8: Apparent wind spectra as seen by a yacht sailing upwind and downwind, and stationary.

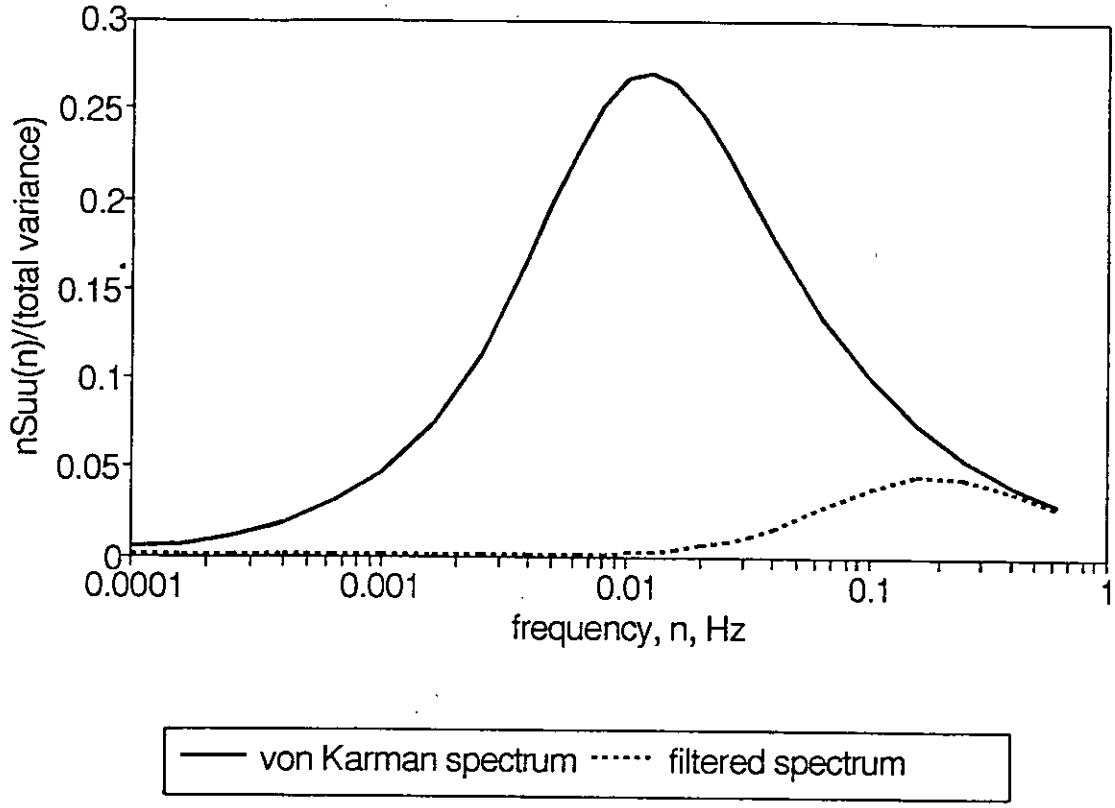

Fig. 9: The effect of high-pass filtering the natural wind spectrum at a cut-off frequency of 0.125 Hz.

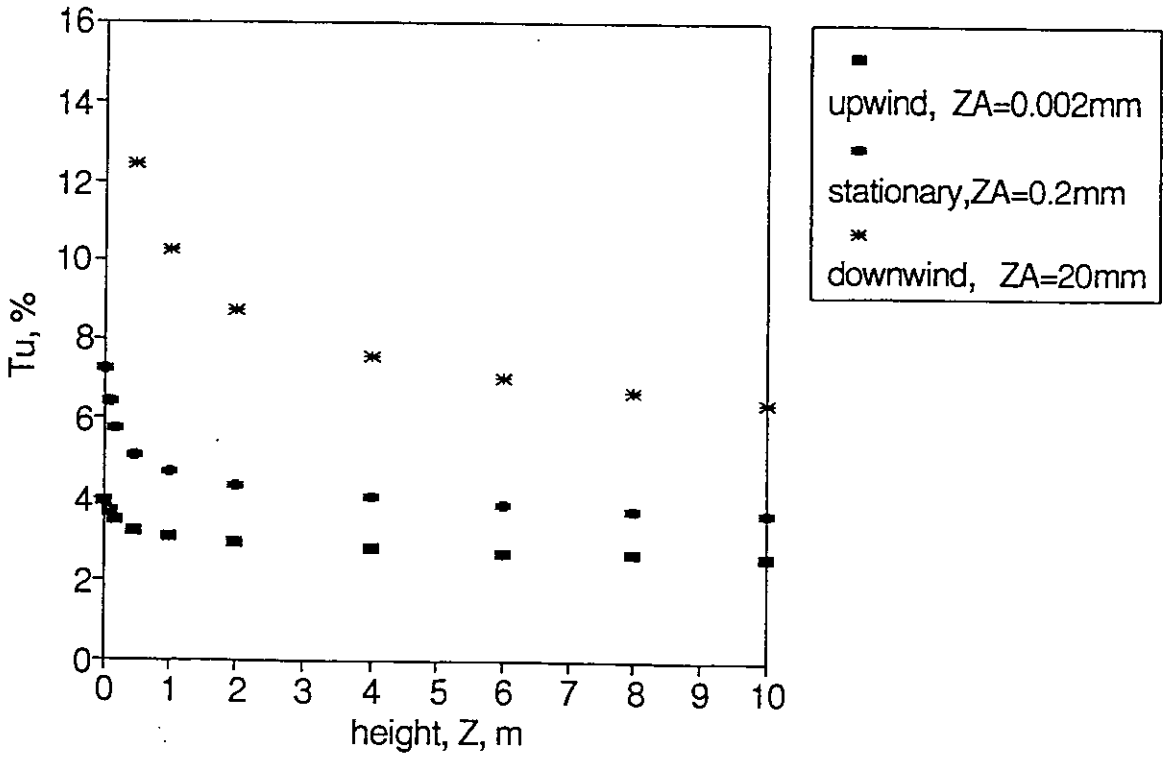

Fig. 10: Idealised turbulence intensity profiles for a yacht sailing upwind and downwind, and stationary.

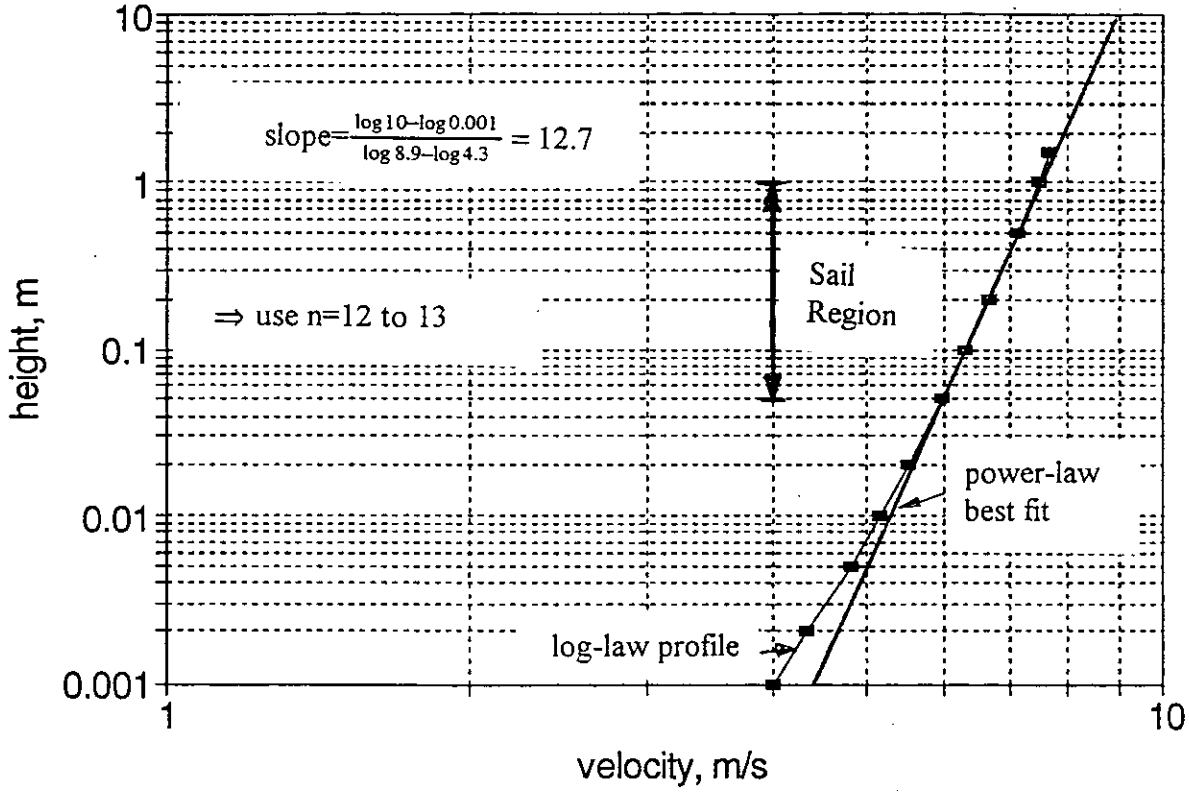

Fig. 11: Comparison of ideal log-law profile with power-law to obtain exponent n in turbulence grid design.

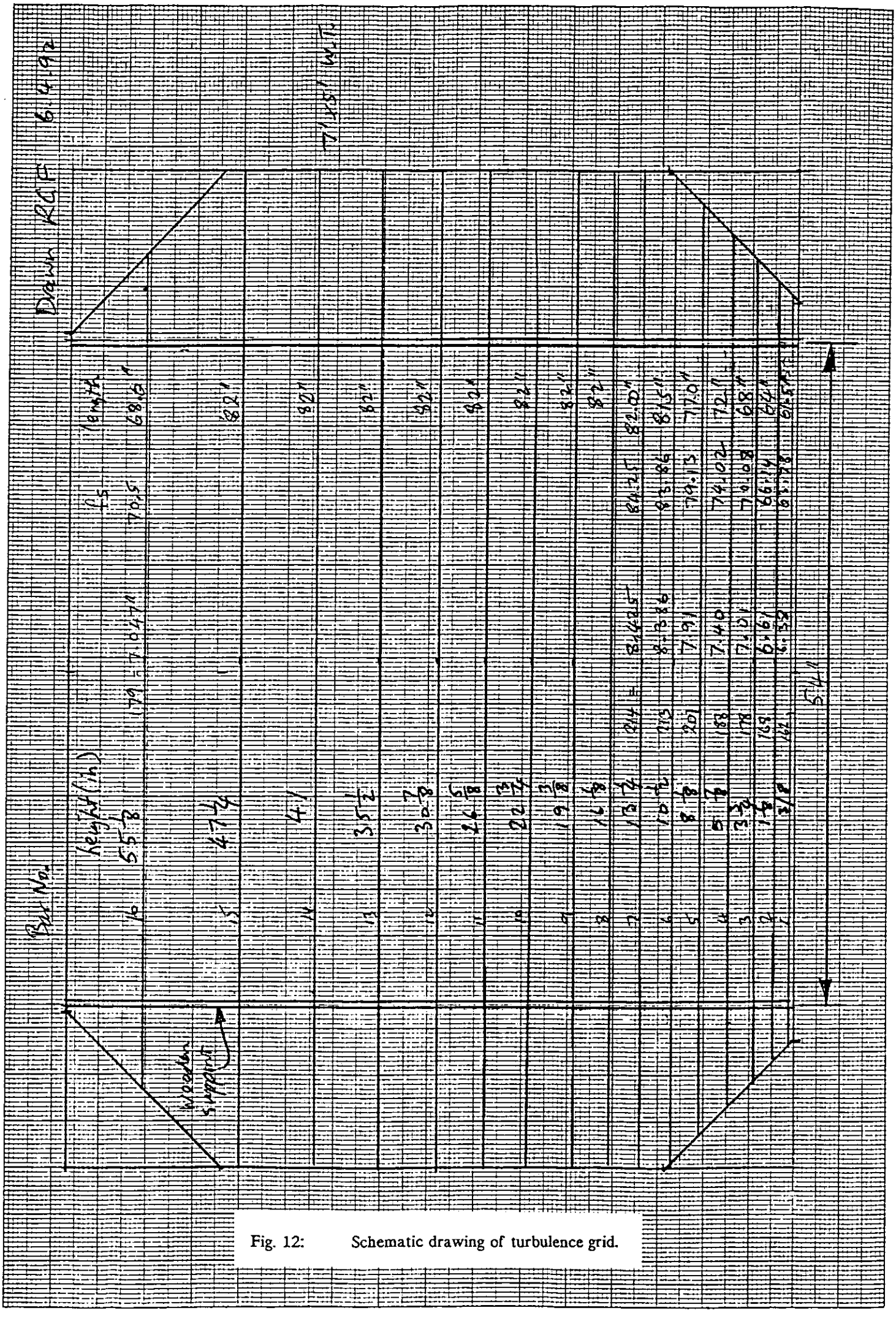

Fig. 12: Schematic drawing of turbulence grid.

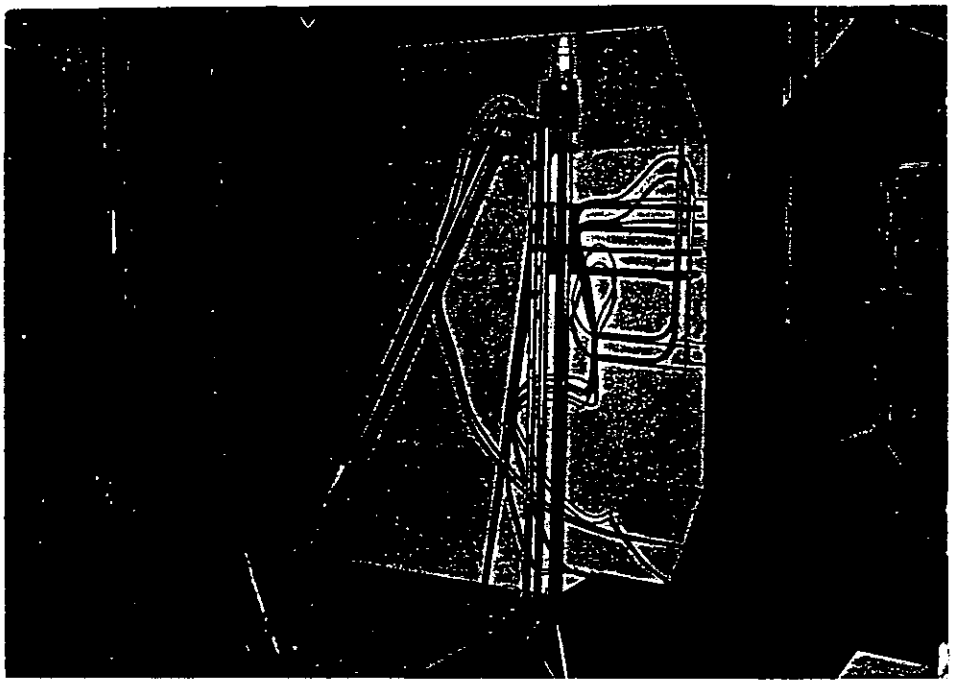

Fig. 13: Photograph of the traversing rig.

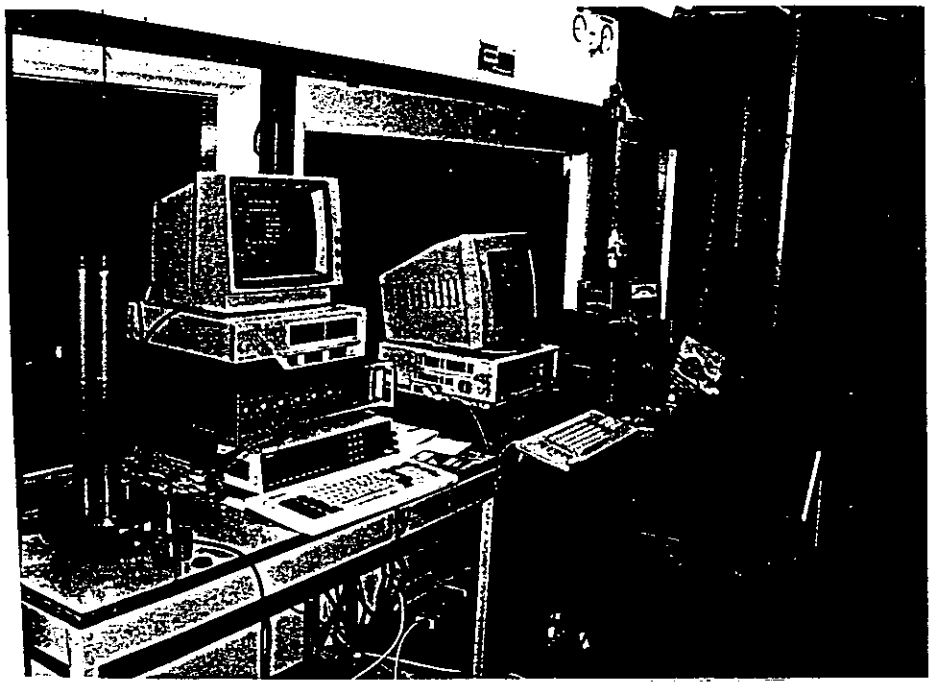

Fig. 14: Photograph of data logging equipment.

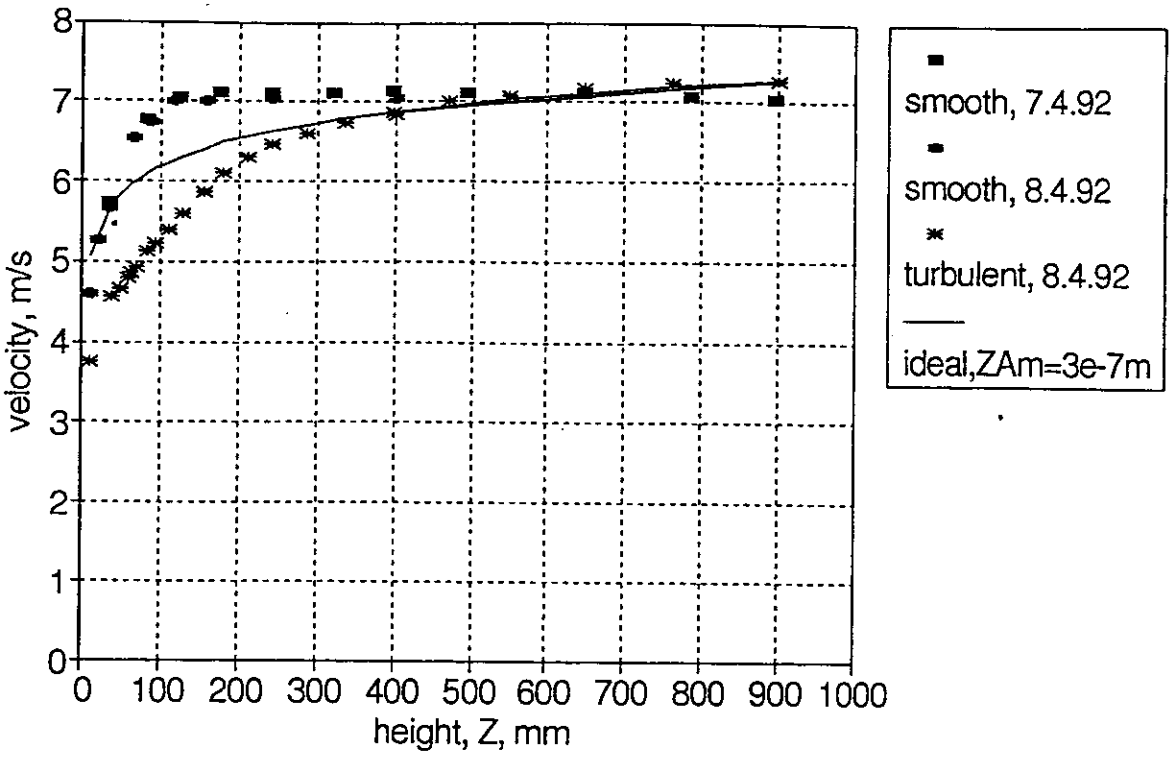

Fig. 15: Ideal and measured velocity profiles, linear axes.

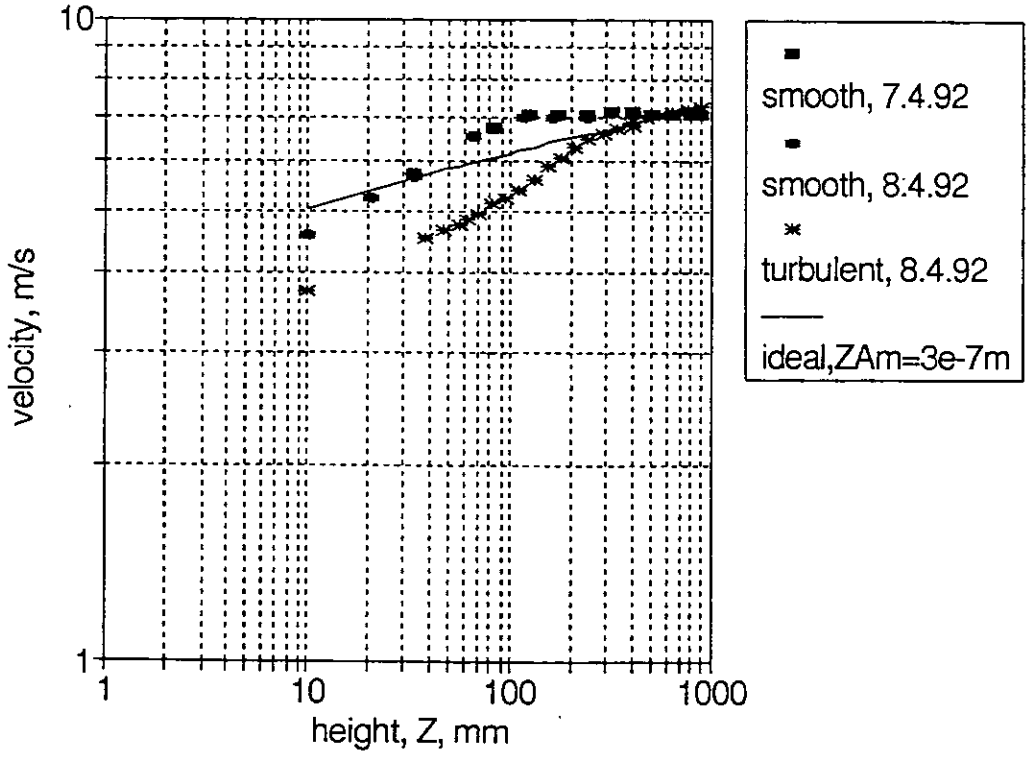

Fig. 16: Ideal and measured velocity profiles, log-log axes.

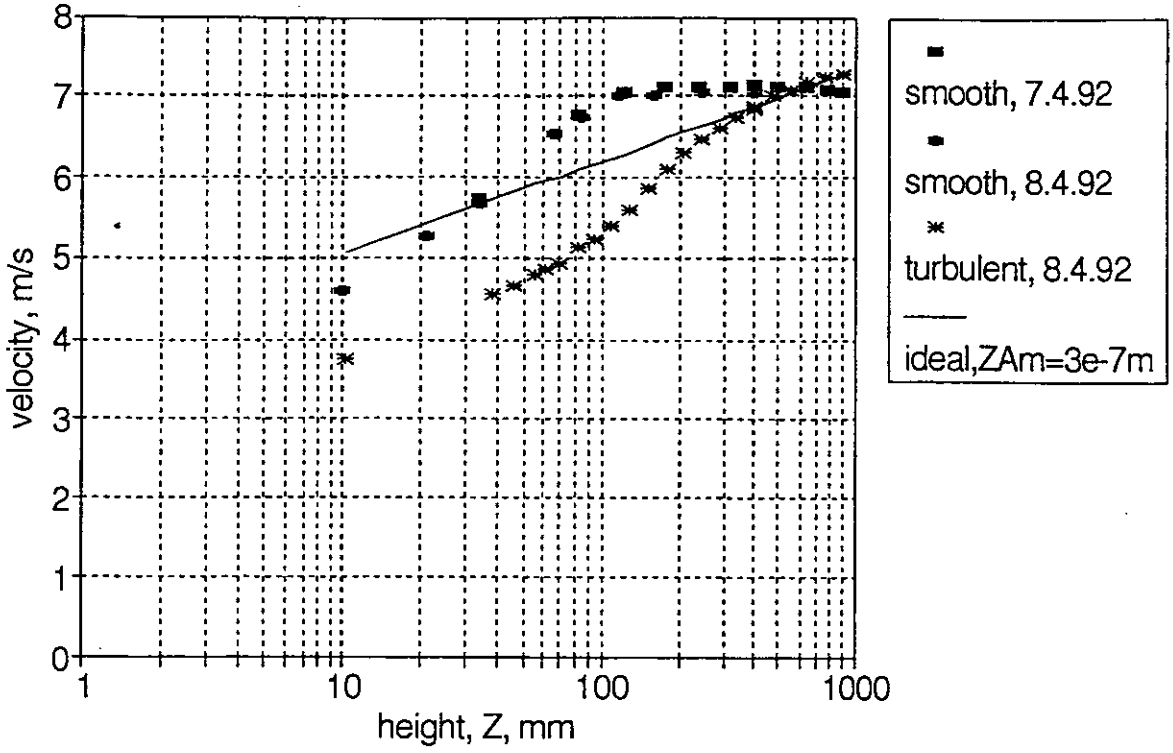

Fig. 17: Ideal and measured velocity profiles, semi-log axes.

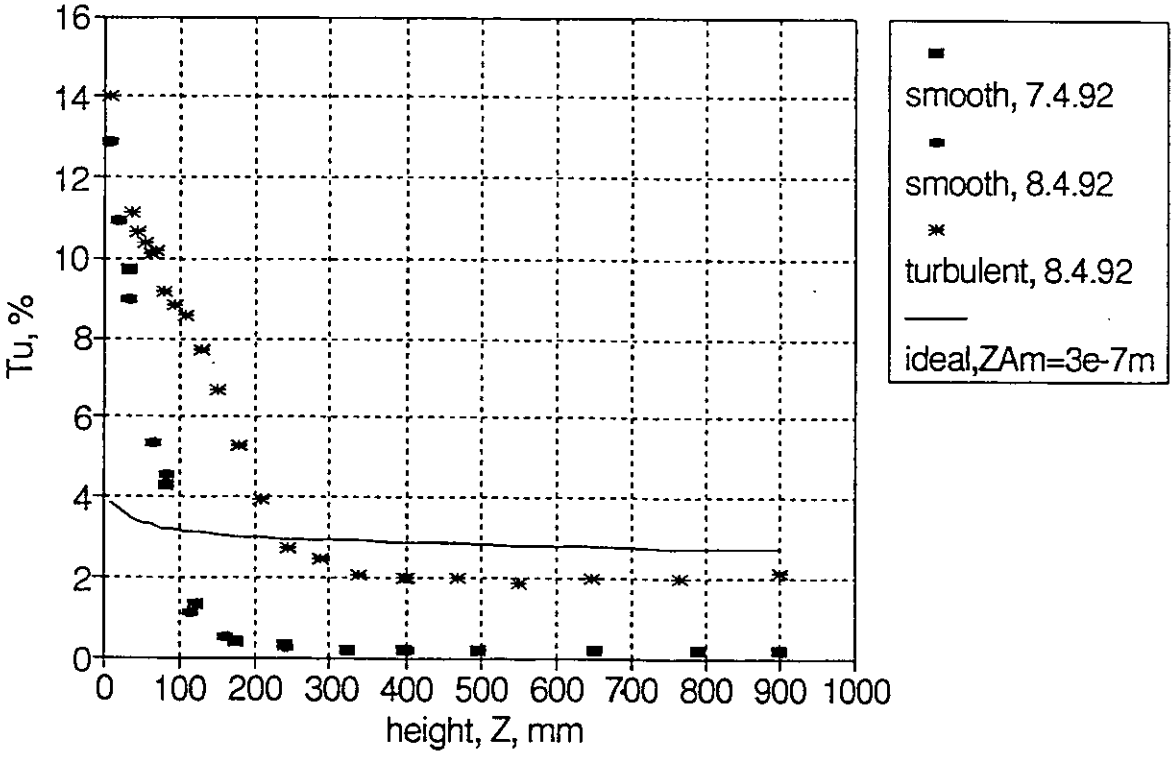

Fig. 18: Ideal and measured turbulence intensity profiles.

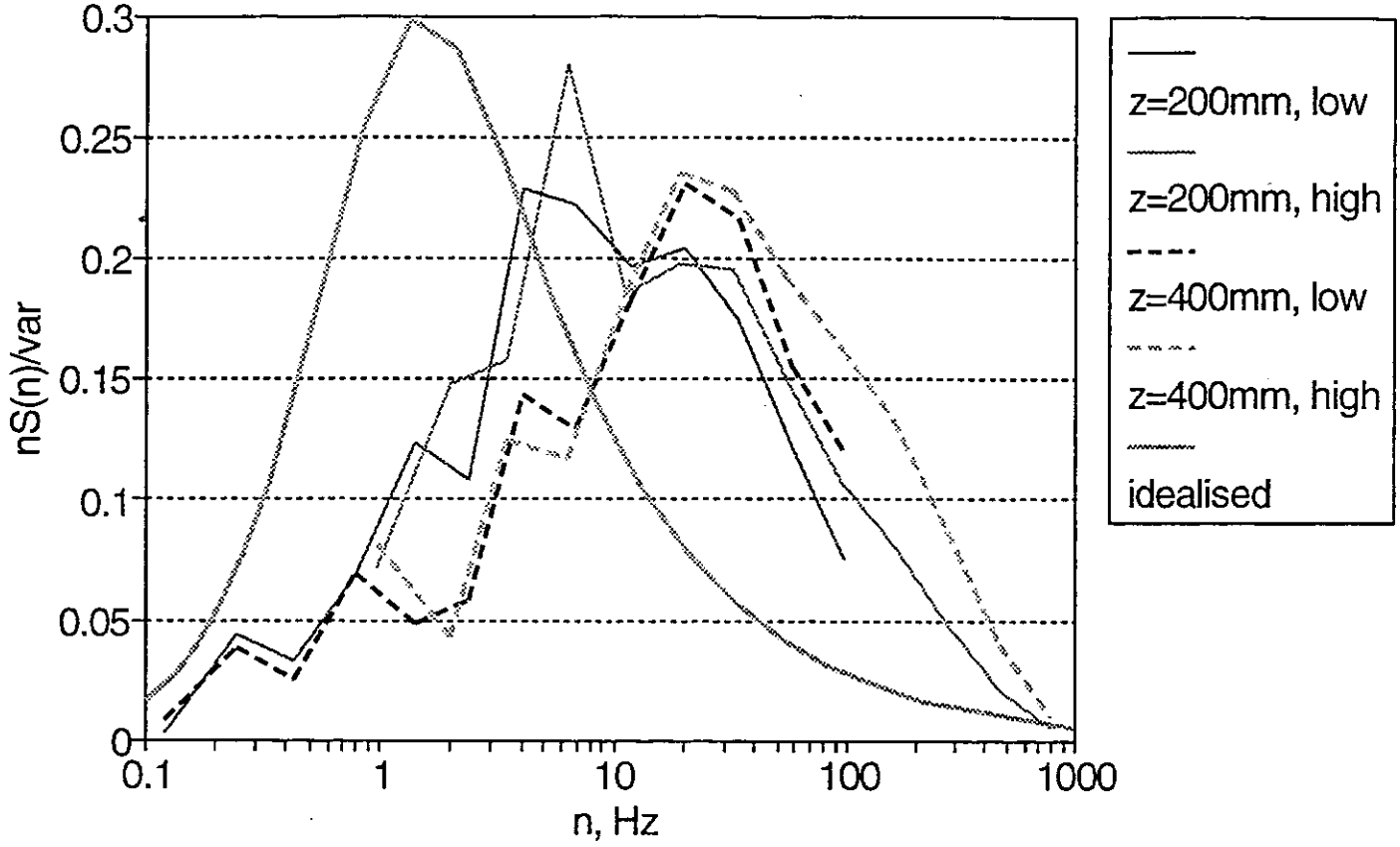

Fig. 19: Ideal and measured turbulence spectra.

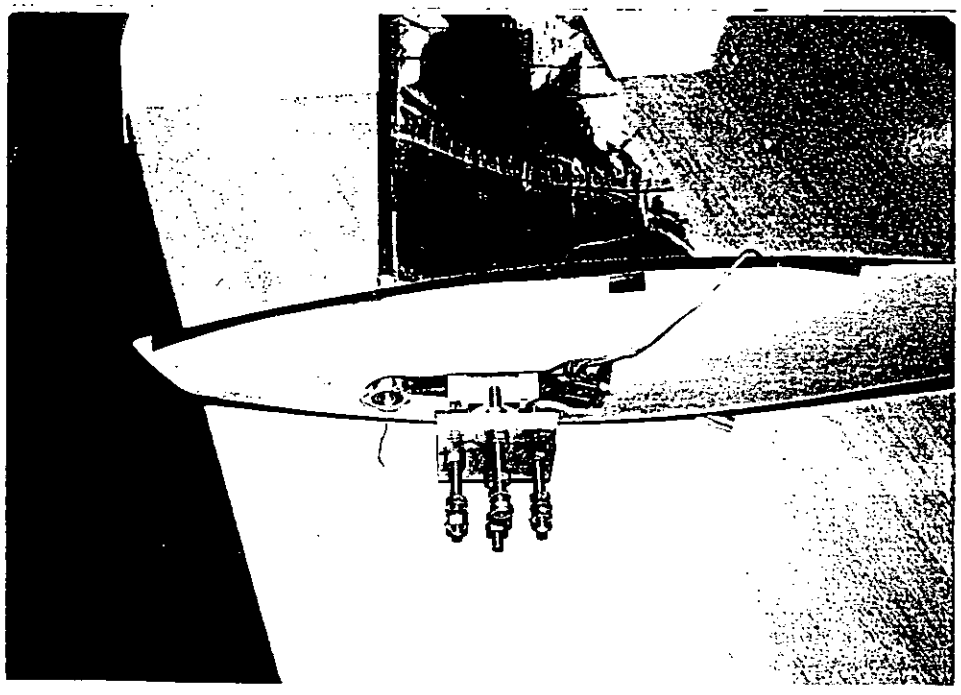

Fig. 20: Photograph of underside of model.

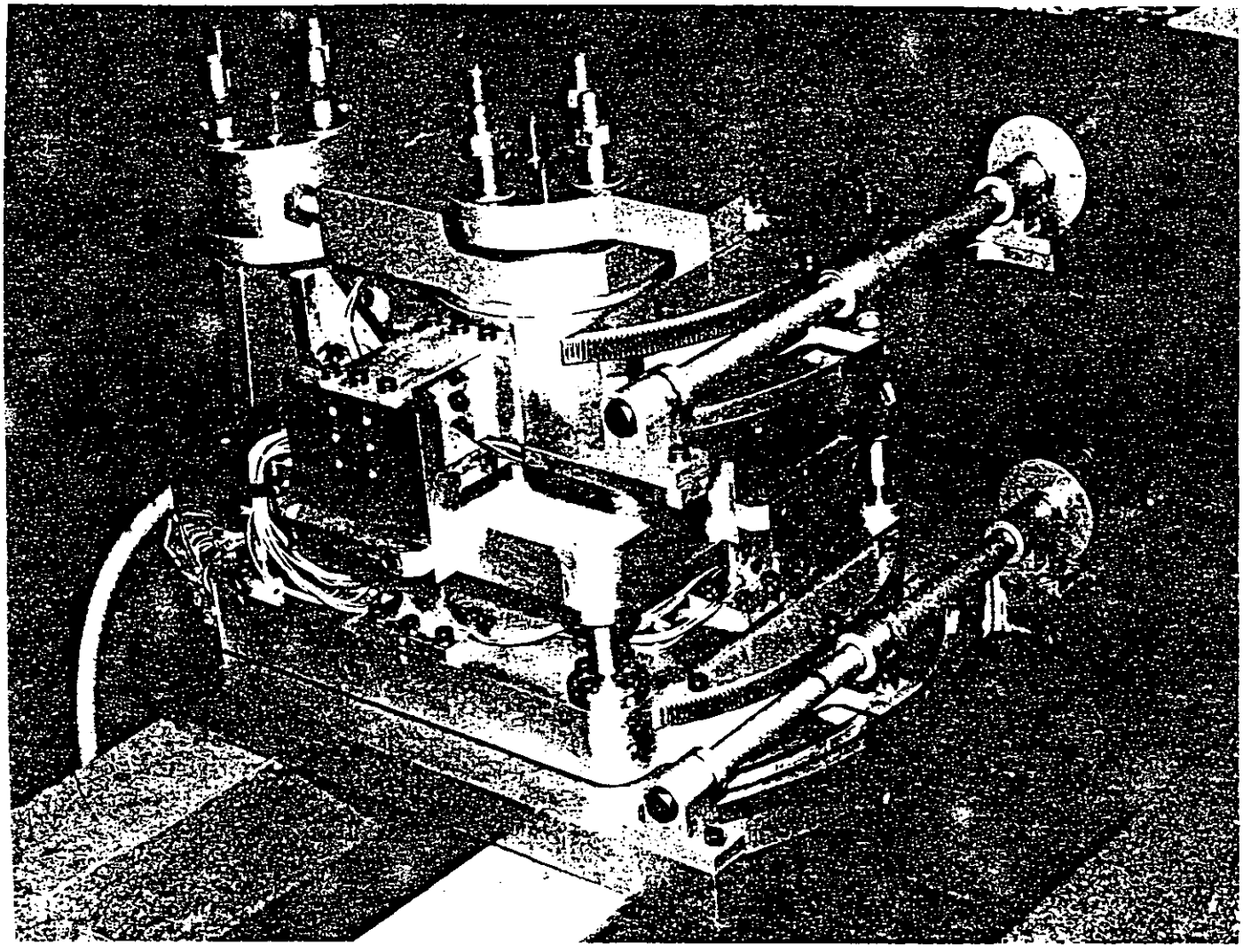

Fig. 21: Dynamometer.

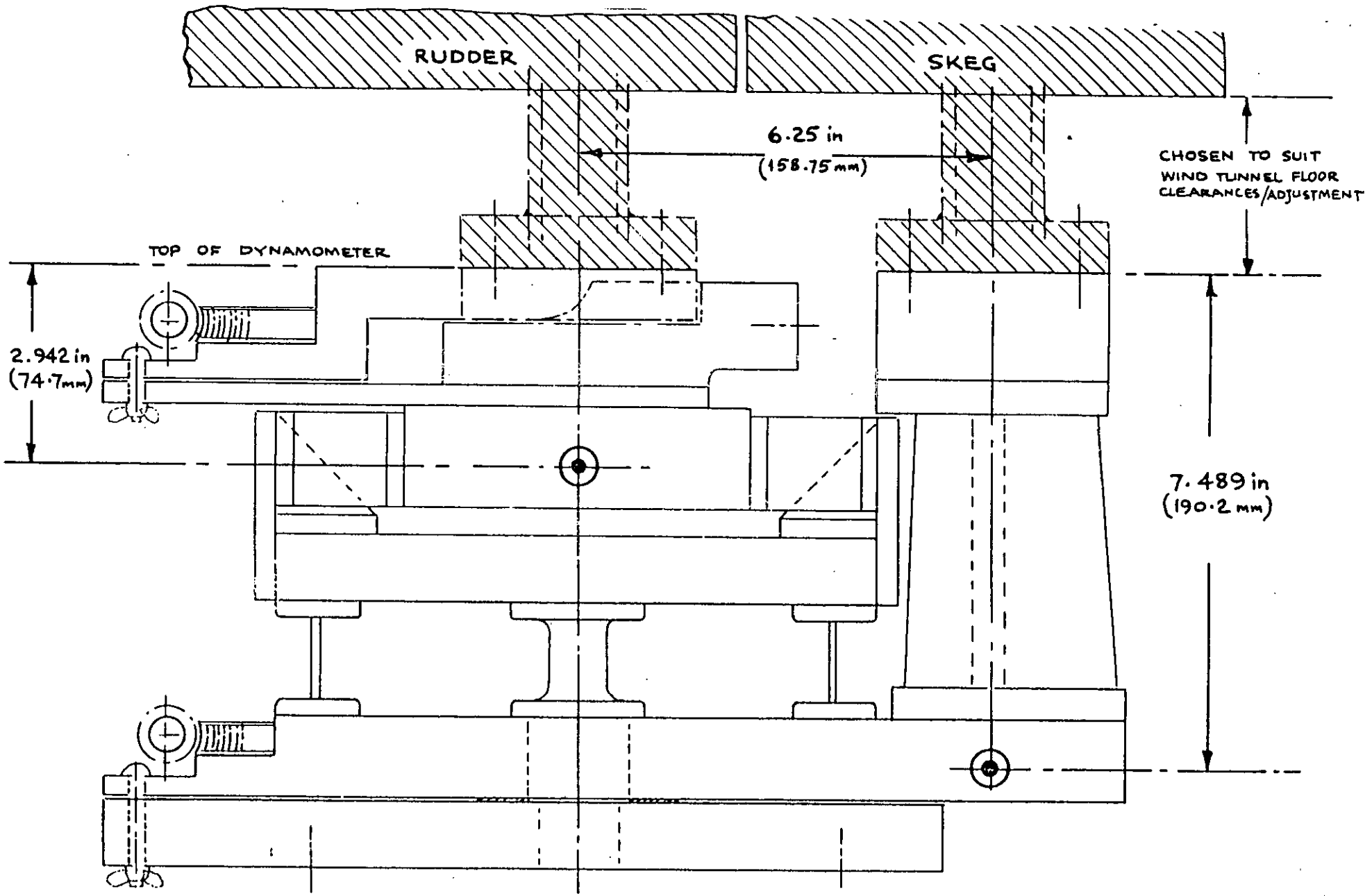

Fig. 22: True roll centres of dynamometer.

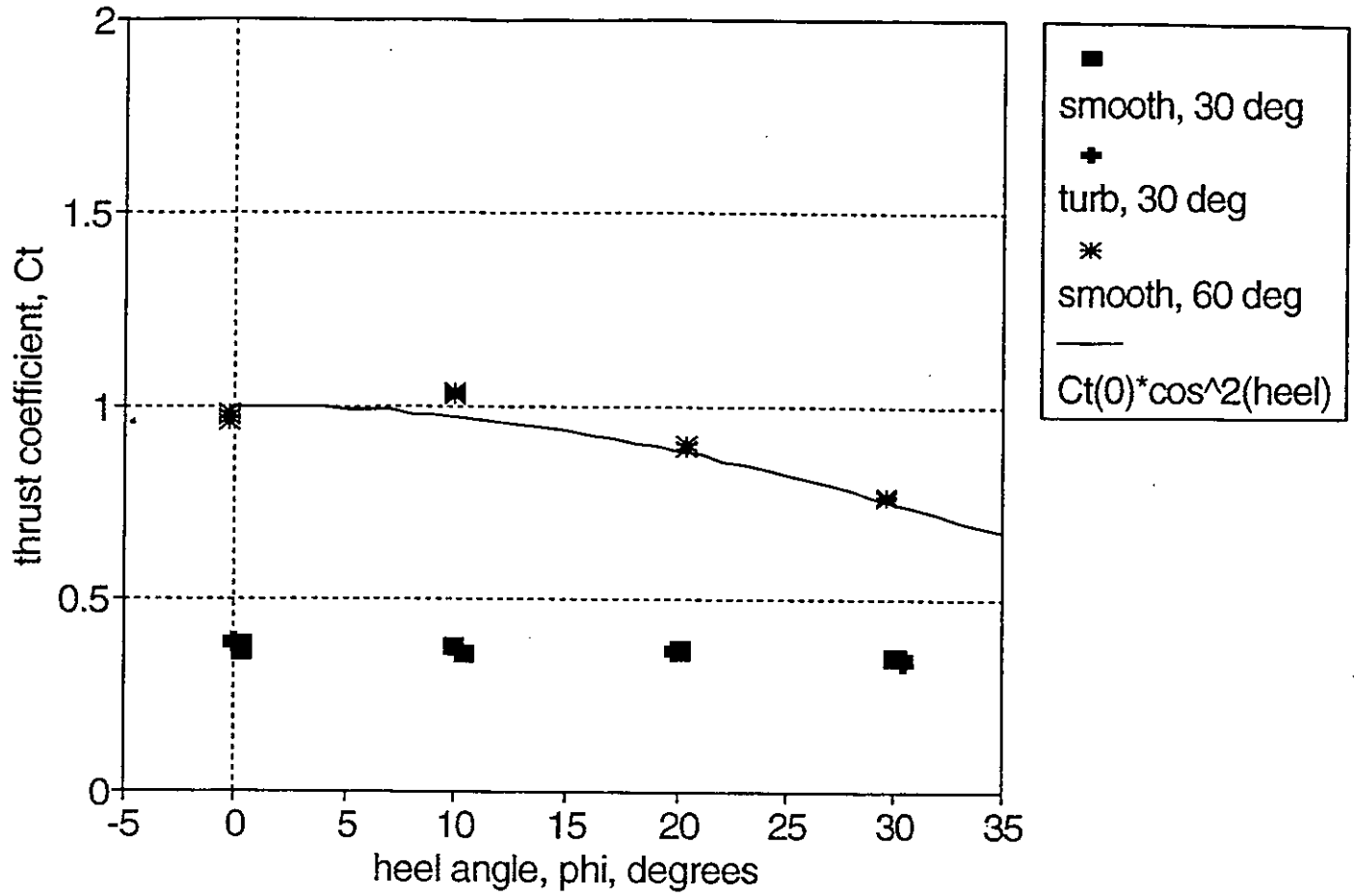

Fig. 23: Thrust coefficient versus heel.

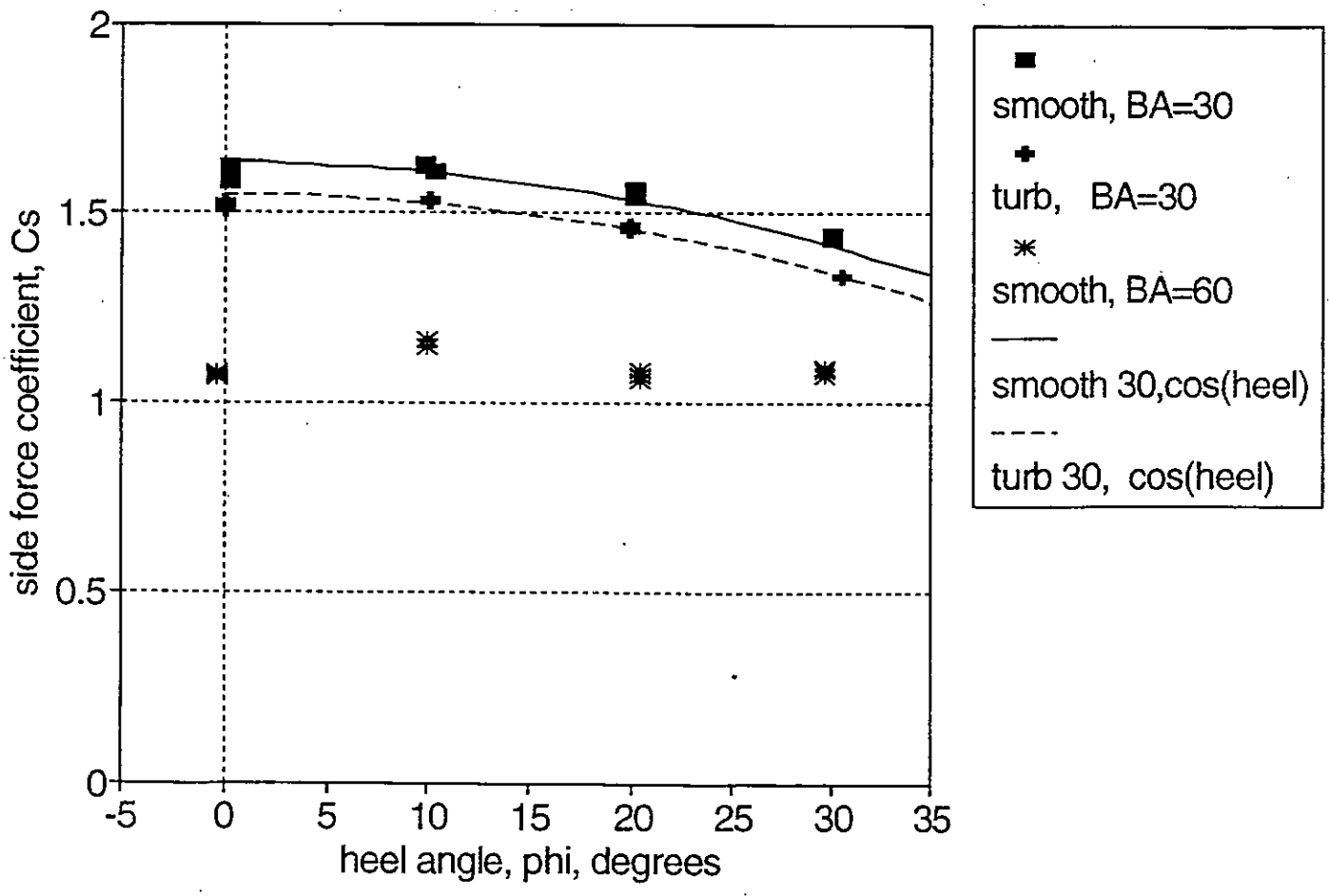

Fig. 24: Horizontal sideforce coefficient versus heel.

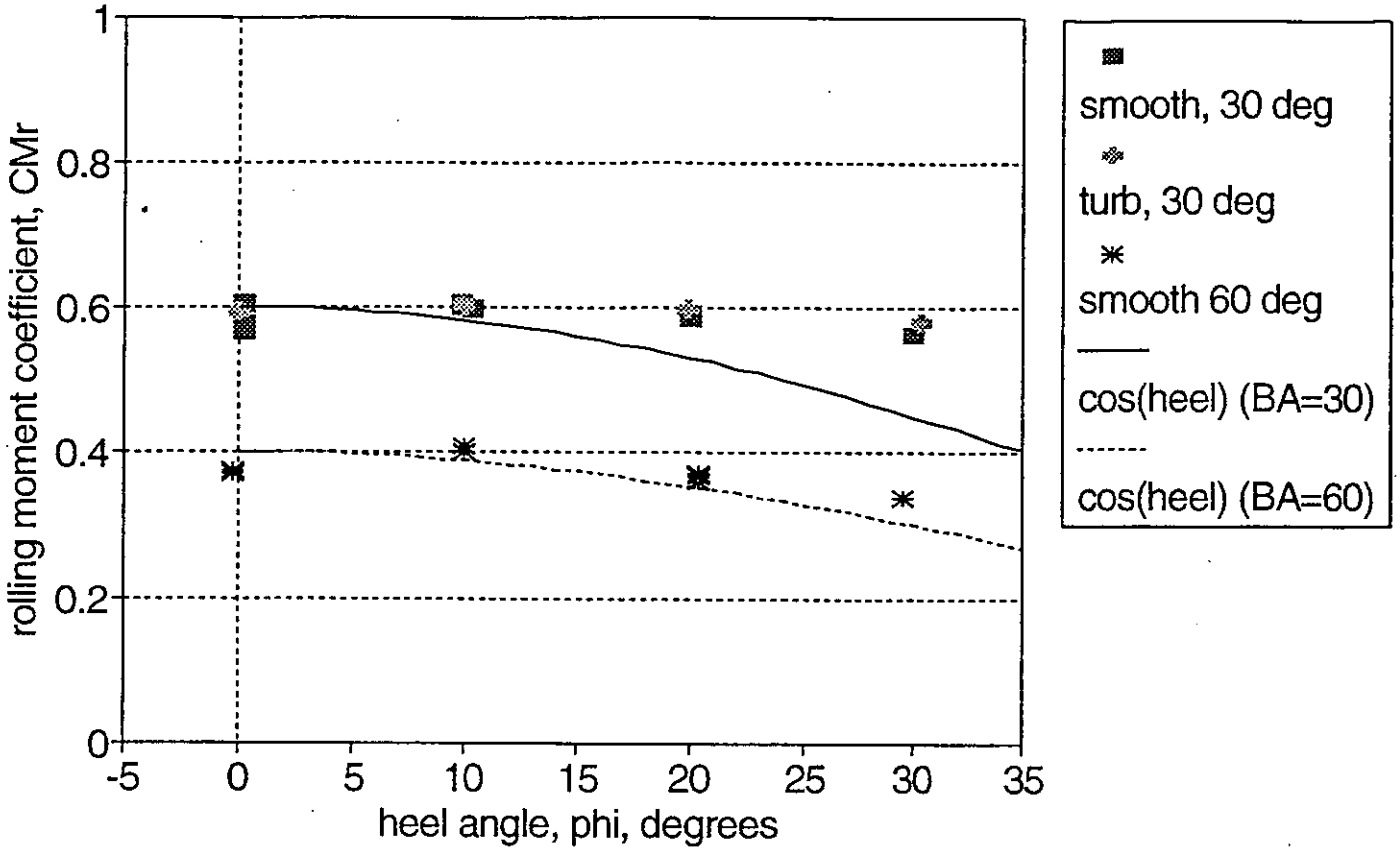

Fig. 25: Rolling moment coefficient versus heel.

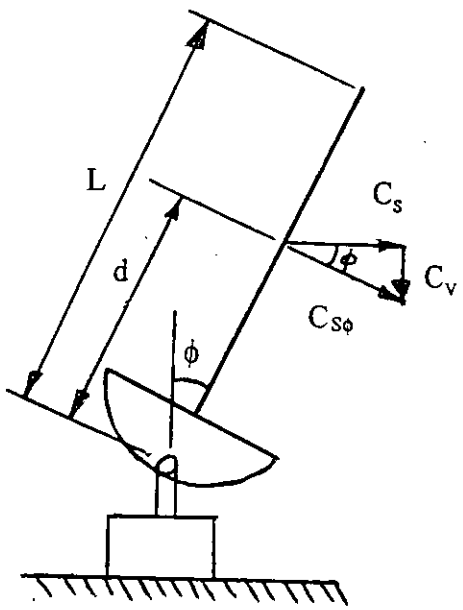

Fig. 26: Sketch showing application of side and vertical forces.

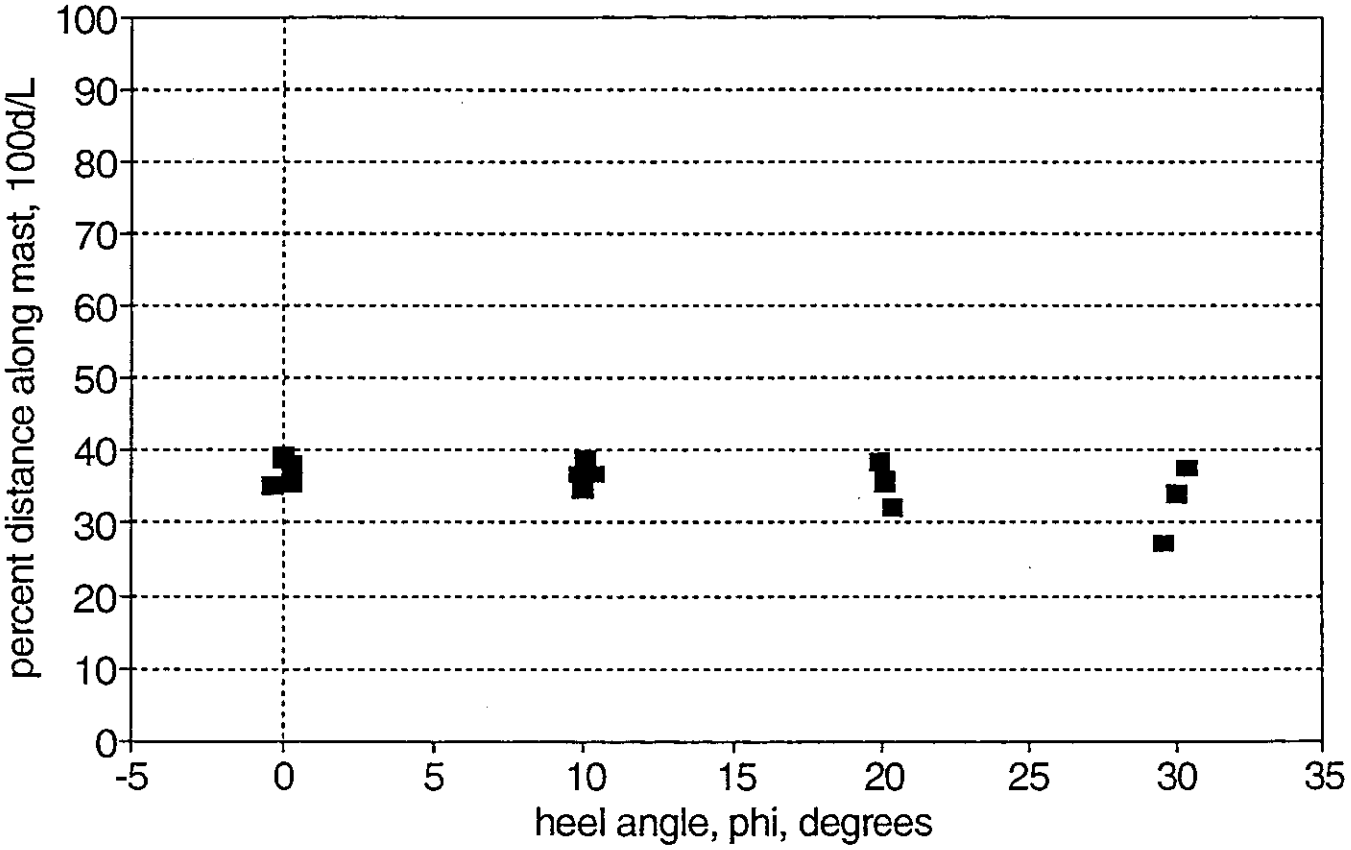

Fig. 27: Effect of heel on the effective height of the sideforce.

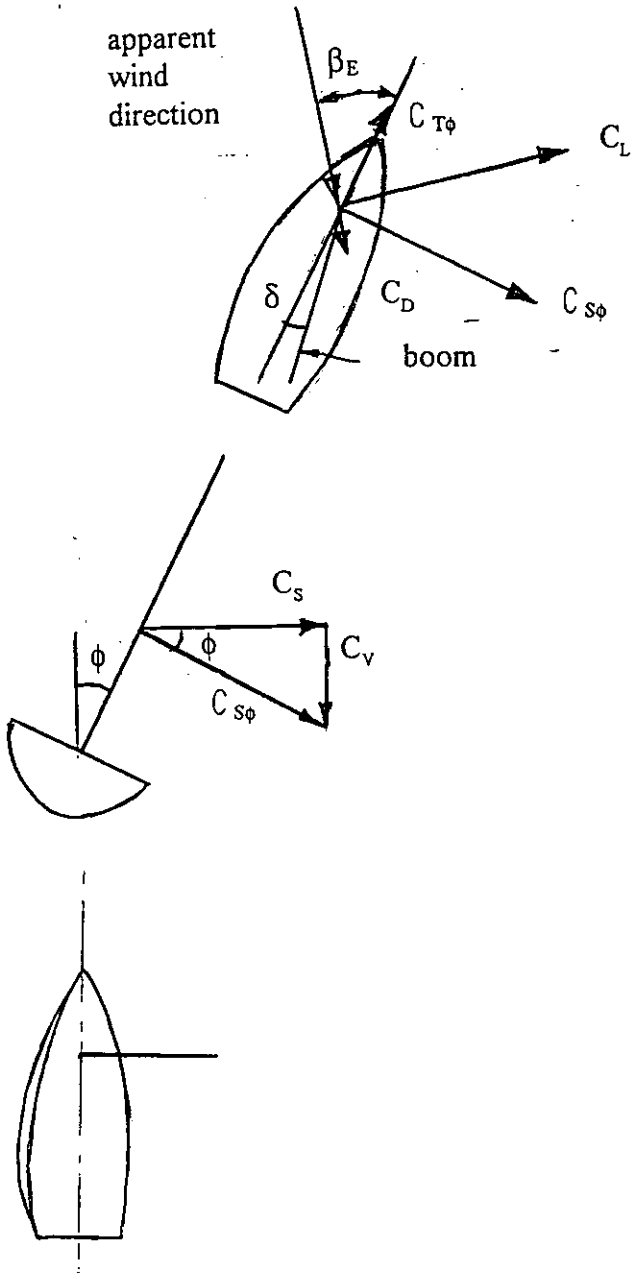

Fig. 28: Sail forces resolved into the plane of the deck.

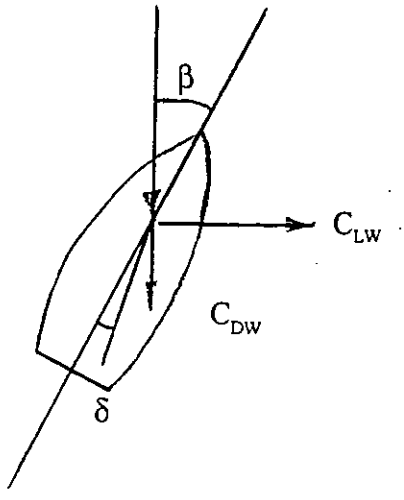

Fig. 29: Resolving forces into wind-tunnel axes.

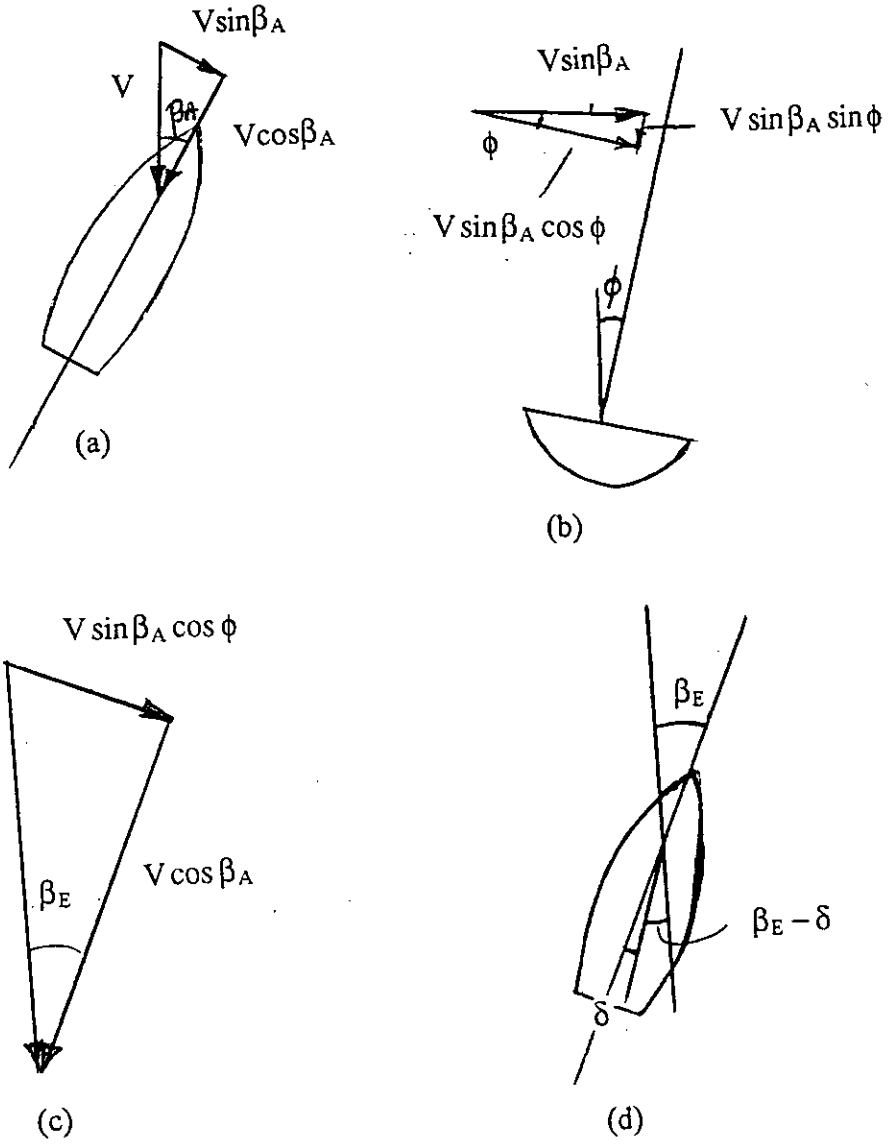

Fig. 30: Definition of the effective wind angle.

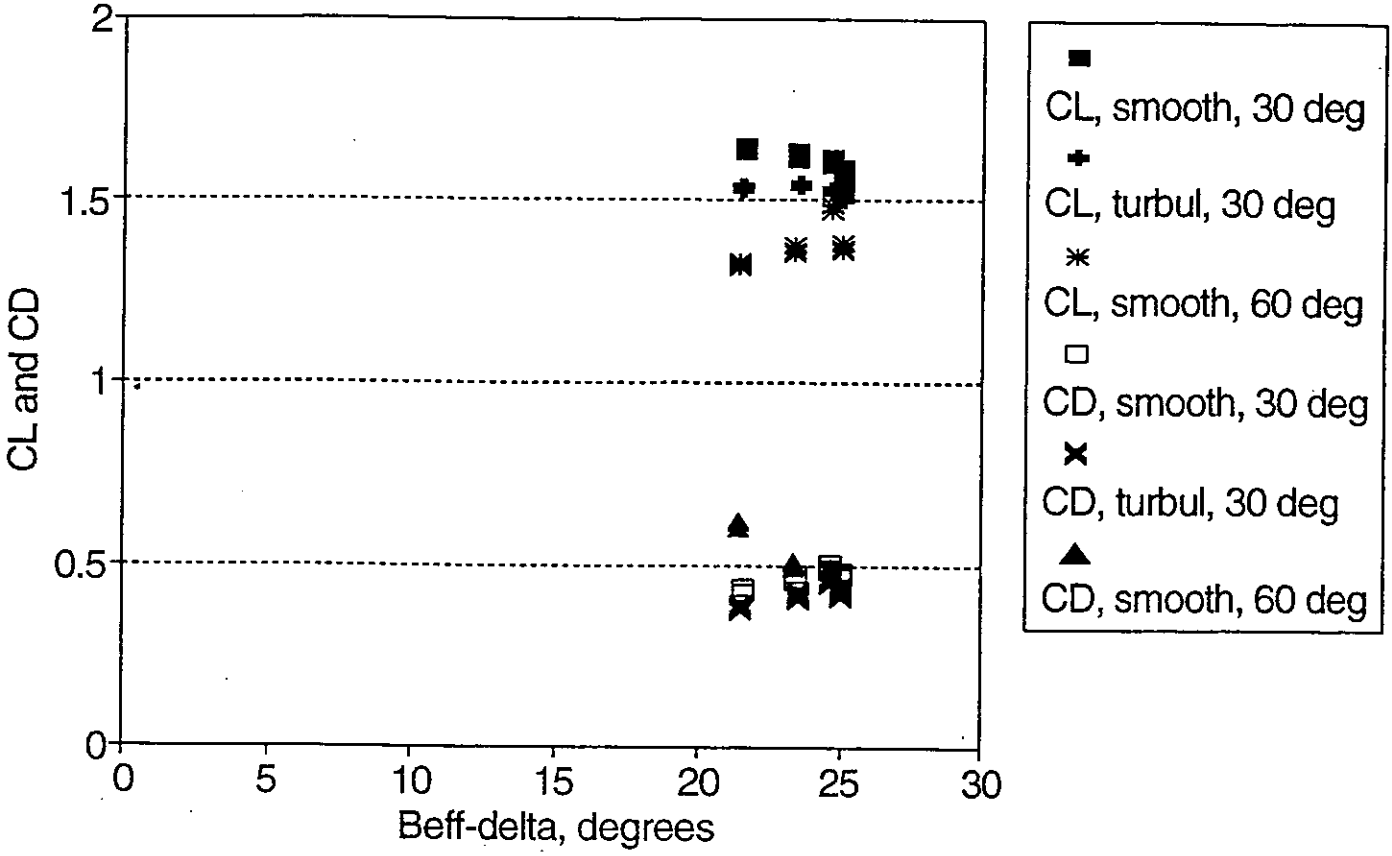

Fig. 31: Lift and drag sail coefficients for δ = 5 and 35°.

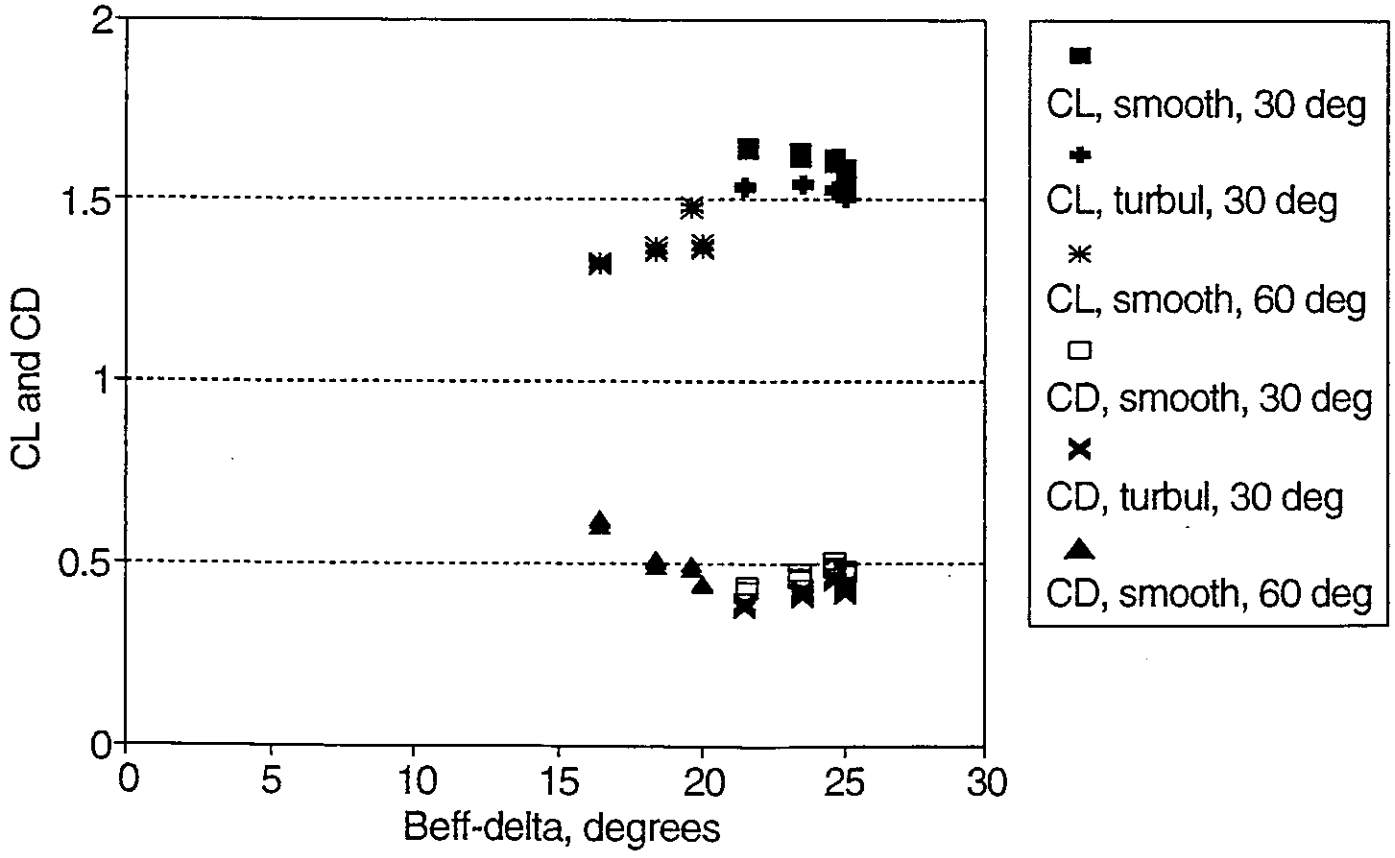

Fig. 32: Lift and drag sail coefficients for δ = 5 and 40°.

APPENDIX 1

COMPUTER PROGRAM FOR TURBULENCE GRID DESIGN AND INPUT AND OUTPUT USED IN THE PRESENT DESIGN

power index = 12.00

tunnel height h = 60.0000

pressure drop coefft k0 = .2500

bar diameter d = .6250

tol = .0020

cowdrey method

no bars = 16

bar no	height(inches)	space
1	.3125	.0000
2	1.8990	1.5865
3	3.7464	1.8474
4	5.8083	2.0619
5	8.0741	2.2658
6	10.5456	2.4714
7	13.2324	2.6868
8	16.1516	2.9192
9	19.3278	3.1762
10	22.7956	3.4678
11	26.6030	3.8074
12	30.8184	4.2154
13	35.5430	4.7246
14	40.9366	5.3936
15	47.2772	6.3406
16	55.1336	7.8563

o and z method

no bars = 16

bar no	height(inches)	space
1	.3125	.0000
2	2.1267	1.8142
3	4.2073	2.0806
4	6.5042	2.2969
5	9.0063	2.5021
6	11.7154	2.7091
7	14.6416	2.9262
8	17.8026	3.1610
9	21.2244	3.4217
10	24.9432	3.7189
11	29.0103	4.0671
12	33.4992	4.4889
13	38.5209	5.0217
14	44.2549	5.7340
15	51.0263	6.7714
16	59.5521	8.5258

```
      real zc,zsc,zoz,zsoz,slast,slost
c     program to calculate grid bar spacing forgiven power
c     law profile using the cowdrey and owenzienkiewicz formulae
      dimension zc(50),zsc(50),zoz(50),zsoz(50),slast(50),slost(50)
      real k,k0,n,h,tol,d,s,x,c,v,q,cldk,a,e,y,b
      integer j,i,m,j0,num1,num2
      open(6,file='prn')
    8 write(*,9)
    9 format(' enter exponent,  tunnel height (in), bar dia (in), dp/q',
     1 '     ',  tolerance separated by commas')
   10 read(*,11) n,h,d,k0,tol
   11 format(5f7.4)
      if(n.eq.0.)go to 1100
c
c     write input parameters
      write(*,12)n,h,k0,d,tol
   12 format(1H0,4x,'power index = ',f6.2,/1h0,4x,'tunnel height h = ',
     1f8.4,/1h0,4x,'pressure drop coefft k0 = ',f7.4,/1h0,4x,'bar diamet
     2er d = ',f7.4,/1h0,4x,'tol = ',f7.4)
      write(*,7)
    7 format(' type 0 if correct?')
      read(j,6)
    6 format(i1)
      if(j.ne.0) go to 8
      write(6,12)n,h,k0,d,tol
c     set initial conditions
   20 j=1
      s=d
      x=0.
      zsc(j)=0.
      zc(j)=d/2.
      c=h*((n/(n+1.))**n)*((1.+k0)**(n/2.))
c
c     write first bar conditions
      write(*,125)
      write(6,125)
  125 format(1h0,'cowdrey iteration')
      write(*,13)j,j,zsc(j),s,x,zc(j)
      write(6,13)j,j,zsc(j),s,x,zc(j)
   13 format(1h0,2x,'zsc(',i2,')',5x,'s',8x,'x',8x,'zc(',i2')',/1h0,4(2x
     1,f7.4))
c
c     calculations for successive bars
   30 j=j+1
      m=1
      write(*,14)j,j
      write(6,14)j,j
   14 format(1h0,2x,'zsc(',i2,')',6x,'s',8x,'x',8x,'zc(',i2,')')
      zsc(j)=zc(j-1)+s/2.
c
c    iteration cycle
   40 v=(zsc(j)/c)**(2./n)
      if((4.-3.*v).lt.0.) go to 1001
      s=(2.*d*(v-1.))/(v-2.+sqrt((2.-v)**2.-4.*(v-1.)*(v-1.)))
      x=zc(j-1)+s/2.
      write(*,15)zsc(j),s,x
      write(6,15)zsc(j),s,x
   15 format(1h0,2x,f7.3,2x,f8.4,2x,f8.4)
```

```
      x=zc(j-1)+s/2.
      write(*,15)zsc(j),s,x
      write(6,15)zsc(j),s,x
   15 format(1h0,2x,f7.3,2x,f8.4,2x,f8.4)
      if(x.ge.h)go to 200
      j0=j*1000
      if(m.eq.10)go to 1000
      m=m+1
      if(abs((zsc(j)-x)/zsc(j)).lt.tol) go to 50
      zsc(j)=x
      go to 40
c
c     centreline height of bar
   50 zc(j)=zc(j-1)+s
      num1=j
      slast(j)=s
      write(*,16)zc(j)
      write(6,16)zc(j)
   16 format(1h+,32x,f8.4)
      q=s-d
      write(*,17)q
      write(6,17)q
   17 format(1h+,50x,21hseparation of bars = ,f7.4)
      if((zc(j)+s+d).ge.h) go to 200
      go to 30
c
c     repeat for owen and zienkienkiewicz method
  200 write(*,60)
      write(6,60)
   60 format(/,'  owen and zienkiewicz method begins',/)
      j=1
      s=d
      zsoz(j)=0.
      zoz(j)=d/2.
  300 j=j+1
      m=1
      if(slast(j).lt.d) slast(j) =s
      zsoz(j)=zoz(j-1)+slast(j)/2.
      oldk=(d/slast(j))/((1.-d/slast(j))**2.)
      a=1.1
      e=(n+1.)/n
c
c     iteration cycle
  400 b=sqrt(1.+oldk)
  410 k=(((h**(2./n))*(1.+k0)*((a+b)**2.))-((e*e)*((a+b)**(2./e))*(zsoz(
     1j)**(2./n))*((b+a*(h/zsoz(j))**(1./n))**(2./(n+1.)))))/(((zsoz(j)*
     2*(1./n))*e*b+a*(h**(1./n)))**2.)
c
c     calculate spacing s
      s=(2.*k*d)/(1.+2.*k-sqrt(1.+4.*k))
      y=zoz(j-1)+s/2.
      j0=j
      if(m.eq.10) go to 1000
      m=m+1
      if(y.ge.h) go to 600
      if(abs((y-zsoz(j))/y).lt.tol) go to 500
      zsoz(j)=y
      oldk=k
      go to 400
c
c     centreline height of bar
  500 zoz(j)=zoz(j-1)+s
      num2=j
      slost(j) = s
      if((zoz(j)+s+d).ge.h) go to 600
      go to 300
c
c     final layouts
  600 write(6,24)
```

```
c     centreline height of bar
  500 zoz(j)=zoz(j-1)+s
      num2=j
      slost(j) = s
      if((zoz(j)+s+d).ge.h) go to 600
      go to 300
c
c     final layouts
  600 write(6,24)
      write(*,24)
   24 format(1h0,8x,'cowdrey method',30x,'o and z method')
      write(6,18)num1,num2
      write(*,18)num1,num2
   18 format(1h0,4x,'no bars = ',i2,32x,'no bars = ',i2)
      write(6,19)
      write(*,19)
   19 format(1h0,4x,'bar no',6x,'height(inches)',4x,'space',9x,'bar no',
     16x,'height(inches)',4x,'space')
      if(num1.lt.num2)num1=num2
  650 do 700 i=1,num1
  700 write(6,21) i,zc(i),slast(i).I,zoz(i),slost(i)
   21 format(1h0,6x,i2,12x,f8.4,5x,f7.4,9x,i2,12x,f8.4,5x,f7.4)
      go to 10
 1000 write(6,22)j0
   22 format(1h0,4x,'j0 = ',i5,2x,'convergence too slow')
      go to 1100
 1001 write(6,23)
   23 format(1h0,4x,'v greater than 4/3')
 1100 stop
      end
```

APPENDIX 2

EXTRACT.PAS - PROGRAM USED TO EXTRACT THE INFORMATION FROM THE DATA RECORD, AND PERFORM PRELIMINARY DATA REDUCTION.

EXTRACT.PAS
printed 13 Nov 1992

```
{$R+}    {Range checking on}
{$B+}    {Boolean complete evaluation on}
{$S+}    {Stack checking on}
{$I+}    {I/O checking on}
{$N+}    {Numeric coprocessor (possibly) }
{$E+}    {Emulate coprocessor if not physically present  }
{$M 65500,16384,655360} {Turbo 3 default stack and heap}

PROGRAM EXTRACT;


Uses
  Crt,dos,Printer; {Units found in TURBO.TPL}

var
   infile,outfile,results:text;

   filename,filename1,filename2,
   comment,
   name
                                  :string[20];

  fileend
                  :boolean;
  ch
    :char;
  i,j,MARKER,noofints,noofreals,testno,day,month,year,
  hours,minutes,sailnumber,noofchs,noofreadings,
  windonoff,turbulenceonoff,
  line,lineno,earlierlineno,
  wind,turb,
  count,
  filecounter
                             :integer;
  rudderangle,skegangle,apparentwindangle,heelangle,
  heightaboveref,baropress,temp,dynpress,area,h,
  reflength
                                          :double;
  chan: array [1..30] of integer;
  volt: array [1..30] of double;
  Vs,zeros,Vsz,F,CF,cwa  : array [1..100,1..8] of double;
  Vcal      : array [1..5] of double;
  linenumber,
  reads,
  turbulence
        : array [1..100] of integer;
  apparent,
  heel,
  height,
  temperature,
  q,heightupmast
        : array [1..100] of double;


function tan(angle:double):double;    {  tangent of an angle  }
begin
  tan:=sin(angle)/cos(angle);
end;   {  end of function tan  }


procedure set_up;
begin
  filecounter:=0;
  wind:=0;
  turb:=0;
```

```
    area:=0.16416;
    reflength:=1.0;
    delete(comment,1,length(comment));
    for i:=1 to 5 do
      Vcal[i]:=7.0;
    Vcal[3]:=11.0;
  end;


  procedure zero;   {   beginning of the file   }
  begin
    rewrite(outfile);
    clrscr;
    writeln('beginning of processing of file ',filename1,
            ' containing balance voltages');
    write('MARKER = ',marker:2);
    readln(infile);
    readln(infile,noofints,noofreals);
    if noofints <>7 then writeln('no of integers = ',noofints:4);
    if noofreals <>5 then writeln('no of reals = ',noofreals:4);
    readln(infile,testno);
    readln(infile,day);
    readln(infile,month);
    readln(infile,year);
    readln(infile,hours);
    readln(infile,minutes);
    readln(infile,sailnumber);
    readln(infile,rudderangle);
    readln(infile,skegangle);
    readln(infile,apparentwindangle);
    readln(infile,heelangle);
    readln(infile,heightaboveref);
    write('  test number = ',testno:3);
    writeln('  sail number = ',sailnumber:2);
    write('date of test = ',day:2,'-',month:2,'-',year:4);
    writeln('   time of test = ',hours:2,':',minutes:2);
    write('rudder ang = ',rudderangle:7:2,' deg');
    writeln('   skeg ang = ',skegangle:7:2,' deg (pos clockwise)');
    write('apparent wind angle = ',apparentwindangle:7:2);
    writeln('heel angle = ',heelangle:7:2,' deg, (positive to leeward)');
    writeln('height of model above reference = ',heightaboveref:7:2,' mm');
  {   write data to file  }

    writeln(outfile,'beginning of processing of file ',filename1,
            ' containing balance voltages');
    write(outfile,'MARKER = ',marker:2);
    write(outfile,'  test number = ',testno:3);
    writeln(outfile,'  sail number = ',sailnumber:2);
    write(outfile,'date of test = ',day:2,'-',month:2,'-',year:4);
    writeln(outfile,'   time of test = ',hours:2,':',minutes:2);
    write(outfile,'rudder ang = ',rudderangle:7:2,' deg');
    writeln(outfile,'   skeg ang = ',skegangle:7:2,' deg (pos clockwise)');
    write(outfile,'apparent wind angle = ',apparentwindangle:7:2);
    writeln(outfile,'heel angle = ',heelangle:7:2,
                    ' deg, (positive to leeward)');
    writeln(outfile,'height of model above reference = ',
                     heightaboveref:7:2,' mm');
    writeln(outfile);
  end;   { end of procedure zero }


  procedure one; {  barometric pressure, air temperature, dynamic pressure  }
  begin
    readln(infile,baropress);
    readln(infile,temp);
    readln(infile,dynpress);
```

```
end;  { end of procedure one  }


procedure twothreeseven;  {  supply volts, zeros, or actual data  }
begin
  readln(infile,noofchs);
  readln(infile,noofreadings);
  readln(infile);
  for i:=1 to noofchs do
    readln(infile,chan[i],volt[i]);
  gotoXY(1,8);
  writeln('MARKER test sail apparent heel height ',
  'baro temp   q    chans readings turb wind');
  writeln(marker:4,testno:6,sailnumber:5,apparentwindangle:8:2,
  heelangle:7:2,heightaboveref:6:1,baropress:6:1,temp:5:1,
  dynpress:6:2,noofchs:6,noofreadings:6,'   ',turb:6,' ',wind:3);
  gotoXY(1,11);  clreol;
  gotoXY(1,12);  clreol;
  gotoXY(1,13);  clreol;
  gotoXY(1,14);  clreol;
  gotoXY(1,11);
  write('chans ');
  for i:=1 to noofchs do
    write(chan[i]:12);
  writeln;
  write('volts  ');
  for i:=1 to noofchs do
    write(volt[i]:12:7);
{  gotoXY(1,16);
  write('hit any key to continue ');
  ch:=readkey;   }

{  write to file  }
  if marker=3 then
  begin
    write(outfile,'MARKER test sail rudder skeg apparent heel height baro ',
    'temp   q    chans readings turb wind');
    chan[noofchs+1]:=16;
    for i:=1 to noofchs+1 do
      write(outfile,chan[i]:11);
    writeln(outfile);
  end;
  if length(comment)>0 then
  begin
    writeln(outfile,' 9  ',comment);
    delete(comment,1,length(comment));
  end;
  write(outfile,marker:4,testno:6,sailnumber:5,rudderangle:6:1,
  skegangle:6:1,apparentwindangle:8:2,
  heelangle:7:2,heightaboveref:6:1,baropress:6:1,temp:5:1,
  dynpress:6:2,noofchs:6,noofreadings:6,'   ',turb:6,' ',wind:3);
  if marker=2 then
    for i:=1 to 8 do
      write(outfile,'           ');
  for i:=1 to noofchs do
    write(outfile,volt[i]:11:7);
  writeln(outfile);

end;  {  end of procedure twothreeseven  }


procedure four;   {  get new height above reference  }
begin
  readln(infile,heightaboveref);
end;  {  end of procedure heightaboveref  }
```

```
procedure fivesix;
begin
  gotoXY(1,16);
  writeln(lst,'procedure 5 6 used by mistake, Marker = ',marker:3);
end;  { end of procedure fivesix }


procedure eight;   { end of input file has been reached }
begin
  gotoXY(10,24);
  writeln('end of input file ',filename1,' reached properly');
  writeln(lst,'end of input file ',filename1,' reached properly');
  writeln(outfile,'8 end of file');
  close(infile);
  close(outfile);
  fileend:=true;
end;  { end of procedure eight }


procedure nine;   { comment }
begin
  gotoXY(1,18);
  write('comment marker  - ');
  clreol;
  readln(infile,comment);
  writeln(comment);
end;  { end of procedure nine }


procedure ten;  { new heel angle }
begin
  readln(infile,heelangle);
end;  { end of procedure 10 }


procedure eleven;  { new apparent wind angle }
begin
  readln(infile,apparentwindangle);
end;


procedure twelve;   { new temperature }
begin
  readln(infile,temp);
end;  { end of procedure twelve }


procedure thirteen;   { new skeg angle }
begin
  readln(infile,skegangle);
end;  { end of procedure thirteen }


procedure fourteen;  { new dynamic pressure }
begin
  readln(infile,dynpress);
end;  { end of procedure fourteen }


procedure fifteen;  { wind on/off }
begin
  readln(infile,wind);
end;  { end of procedure fifteen }
```

```
procedure sixteen;  {  turbulence on/off  }
begin
  readln(infile,turb);
end;  {  end of procedure sixteen  }


procedure get_file;
begin
  fileend:=false;
  clrscr;
  repeat
    gotoXY(1,10);
    writeln('enter input file name (without extension) ');
    clreol;
    write('                or q to quit                  ');
    readln(filename);
    for i:=1 to length(filename) do
      filename[i]:=upcase(filename[i]);
    if filename='Q' then halt;
    filename1:=filename+'.YRF';
    filename2:=filename+'.VLT';
    assign(infile,filename1);
    {$I-}
    reset(infile);
    {$I+}
    if IOresult<>0 then
       write(filename1,' does not exist - try again');
    {$I-}
    reset(infile);
    {$I+}
  until IOresult=0;
  assign(outfile,filename2);
end;  {  end of procedure get_file  }


procedure extractdata;
begin
  repeat
    readln(infile,marker);
    case marker of
      0: zero;
      1: one;
      2,3,7: twothreeseven;
      4: four;
      5,6: fivesix;
      8: eight;
      9: nine;
      10: ten;
      11: eleven;
      12: twelve;
      13: thirteen;
      14: fourteen;
      15: fifteen;
      16: sixteen;
    else
      writeln(lst,'not in range 0 - 16, MARKER = ',marker:6);
    end;
  until fileend;
end;  {  end of procedure extractdata  }

procedure supplyvoltages;  {  get the supply voltages  }
begin
  reset(outfile);
  for i:= 1 to 7 do
    readln(outfile);
  repeat
```

```
    readln(outfile);
    read(outfile,marker)
  until marker=2;
  lineno:=1;
  earlierlineno:=lineno;
  read(outfile,testno,sailnumber,rudderangle,
  skegangle,apparentwindangle,
  heelangle,heightaboveref,baropress,temp,
  dynpress,noofchs,noofreadings,turb,wind);
  for i:=1 to noofchs do
    read(outfile,Vs[lineno,i]);
  repeat
     repeat
       readln(outfile);
     ' read(outfile,marker);
       if marker<>9 then lineno:=lineno+1;
     until (marker=2) or (marker=8);
     if marker=2 then
     begin
       read(outfile,testno,sailnumber,rudderangle,
       skegangle,apparentwindangle,
       heelangle,heightaboveref,baropress,temp,
       dynpress,noofchs,noofreadings,turb,wind);
       for i:=1 to noofchs do
         read(outfile,Vs[lineno,i]);
       for line:=earlierlineno+1 to lineno-1 do
         for i:=1 to noofchs do
           Vs[line,i]:=Vs[earlierlineno,i]+(Vs[lineno,i]-
           Vs[earlierlineno,i])*(line-earlierlineno)/(lineno-earlierlineno);
      earlierlineno:=lineno;
    end;
    if marker=8 then
    begin
      lineno:=lineno-1;
      for line:=earlierlineno+1 to lineno do
        for i:= 1 to noofchs do
          Vs[line,i]:=Vs[earlierlineno,i];
    end;
  until marker=8;
  close(outfile);
  writeln(lst);
  writeln(lst,'supply voltages');
  write(lst,'channel ');
  for i:=1 to noofchs do
     write(lst,i:12);
  writeln(lst);
  writeln(lst,'line no.');
  for line:=1 to lineno do
  begin
    write(lst,line:5,'    ');
    for i:=1 to noofchs do
      write(lst,Vs[line,i]:12:7);
    writeln(lst);
  end;
end;  { end of procedure supplyvoltages }


procedure findzeros;  { get the windoff balance voltages }
begin
  reset(outfile);
  for i:= 1 to 7 do
    readln(outfile);
  repeat
    readln(outfile);
    read(outfile,marker)
  until marker=2;
```

```
    lineno:=1;
    earlierlineno:=lineno;
    read(outfile,testno,sailnumber,rudderangle,
    skegangle,apparentwindangle,
    heelangle,heightaboveref,baropress,temp,
    dynpress,noofchs,noofreadings,turb,wind);
    for line:=1 to 100 do zeros[line,noofchs+1]:=0.0;
    repeat
       repeat
         readln(outfile);
         read(outfile,marker);
         if marker<>9 then lineno:=lineno+1;
       until (marker=7) or (marker=8);
       if marker=7 then
       begin
         read(outfile,testno,sailnumber,rudderangle,
         skegangle,apparentwindangle,
         heelangle,heightaboveref,baropress,temp,
         dynpress,noofchs,noofreadings,turb,wind);
         if wind=0 then
         begin
           if dynpress<> 0.0 then
             writeln(lst,'zero block and dynamic pressure = ',dynpress:6:2,
                         '  line number = ',lineno:3);
           for i:=1 to noofchs do
             read(outfile,zeros[lineno,i]);
           if earlierlineno=1 then
             for line:=1 to lineno-1 do
               for i:=1 to noofchs do
                 zeros[line,i]:=0.0;
           if earlierlineno<>1 then
             for line:=earlierlineno+1 to lineno-1 do
               for i:=1 to noofchs do
                 zeros[line,i]:=zeros[earlierlineno,i]
                              +(zeros[lineno,i]-zeros[earlierlineno,i])
                              *(line-earlierlineno)/(lineno-earlierlineno);
           zeros[lineno,noofchs+1]:=-99.0;
           earlierlineno:=lineno;
         end;
       end;
       if marker=8 then
       begin
         lineno:=lineno-1;
         for line:=earlierlineno+1 to lineno do
           for i:= 1 to noofchs do
             zeros[line,i]:=zeros[earlierlineno,i];
       end;
    until marker=8;
    close(outfile);
    writeln(lst);
    writeln(lst,'zeros');
    write(lst,'channel ');
    for i:=1 to noofchs do
       write(lst,i:12);
    writeln(lst);
    writeln(lst,'line no.');
    for line:=1 to lineno do
    begin
      write(lst,line:5,'    ');
      for i:=1 to noofchs do
        write(lst,zeros[line,i]:12:7);
      if zeros[line,noofchs+1]=-99.0 then write(lst,'  zero');
      writeln(lst);
    end;
  end;  {  end of procedure zeros  }
```

```
procedure balance_matrix;
begin
{  fudge the pitch voltage, which is garbage, measured from the balance
   this is done so that the interactions from pitch will not cause
   incorrect errors                                                  }

  Vsz[count,5]:=0.2525*Vsz[count,2]*(122+height[count]+400*
                    cos(heel[count]*pi/180))/(4.84685e-2*1e3);
{ writeln(lst,'pitch voltage is = ',Vsz[count,5]:11:7);             }

  F[count,1]:= (0.338035   * Vsz[count,1]+
               -1.188100e-3* Vsz[count,2]+
               -3.952000e-4* Vsz[count,3]+
               -1.484800e-3* Vsz[count,4]+
               -3.260500e-3* Vsz[count,5])*1e6;

  F[count,2]:= (2.120000e-5* Vsz[count,1]+
                0.252512   * Vsz[count,2]+
               -6.659000e-4* Vsz[count,3]+
                1.682300e-3* Vsz[count,4]+
               -9.901000e-4* Vsz[count,5])*1e6;

  F[count,3]:=(-0.000182   * Vsz[count,1]+
                2.845000e-4* Vsz[count,2]+
                3.936600e-2* Vsz[count,3]+
                1.344000e-4* Vsz[count,4]+
                0.00032    * Vsz[count,5])*1e6;

  F[count,4]:= (7.002000e-4* Vsz[count,1]+
               -2.370000e-5* Vsz[count,2]+
               -3.403600e-3* Vsz[count,3]+
                6.349250e-2* Vsz[count,4]+
                2.049000e-4* Vsz[count,5])*1e6;

  F[count,5]:=(-3.300000e-6* Vsz[count,1]+
                6.333000e-4* Vsz[count,2]+
                1.470000e-5* Vsz[count,3]+
               -3.008000e-4* Vsz[count,4]+
                4.846850e-2* Vsz[count,5])*1e6;

{  estimate vertical force assuming that the sideforce acts perpindicular
   to the mast }
   F[count,6]:=F[count,1]*tan(heelangle*pi/180.0);

end;  {  end of procedure balance_matrix  }


procedure moveMRC;
begin

   F[count,3]:=F[count,3]+0.085*F[count,1];
   F[count,4]:=F[count,4]-F[count,1]*(0.122+height[count]/1000.0);
   F[count,5]:=F[count,5]-F[count,2]*(0.122+height[count]/1000.0)
                         -F[count,6]*0.085;

  if F[count,1]<>0.0 then
    heightupmast[count]:=F[count,4]*cos(heelangle*pi/180.0)*1000/F[count,1]
  else
    heightupmast[count]:=0.0;

end;   {   end of procedure moveMRC    }


procedure coefficients;
begin
```

```
  h:=400.0*cos(heelangle*pi/180.0)+heightaboveref-115.0+5.0;
  if turb=1 then
    q[count]:=3*9.81*(0.76239+0.0005326*h)
  else
    q[count]:=3*9.81*1.03;
  for i:=1 to 2 do
    CF[count,i]:=F[count,i]/(area*q[count]);
  for i:=3 to 5 do
    CF[count,i]:=F[count,i]/(area*reflength*q[count]);
  CF[count,6]:=F[count,6]/(area*q[count]);
end;   { end of procedure coefficients }


procedure wind_axes;
begin

  cwa[count,1]:=CF[count,2]*sin(apparent[count]*pi/180.0)
               +CF[count,1]*cos(apparent[count]*pi/180.0);
  cwa[count,2]:=CF[count,1]*sin(apparent[count]*pi/180.0)
               -CF[count,2]*cos(apparent[count]*pi/180.0);
  cwa[count,3]:=CF[count,3];
  cwa[count,4]:=CF[count,4]*cos(apparent[count]*pi/180.0)
               +CF[count,5]*sin(apparent[count]*pi/180.0);
  cwa[count,5]:=CF[count,5]*cos(apparent[count]*pi/180.0)
               -CF[count,4]*sin(apparent[count]*pi/180.0);
  cwa[count,6]:=CF[count,6];
end;   { end of procedure wind_axes }


procedure correctdata;
begin
  reset(outfile);
  for i:= 1 to 7 do
    readln(outfile);
  repeat
    readln(outfile);
    read(outfile,marker)
  until marker=2;
  lineno:=1;
  count:=0;
  read(outfile,testno,sailnumber,rudderangle,
  skegangle,apparentwindangle,
  heelangle,heightaboveref,baropress,temp,
  dynpress,noofchs,noofreadings,turb,wind);
  repeat
     repeat
       readln(outfile);
       read(outfile,marker);
       if marker<>9 then lineno:=lineno+1;
     until (marker=7) or (marker=8);
     if marker=7 then
     begin
       read(outfile,testno,sailnumber,rudderangle,
       skegangle,apparentwindangle,
       heelangle,heightaboveref,baropress,temp,
       dynpress,noofchs,noofreadings,turb,wind);
       if wind=1 then
       begin
         if dynpress<>3.0 then
           writeln(lst,'data block and dynamic pressure = ',dynpress:6:2,
                       '  line number = ',lineno:3);
         count:=count+1;
         linenumber[count]:=lineno;
         apparent[count]:=apparentwindangle;
         heel[count]:=heelangle;
```

```
          height[count]:=heightaboveref;
          temperature[count]:=temp;
          q[count]:=dynpress;
          reads[count]:=noofreadings;
          turbulence[count]:=turb;
          for i:=1 to noofchs do
            read(outfile,Vsz[count,i]);
          for i:=1 to noofchs do
            Vsz[count,i]:=(Vsz[count,i]-zeros[lineno,i])*Vcal[i]/Vs[lineno,i];
          balance_matrix;
          moveMRC;
          coefficients;
{         wind_axes;                        }
        end;
      end;
  until marker=8;
  close(outfile);
  writeln(lst);
  writeln(lst,'voltages corrected for supply and zero offsets');
  write(lst,'channel  ');
  for i:=1 to noofchs do
     write(lst,i:12);
  writeln(lst);
  writeln(lst,'count  line no.');
  for line:=1 to count do
  begin
    write(lst,line:3,'    ',linenumber[line]:3,'  ');
    for i:=1 to noofchs do
      write(lst,Vsz[line,i]:12:7);
    writeln(lst);
  end;
  writeln(lst);
  writeln(lst,'balance matrix applied and MRC moved to boat');
  write(lst,'channel  ');
     write(lst,'       sideforce     thrust    yaw moment   roll momt',
                    '  pitch momt');
  writeln(lst);
  writeln(lst,'count  line no.');
  for line:=1 to count do
  begin
    write(lst,line:3,'    ',linenumber[line]:3,'  ');
    for i:=1 to noofchs do
      write(lst,F[line,i]:12:7);
    writeln(lst);
  end;
  writeln(lst);
  writeln(lst,'                                                    COEFFICIENTS');
  write(lst,'channel  ');
     write(lst,'                              side  thrust yaw mom',
              '  roll pitch   Fv  hupmst');
  writeln(lst);
  writeln(lst,'     line height  heel tu apprnt');
  for line:=1 to count do
  begin
    write(lst,line:2,'    ',linenumber[line]:2,'  ',height[line]:6:1,
    heel[line]:6:1,turbulence[line]:2,apparent[line]:6:1);
    for i:=1 to noofchs do
      write(lst,CF[line,i]:7:3);
    write(lst,CF[line,6]:7:3,heightupmast[line]:6:1);
    writeln(lst);
  end;
  writeln(lst);
{ writeln(lst);
  writeln(lst,'                                        WIND AXIS     COEFFICIENTS');
  write(lst,'channel  ');
     write(lst,'                                lift  drag   yaw ',
```

```
                ' roll   pitch   Fv   hupmst');
  writeln(lst);
  writeln(lst,'     line  height heel tu apprnt');
  for line:=1 to count do
  begin
    write(lst,line:2,'    ',linenumber[line]:2,'  ',height[line]:6:1,
    heel[line]:6:1,turbulence[line]:2,apparent[line]:6:1);
    for i:=1 to noofchs do
      write(lst,cwa[line,i]:7:3);
    write(lst,cwa[line,6]:7:3,heightupmast[line]:6:1);
    writeln(lst);
  end;
  writeln(lst);                                                    }
  writeln(lst);
end;  {  end of procedure correctdata  }


procedure saveresultsinafile;
begin
  if filecounter=0 then
     begin
       writeln;
       write('enter results file name (without extension) ');
       readln(name);
       for i:=1 to length(name) do
         name[i]:=upcase(name[i]);
       name:=name+'.CPS';
       assign(results,name);
       rewrite(results);
     end
     else
       append(results);
  writeln(results,'0  processed results from ',filename1,' and ',filename2);
  writeln(results,'test no. date    time    sail no. baro press');
  writeln(results,testno:3,'    ',day:2,'-',month:2,'-',year:4,'  ',
                  hours:2,':',minutes:2,'  ',sailnumber:3,'    ',baropress:7:3);
  write(results,'      line  apprnt heel height',
                    '  temp  q  reads turb hupmast');
{    write(results,' Vsz                                              ',
    '             ');
     write(results,' F                                               ',
    '             ');
}    write(results,' CF                                              ',
    '             ');
{    write(results,' cwa');        }
     writeln(results);
  for i:=1 to count do
  begin
    write(results,i:3,linenumber[i]:6,apparent[i]:8:2,heel[i]:6:1,
          height[i]:7:2,temperature[i]:6:1,q[i]:5:1,reads[i]:3,
          turbulence[i]:5,heightupmast[i]:7:1);
{    for j:=1 to noofchs do
       write(results,Vsz[i,j]:11:7);
     for j:=1 to noofchs do
       write(results,F[i,j]:11:7);
}    for j:=1 to noofchs+1 do
       write(results,CF[i,j]:11:7);
{    for j:=1 to noofchs+1 do
       write(results,cwa[i,j]:11:7);                    }
     writeln(results);
  end;
  close(results);
end;  {  end of procedure saveresultsinafile  }


function finished:boolean;   {  finished all files?  }
```

```
begin
  write('process another file (y/n) ? ');
  repeat
    ch:=upcase(readkey);
  until ch in ['Y','N'];
  finished:=(ch='N');
end;

{  main  }

begin
  set_up;
  repeat
    get_file;
    extractdata;
    supplyvoltages;
    findzeros;
    correctdata;
    saveresultsinafile;
    filecounter:=filecounter+1;
  until finished;
end.
```